UNIVERSITY*of*
TASMANIA

Multi-System Pathophysiology and Molecular Signalling in a *Ccr6*- Deficient Murine Model of Spontaneous Colitis

by

Ranmali Ranasinghe

Submitted in fulfilment of the requirements for the
Degree of Master of Medical Science by Research
University of Tasmania, January 2020

Dedication

To Anurasiri and Anushka

Declaration of Originality

This thesis contains no material which has been accepted for a degree or diploma by the university or any other institution, except by way of background information and duly acknowledged in the thesis and to the best of my knowledge and belief, no material previously published or written by another person except where due acknowledgement is made in the text of the thesis, nor does the thesis contain any material that infringes copyright.

Full Name: Ranmali Ranasinghe

Signed: Date: January 2020

Authority of Access

This thesis is not to be made available for loan or copying for two years following the date this statement was signed. Following that time, the thesis may be made available for loan and limited copying and communication in accordance with the Copyright Act 1968.

Full Name: Ranmali Ranasinghe

Signed: Date: January 2020

Statement of Ethical Conduct

The research associated with this thesis abides by the international and Australian codes on human and animal experimentation, the guidelines of the Australian Government's office of the Gene Technology Regulator and the rulings of the Safety, Ethics and Institutional Biosafety Committees of the University. All animal experiments conducted in this thesis were approved by the University's Animal Ethics Committee (approval number, A0017541).

Statement Regarding Published Work Contained in Thesis

The publishers of the papers comprising Chapters 1 and 4 hold the copyright for that content, and access to the material should be sought from the respective journals. The remaining non-published content of the thesis may be made available for loan and limited copying and communication in accordance with the Copyright Act 1968, following the two year, withholding period (see Authority of Access).

Publications and Statements of Co-Authorship

The following people and institutions contributed to the publication of work undertaken as part of this thesis:

Paper 1: **Pleiotropic Immune Functions of CCR6 in Health and Disease**

Journal: Medicines

MDPI Publishing; Medicines **2018**, 5(3), 69; **https://doi.org/10.3390/medicines5030069**

Location of thesis: Chapters 1 and 4

Author 1: Ranmali Ranasinghe, School of Health Sciences, University of Tasmania

Author 2: Rajaraman Eri, School of Health Sciences, University of Tasmania

Author 1: Concept, writing and diagrams. Author 2: Editing and constructive criticism

This paper has received 17 citations up to date.

Paper 2: **Modulation of the CCR6-CCL20 Axis: A Potential Therapeutic Target in Inflammation and Cancer**

Journal: Medicina

MDPI Publishing: Medicina **2018**, 54(5), 88; **https://doi.org/10.3390/medicina54050088**

Location of thesis: Chapters 1 and 4

Author 1: Ranmali Ranasinghe, School of Health Sciences, University of Tasmania

Author 2: Rajaraman Eri, School of Health Sciences, University of Tasmania

Author 1: Concept, writing and diagrams. Author 2: Editing and constructive criticism

This paper has received 10 citations up to date.

Paper 3: **CCR6–CCL20-Mediated Immunologic Pathways in Inflammatory Bowel Disease**

Journal: Gastrointestinal Disorders

MDPI Publishing:

Gastrointest. Disord. **2019**, 1(1), 15-29; **https://doi.org/10.3390/gidisord1010003**

Location of thesis: Chapters 1 and 4

Author 1: Ranmali Ranasinghe, School of Health Sciences, University of Tasmania

Author 2: Rajaraman Eri, School of Health Sciences, University of Tasmania

Author 1: Concept, writing and diagrams. Author 2: Editing and constructive criticism

Paper 4: **CCR6–CCL20 Axis in IBD: What Have We Learnt in the Last 20 Years?**

Journal: Gastrointestinal Disorders

MDPI Publishing:

Gastrointest. Disord. **2019**, 1(1), 57-74; **https://doi.org/10.3390/gidisord1010006**

Location of thesis: Chapters 1 and 4

Author 1: Ranmali Ranasinghe, School of Health Sciences, University of Tasmania

Author 2: Rajaraman Eri, School of Health Sciences, University of Tasmania

Author 1: Concept, writing and diagrams. Author 2: Editing and constructive criticism

Poster Presentations

Understanding the CCR6-CCL20 Axis in the Gut

Presenter: Ranmali Ranasinghe, School of Health Sciences, University of Tasmania

Supervision: Rajaraman Eri, School of Health Sciences, University of Tasmania

Graduate Research Conference of University of Tasmania (2018)

Paper 5: ***Ccr6*-Deficiency Attenuates Spontaneous Chronic Colitis in Winnie**

Journal: Gastrointestinal Disorders

Published in Open Access Preprints:

DOI: https://doi.org/10.3390/gidisord2010004

Location of thesis: Chapters 1 to 4

Author 1: Ranmali Ranasinghe, School of Health Sciences, University of Tasmania

Author 2: Ruchira Fernando, Department of Histopathology, Launceston General Hospital, Launceston 7250, Tasmania.

Author 3: Agampodi Promoda Perera, School of Health Sciences, University of Tasmania

Author 4: Madhur Shastri, School of Health Sciences, University of Tasmania

Author 5: Waheedha Basheer, School of Health Sciences, University of Tasmania

Author 6: Paul Scowen: School of Medicine, University of Tasmania, Hobart, Tasmania

Author 7: Terry Pinfold, School of Medicine, University of Tasmania, Hobart, Tasmania

Author 8: Rajaraman Eri, School of Health Sciences, University of Tasmania

Author 1: Concept, writing and diagrams. Author 2: Analysis of Histopathology Data

Author 3: Data collection and constructive criticism, Author 4: Supervision, Author 5: Data collection, Author 6: Animal breeding, Author 7: Flowcytometry Supervision Author 8: Concept, supervision, manuscript editing, constructive criticism

_____ _____ _____

HDR Candidate **Primary Supervisor** **Head of School**

Acknowledgements

First and foremost, my grateful thanks go to my primary supervisor, Associate Professor Raj Eri for giving me the opportunity to re-kindle my enthusiasm for medical research and for the unwavering support given from the time I met him until I gained admission to join UTAS as an HDR candidate. Since then, he has been my tower of strength, and the kindest mentor and supervisor; he did not stall in the face of adversity, but wholeheartedly and optimistically helped me over the numerous hurdles I encountered during my course of study.

Secondly, I gratefully acknowledge the Australian Government and the University of Tasmania for giving me a much - valued Research Training Programme (RTP) scholarship which paid my tuition fees in full, a heavy financial burden off my shoulders. Without it, I could not have realised my dream of pursuing a higher degree in research after a long lapse away from the research arena.

I am very thankful to Professor Dominic Geraghty, my secondary supervisor, who helped me to gain admission to UTAS by supporting my application and has continued to provide steady support and for editing and proofreading the draft thesis.

I cannot describe the kind motivation and valuable support that I received from Dr Terry Pinfold, an enthusiastic research scientist who, in a short space of time, taught me flowcytometry and allowing me. His sincere criticism and invaluable guidance in all my flowcytometry experiments proved to be well worth the trouble of commuting to Hobart numerous times.

I would like to thank Peta Lawrie for her patience and diligence in training me in animal handling techniques, which is a pre-requisite for my study. I am also greatly indebted to Paul Scowen for his enthusiastic support, especially in helping me at a time when help was much needed.

My sincere gratitude goes to Dr Ruchira Fernando, Histopathologist at the LGH, whose magnanimous support made the completion of the histological assessments possible. Karen Wolfswinkle and Cassie, scientists at LGH pathology, are gratefully remembered for their kind support at a time I was rendered helpless, not being able to reach my goal.

Numerous people have helped me through my two- year journey towards the completion of my degree. To all those who have given me enormous encouragement by helping me either in a small or big way, I say a heartfelt thank you and I will be forever indebted for your unequivocal support.

My sincere thanks go to Promoda Perera, who became my best friend at UTAS, who has been a loyal critic, walking with me every step of the way on this arduous journey, helping me countless times to complete my research study successfully. Among those who have helped me at UTAS and who deserve to be mentioned as kind, good friends who assisted me in my times of need are Kate Edwards, Sonia Shastri, Tanvi Shinde, Ravi Vemuri, Tauseef Ahmed, Madhur Shastri, Archana Gaikwad and John Adulcikas.

I am ever so indebted to Dr Leonie Constable, Head of Histopathology at the Melbourne Pathology in Victoria, and Husni Hussain, Chairperson of the Ilma International Girls' School, in Colombo Sri Lanka, being my superiors at both these places where I worked for giving me excellent references to support my application at the UTAS, which I believe had helped me enormously to gain admission to this degree course.

Finally, it is my beloved husband Anura and loving little son, Anushka, who made this dream a reality, believing in me and taking a big risk coming and living in unknown Tasmania, foregoing lucrative employment opportunities elsewhere and doing all the housework, bearing the brunt of menial jobs and accompanying me back and forth on my many trips to Hobart. They have been my greatest strength and the two most precious gifts that god has choicely blessed me with.

Contents

List of Figures

List of Tables

Abbreviations

APC	Antigen presenting cells
bp	Base pairs
CCL20	C-C-Chemokine ligand 20
CCR6	C-C-Chemokine receptor 6
CD	Crohn's disease
DCs	Dendritic cells
DSS	Dextran sodium sulphate
ER stress	Endoplasmic reticulum stress
EAE	Experimental autoimmune encephalitis
FAE	Follicle-associated epithelium
FOXP3	Forkhead box transcription factor 3
GWAS	Genome-wide association studies
H&E	Haematoxylin and eosin
IBD	Inflammatory bowel disease
ILFs	Isolated lymphoid follicles
IFN-γ	Gamma interferon
IL	Interleukin
KO	Knockout
LARC	Liver activation-regulated chemokine
LPS	Lipopolysaccharide
MHC	Major histocompatibility complex
mRNA	Messenger ribonucleic acid
Muc2	Mucin 2 gene
M cell	Microfold cell
MALT	Mucosal-associated lymphoid tissue
MLNs	Mesenteric lymph nodes
MIP-3α	Macrophage inflammatory protein -3 alpha
NF-kB	Nuclear factor kappa B
NOD	Nucleotide-binding oligomerization domain
PAMP	Pathogen associated molecular pattern

PRRs	Pattern recognition receptors
PBS	Phosphate buffered saline
PPs	Peyer's patches
RT-PCR	Real time polymerase chain reaction
RORγt	RAR-retinoic acid-related orphan receptor gamma
SAMP1	Senescence-accelerated mouse P series
SCID	Severe combined immunodeficiency
SNP	Single nucleotide polymorphism
STAT3	Signal transducer and activator of transcription 3
TCR	T cell receptor
TGF-β1	Transforming growth factor beta 1
TNBS	2,4,6-trinitrobenzene sulfonic acid
TNF- α	Tumour necrosis factor-alpha
UC	Ulcerative colitis
UPR	Unfolded protein response
WT	Wild type

Abstract

Background: Inflammatory Bowel Disease (IBD) is an immune-deficient gut diseases complex [Crohn's Disease (CD) and Ulcerative Colitis (UC)] which cause serious digestive problems from prolonged inflammation. A multitude of immunological, microbial and environmental reasons have been named as its causative agents although its true aetiology is still unknown. There is no known definite treatment regime, nor a permanent cure has yet been established for these serious chronic illnesses in the gut. This study has attempted to investigate the influence of the C-C Chemokine Receptor 6 (CCR6) and its sole ligand C-C Chemokine Ligand (CCL20) as a potential therapeutic target for IBD given the important immunological role played by this chemokine pair. The immunomodulatory behaviour of the CCR6/CCL20 axis on multi-system pathophysiology was investigated at two clinically significant time points, using a *Ccr6*-deficient mouse model of spontaneous colitis. **Methods:** Four groups of mice, [(i) C57BL/6J which was the Wild Type abbreviated as WT and having (Winnie +/+, *Ccr6* +/+) genotype (ii) homozygous *Ccr6*-/- mutant of the WT having (Winnie +/+, *Ccr6*-/-) genotype (iii) Winnie x *Ccr6* -/-, the double knockout experimental model derived from the WT background (denoted by Winnie m/m, *Ccr6*-/-) and (iv) Winnie, also derived from the WT background, having the (m/m, *Ccr6*+/+) genotype] were utilized and (1) colonic inflammatory parameters, (2) colonic histology, (3) histology of spleen, kidney and liver (4) T and B lymphocyte quantification in the spleen and mesenteric lymph nodes (MLN) by flow cytometry, (5) colonic CCL20, phosphorylated phosphoinositide – 3 – kinase ($PI3K^P$) and phosphorylated protein kinase B also known as (Akt^P) expression by immunohistochemistry, and (6) cytokine expression in the colon by real time – polymerase chain reaction (RT-PCR) were evaluated. **Results:** CCR6 influenced upregulation of inflammation during murine colitis in the gut, spleen and liver while renal histology remained unaffected. Marked focal lobular inflammation with reactive nuclear features were observed in hepatocytes and a significant neutrophil infiltration in red pulp with extra medullary hemopoiesis existed in the spleen. These changes were

considerably reduced in the gut, spleen and liver of Winnie x *Ccr6*-/- [also known as the *Ccr6*-deficient-Winnie] with elevated goblet cell numbers and a conspicuously high mucus production in the colonic epithelium. In its spleen, the splenic lymphocyte percentage during early inflammation remained static but declined considerably towards the acute inflammatory stage compared to the WT, indicating decreased lymphocyte egression. The reverse of splenic hemopoiesis was seen in the MLN of the same model which had suppressed lymphocyte presence at 8 weeks which was restored with increased presence during acute disease. Cytokine expression in the Winnie x *Ccr6*-/- was below that of Winnie in all the cytokines tested. As an effect of CCR6 deficiency during chronic colitis, Winnie x *Ccr6*-/- produced upregulation of AKT^{P} and downregulation of $PI3K^{P}$ in its molecular signalling apparatus, compared to those of Winnie. **Conclusion:** CCR6/CCL20 are known to produce detrimental effects in the gut and this is further substantiated by our study. We report inflammation and tissue injury in the spleen and liver during chronic colitis in the Winnie model for the first time. Results indicated that *Ccr6* deficiency in the experimental colitis model contributed towards ameliorating colitis. Consequently, they displayed reduced inflammation in the gut, spleen and liver. These findings demonstrate an intricate networking role for CCR6 in pre-clinical immune activation, which was substantially diminished in Winnie x *Ccr6*-/- and need clinical investigation to determine whether it could provide newer clinical therapies in colitis.

1.0 Introduction

1.1 Inflammatory Bowel Disease

1.1.1 Epidemiology and Economic Impact

Inflammatory bowel disease (IBD) is a complex, chronic gut disease comprising two concordant phenotypes; Crohn's disease (CD) and ulcerative colitis (UC) (1). Both CD and UC feature a relapsing–remitting disease course with colectomy as the final treatment option and a high risk of developing colorectal cancer (CRC) (2). Symptoms of both the disease phenotypes can include rectal bleeding, abdominal pain, tenesmus, urgency to evacuate, prolonged intermittent diarrhea, anorexia, fatigue, and weight loss (3). Extraintestinal manifestations include arthritis, skin rashes, dysfunction of the eyes, liver and kidneys (4). The severity of the symptoms varies from mild to severe. The most common complication of CD is the blockage of the intestine due to swelling, which results in the thickening of the bowel wall (5). Afflicted persons often encounter problems related to malnutrition, triggered by poor nutrient absorption (6).

CD and UC can be differentiated by their location in the gastrointestinal tract, with severity of inflammation appearing in the intestinal wall and the specific nature of pathophysiology (7). CD is a chronic, transmural, segmental, inflammatory disease that involves any part of the gut from mouth to anus but mostly affects the terminal ileum (8). CD is characterized by mucosal granuloma and can be complicated by the development of fistulas and strictures (9). UC is a chronic, inflammatory disease which affects only the mucosa of the colon and the rectum (10).

Studies also show that IBD most commonly presents in young adults aged between 15 and 29 years of age. Another prominent age group are those aged between 60 and 70 years (11). IBD causes severe morbidity in young adults at their most productive age (12). The disease itself places a heavy burden on the patients by causing psychological distress, annihilating career objectives, instilling social stigma and degrading their quality of life (13).

Population-based studies reveal IBD to be a global disease of the 21st century, with the highest prevalence in Europe and North America (14). A 2016, USA-based study reported an increase of 1.3% in IBD prevalence rates, and showed that the disease was more common in people who were unemployed, living in poverty, and lacking a high school education (15). Increasing rates of IBD have been shown in several newly industrialized countries in Asia, Africa, South America, and the Middle East since the 1990s (16).

A recent population survey identified Australia as also having the highest prevalence of IBD alongside Canada, Denmark, and New Zealand, with CD being more common than UC in the Australian population (17). The data also showed that IBD is becoming more severe and more complex in Australia, also with a projected estimate of 100,000 patients in 2022 (18). Among the Australians surveyed, factors such as smoking, childhood immunological events, namely, tonsillectomy or chickenpox, and frequent intake of fast food, were factors associated with the high risk of developing IBD, while frequent caffeine consumption and pet ownership provided protection against developing the disease (19). Another survey had estimated the cost of IBD to the Australian State, for 242 Australian patients, in their first 12 months from diagnosis, was over 2 million Australian Dollars (20).

1.1.2 Aetiology and Pathogenesis

The aetiology of IBD is not completely understood yet, but it is commonly attributed to the gastrointestinal (GI) tract stimulation by excessive and abnormal adaptive immune responses *via* induction of pro-inflammatory cytokines (21). Such immune activation is produced against the 100 trillion or so luminal microbial flora inhabiting the intestine, which spans about 200–400 m^2 (22). Dysregulated innate and adaptive immunity followed by microbial dysbiosis, due to the disruption of the mucosal barrier, which exposes persons to numerous luminal antigens, play a significant role in the disease development (23). Decreased rates of IBD in rural environments and

increased rates of IBD in overly clean environments too, have been reported, while enteric infections may trigger the onset in settings such as refugee camps (24) (25).

IBD is considered as a group of highly complex, heritable diseases, where more than 200 genetic loci including, Nucleotide-binding oligomerization domain-containing protein 2 (*NOD2),* Autophagy related like 16 gene (*ATR16GL*), X-Box binding protein 1 *(XBPI),* Interleukin twenty three receptor (*IL23R*), Signal transducer and activator of transcription 3 (*STAT3*), Janus Kinase 2 (*JAK2*) and C-C Chemokine Receptor six (*CCR6*), have been implicated as predisposing factors (26). Recently, heritability was endowed with only a 25% probability, being recognized as the cardinal factor causing IBD, because a multitude of environmental factors are also now held accountable (27).

Multiple causative factors, newly defined as the "exposome", consisting of all the environmental contributory agents, are now implicated in IBD (28). These include the gut microbiota (both commensal and pathogenic), excessive usage of antibiotics, nutrition, smoking, industrialization with more exposure to pollutants, a westernized lifestyle, poor access to hygienic toileting, sleep disorders, anxiety and depression, appendectomy, exposure to bright sunlight, increased vitamin D and the use of oral contraceptives (29).

Rather than being attributed to entirely genetic predisposition and microbiome status, more recent explanations focus on dysfunctional signalling pathways. One of these pathways involved endoplasmic reticulum stress (ER-stress)-induced apoptosis, due to the unfolded protein response, which had resulted in the autophagy of Paneth, goblet, and intraepithelial cells (30) (31).

1.1.3 Diagnosis and Treatment

There are a number of biomarkers [blood c-reactive protein, faecal calprotectin, magnetic resonance imaging (MRI), computer tomography (CT) scans and ultrasound scans with many more serological and stool biomarkers] are utilised in IBD diagnosis, including perinuclear anti-neutrophil cytoplasmic antibodies (pANCA) and anti-

Saccharomyces cerevisiae antibodies (pASCA), but no single blood test of definite diagnostic value exists (32). Abnormalities include anaemia, elevated inflammatory markers, electrolyte abnormalities due to diarrhea, vitamin deficiencies as seen in CD and low albumin, indicative of both inflammation and poor absorption of nutrients (33). Those individuals with severe or complicated disease may require surgical intervention (34).

A wide range of pharmacological agents are currently used in the treatment of IBD (35). These include, the mesalamine derivatives (mesalamine, sulfasalazine, olsalazine, and balsalazide), glucocorticoids (prednisolone, methylprednisolone, hydrocortisone, and budesonide), and immunomodulators (6-mercaptopurine, azathioprine, methotrexate, cyclosporine, and tacrolimus) (36). New biologics consist of monoclonal antibody therapy – TNF-α inhibitors (infliximab, adalimumab, certolizumab, and golimumab), integrin receptor antagonists (vedolizumab and natalizumab), and interleukin (IL)-12 and IL-23 antagonists (ustekinumab) which are approved for the use in IBD (36).

Other novel agents include Janus kinase inhibitors (tofacitinib), antisense oligonucleotides (mongersen), sphingosine-1-phosphate (S1P) receptor agonists (ozanimod), and anti-integrin inhibitors. Janus kinase inhibitors interfere with the signalling pathway that is required for the inflammatory process, whereas the antisense oligonucleotides prevent the translation process by binding to mRNA from which the protein is usually synthesized. S1P receptor agonists decrease the total circulating lymphocyte count, especially $CD4^{+}CCR7^{+}$ and $CD8^{+}CCR7^{+}$ T cells (36). Other experimental treatments included intravenous immunoglobulins, exclusive enteral nutrition and granulocyte colony-stimulating factors. Micro-RNAs have also demonstrated their role as disease biomarkers and could become useful for the treatment of IBD. Finally, cellular therapy is another therapeutic approach which is still under development, but aimed at severe and/or refractory CD (37).

The available treatments have several drawbacks, the most important of which is the 30% primary non-responder rate (38). Some patients transiently show a loss of response which are namely, the secondary non-responders (38). Also, the available agents are associated with serious adverse effects such as antibody formation, malignancies, reactivation of tuberculosis and hepatitis (36). Additionally, two chemokine inhibitors have undergone clinical trials to evaluate their efficacy in treating IBD, including bertilimumab which is the chemokine CCL11 – inhibitor, trialled in both, phase II CD and UC, and E6011 which is a CX3CLI – inhibitor, that is used in both phases I and II CD (36).

1.2 Chemokines CCR6 and CCL20

Chemokines are a superfamily of immune-modulatory small protein molecules, which regulate leukocyte migration to inflammatory sites through their chemoattractant properties (39). The total chemokine repertoire consists of 50 chemokines and they belong to receptor and ligand cohorts (40). Chemokines consists of four subgroups named, XC, CX3C, CXC, and CC, in which the naming is based on their receptors (41). A receptor is denoted by R, and therefore, Cysteine-Cysteine (C-C) chemokines bind with CCR chemokine receptors (42). Chemokines display a common molecular structure, having three beta-pleated sheets with an alpha helix at the carbon terminal, in which the cysteine motifs are joined by disulphide bonds. The entire chemokine is composed of 67–127 amino acid residues (42). Chemokine receptors are expressed on the cell surface and they are seven transmembrane, guanine nucleotide-linked, G1 class receptors (43). Several chemokine receptors can be activated by many ligands, whereas other receptors are activated by a single ligand (44). Chemokines play a prominent role in inflammation and the spreading of cancer and chemokine inhibition, has yielded anti-inflammatory attributes in inflammatory disorders (45).

Chemokine receptors are present on a wide range of immune and non-immune cell types (46). The C-C motif chemokine ligand 20 (CCL20), the only known monogamous

ligand which binds with C-C motif chemokine receptor six (CCR6), has been evaluated in this study as an inflammatory biomarker. CCL20 is produced in copious amounts by the gut epithelium, in response to infectious microbial penetration that attracts the $CCR6^+$ immune cells to the site of infection (47). In spite of the many varied biological functions performed by the CCR6-CCL20 axis, one of its primary functions is to aid leukocyte homeostasis in the intestines (48).

Among a plethora of functions, chemotactic navigation of effector T helper cell cohorts to the gut mucosa from lymphatics appears to be primarily a CCR6-driven mechanism, (where chemotaxis of $CCR6^+$ immune and non-immune cells occur in response to CCL20 produced by the gut epithelial cells), which synchronizes immune homeostasis during IBD pathophysiology (49). The CCR6–CCL20 axis is a prominent immune modulator in both the innate and the adaptive immune responses of a wide range of inflammatory diseases (50). It is also associated with tissue damage and injury, human immunodeficiency virus (HIV), ophthalmic disorders, lung and kidney disorders, autoimmune diseases, brain disease, arthrosclerosis, obesity, diabetes and cancer (Figure 2) (42).

1.2.1 C-C motif Chemokine Receptor 6 (CCR6)

CCR6 is denoted by a string of different gene codes, (for some which do not have expanded names), such as cluster of difference 196 (CD196), CKRL3, G - protein coupled receptor 29 (GPR29)-, CKR-L3, CMKBR6, GPRCY4, STRL22, BN-1, DCR2, DRY6, CCR-6, and C-C CKR-6. CCR6 is understood to transduce signals that mobilize intracellular calcium ion influx upon binding to its ligand, CCL20 (51). CCR6 is a commonly expressed molecule on the T lymphocyte subdivisions of TH17 and Treg cells, innate lymphoid cells-3 (ILC)-3, neutrophils, natural killer T cells (NKT) cells, macrophages, B cells, and immature dendritic cells (52).

Tissue - specific imprinting of $CCR6^+$ cell types have been identified. Given the numerous organ systems in which CCR6 is present and activated, in addition to T

helper lymphocytes (TH1, TH2, TH17 and Treg subsets), are alveolar macrophages, alveolar epithelial cells, fibroblasts, gamma-delta T cells and dendritic cells (Table 1, Figure 2) (42). CCR6 is predominantly expressed in the appendix, pancreas, lymph nodes, and spleen, with lesser expression in the foetal liver, testis, colon, small intestine, and thymus (53). Distinctively, CCR6 is thought to trigger the phosphoinositide - 3 kinase (PI3K) signal transduction cascade, which leads to phosphorylation that provides energy for cell chemotaxis (54). This receptor is important for B-lineage maturation and antigen-driven B cell differentiation, and it may regulate the migration and recruitment of dendritic cells, T and B cells during inflammatory and immunological responses (55). Among the ligand independent, biological functions of CCR6 are; (i) embryonic development (ii) angiogenesis (iii) wound healing (iv) lymph organogenesis and (v) tumour proliferation and metastasis (42).

1.2.2 C-C motif Chemokine Ligand 20 (CCL 20)

CCL20 was recognized as the principal ligand of CCR6 through calcium ion influx experiments in the first human immortalised myelogenous leukemia cell line (K562), devoid of other chemokine receptors (CCR1-5), but transfected with CCR6 (53). CCL20 has synonyms, such as LARC (liver and activation-regulated chemokine), MIP-3α (macrophage inflammatory protein), and Exodus-1. Expression of CCL20 is upregulated by intestinal enterocytes responsive to bacteria displaying flagellar movement, as well as, antigen-presenting dendritic and macrophage subsets, Langerhans cells in the skin, endothelial cells, natural killer (NK cells), neutrophils, B cells, and TH17 cells (53).

Apart from CCL20, human beta defensins (HBD), which are a group of microbicidal peptides, have been identified as additional epitopes, although this needs thorough validation (56). There is increasing evidence that the counterpart of the CCL20 ligand, HBD2, concomitantly contributes to epithelial cell migration, in maintaining intestinal epithelial barrier integrity, and as such, acts as a frontline defence against microbial

invasion (57). Vongsa *et al.*, (2009) reported equipotent functionality of HBD2 to CCL20, demonstrating that it stimulates active migration of the human intestinal cell lines; human epithelial colorectal adenocarcinoma cell line 2 (Caco2), transplantable human carcinoma cell line (T84) and non-transformed intestinal epithelioid cell line number six (IEC6), *ex vivo*. These investigations further confirmed that HBD2 can stimulate intracellular calcium influx, which innervates the PI3K signal transduction *via* mobilizing the guanosine triphosphatase (GTPase), Ras homolog family member A (RhoA), and phosphorylated myosin light chain, leading to F-actin accumulation, which is a possible canonical wound healing mechanism (57). Therefore, HBD is thought to augment immune cell patrolling, microbial defence and intestinal barrier restitution. These results significantly underpin the notion that HBD2 parallels the functions of CCL20 in its role as an additional partnering ligand of CCR6 (44).

1.2.3 Signalling Pathway Modulated by CCR6-CCL20.

Chemokines act by binding to specific cell surface receptors that are differentially expressed on diverse cell types (58). The receptors are members of a large subfamily within the seven-transmembrane domain G - protein coupled receptor superfamily (59). At the biochemical level, chemokine receptors act as guanine nucleotide exchange factors, restricted mainly to the pertussis–toxin sensitive G1 class of G - proteins (60). At the immunological level, they coordinate the development, differentiation, anatomical distribution, chemotactic migration and effector capabilities of leukocytes (61).

Cell responses to chemo-attractants typically make them sensitive to pertussis toxin, which indicates heterotrimeric G - proteins from the G1 class are coupled to the signalling pathway downstream of the receptor as shown in Figure 1 (42). Activated G - protein heterotrimers (G-alpha, G-beta, G-gamma), release guanosine di phosphate (GDP) and bind guanosine tri phosphate (GTP), which dissociates afterwards into G-beta, gamma (G$\beta\gamma$) subunit complexes and G-alpha (Gα) subunits. In leukocytes, G$\beta\gamma$ activates membrane-associated phospholipase C-β2 (PLC) and

phosphoinositide 3-kinase (PI3K) (42). PI3K catalyses phosphatidylinositol 4,5-bisphosphate (PIP_2) into phosphatidylinositol (3,4,5)-trisphosphate (PIP_3) which is subsequently converted into inositol triphosphate (IP_3) and di acyl glycerol (DAG) by activated PLC (42). IP_3 regulates the mobilization of calcium ions from intracellular stores and DAG acts in conjunction with calcium to activate various isoforms of protein kinase C (PKC) (42). Activated PKC and various calcium (Ca)–sensitive protein kinases catalyse phosphorylation, thereby activating a series of signalling events ending up in cell migration (42).

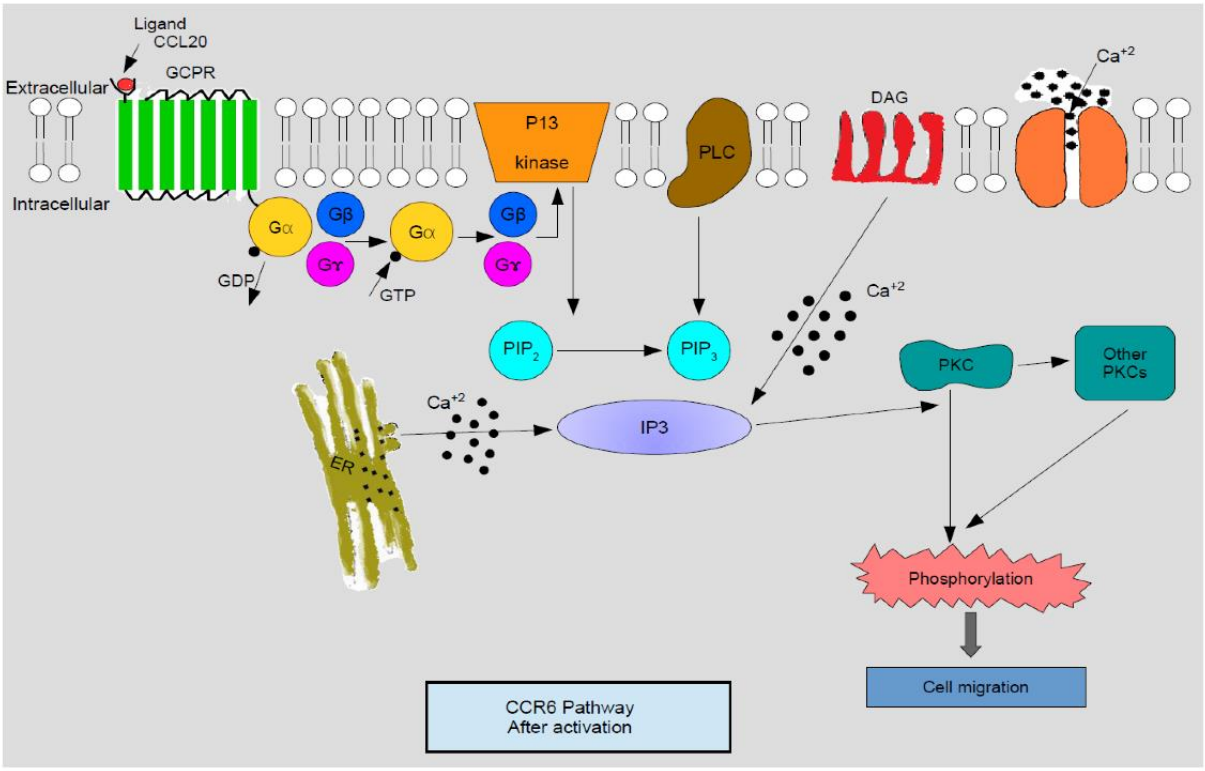

Figure 1. Schematic representation of C-C chemoattractant cytokine (chemokine) receptor 6 (CCR6) activation pathway. After binding with the ligand, G - Protein Coupled Receptors (GPCR) are activated to release the G-beta (Gβ) and G-gamma (Gγ) subunits which in turn activate PLC and PI3K. PI3K then converts PIP2 to PIP3 which activates calcium ion mobilization across IP3. IP3 with DAG stimulated by calcium ions activate PKC and other PKCs which trigger phosphorylation causing cell

migration. Legend for abbreviations: G-alpha (Gα), G-beta (Gβ), G-gamma (Gγ) — Subunits of G-protein coupled receptor (GPCR), PI3K—Phosphoinositide 3 kinase, PLC—Phospholipase Cβ2, DAG—diacylglycerol, PIP2—Phosphatidylinositol 4,5-bisphosphate, PIP3—Phosphatidylinositol 3,4,5-triphosphate, IP3—Inositol triphosphate, PKC—Protein kinase C, ER—endoplasmic reticulum, Ca+2—Calcium ions. Reproduced from Copyright 2003, CRC Press: Boca Raton, FL, USA. (40).

CCR6 and CCL20 have exhibited characteristics in line with both immune homeostasis and immune activation. It is already established that the immunological impact of this chemokine receptor–ligand partnership has far reaching consequences in health and disease that affect multiple organs of the human body (42). Several research studies have demonstrated that the CCR6-CCL20 axis directly influences the nervous, respiratory, gastrointestinal, excretory, skeletal, and reproductive systems via pleiotropic immune mechanisms, manifesting as diseases with high mortality rates as shown in Table 1 and Figure 2. Given the exclusive roles that CCR6 and CCL20 play in clinical pathophysiology, this chemokine pair is considered as a potential therapeutic target, whereby the blockade or inhibition of either partner is expected to produce successful pharmacotherapy, as a treatment for its related diseases (42). Hence the effect of gene ablation of *Ccr6* locus on secondary lymphoid organs was investigated. No studies have been conducted so far on investigating the impact of chronic colitis on other organ systems in Winnie and therefore, spleen, liver and kidneys were examined to understand the multi-system pathophysiology arising because of IBD. Further, since CCR6 plays a pivotal role in immune cell chemotaxis, the upregulation of CCL20, $PI3K^{P}$ and Akt^{P} in colon tissue during colitis was also investigated.

Table 1. Organ systems and the diseases in which CCR6/CCL20 axis is operative along with the cell types involved in the disease progression which express CCR6.

Organ	CCR6/CCL20 Axis	Cell Types Involved	Disease Produced	References
Lung	Operative	Fibroblasts, AEC, DC, T_H1, AM	IPFL, Sarcoidosis	(62), (63),(39)
Liver	Operative	T_H17, T_{reg}, (γδ) T cells	Chronic liver disease	(64),(64)
Kidney	Operative	T_H1, T_H17, T_{reg}	Glomerular nephritis	(65),(66)
Brain	Operative	T_H1, T_H17, (γδ) T cells	EAE, Stroke	(67)
Eye	Operative	T_H17	Dry eye disease	(68)
Skin	Operative	T_H17	Psoriasis	(69)
Joints	Operative	$CD25^{-}FoxP3^{+}$	Rheumatoid arthritis	(70)
Gut	Operative	T_H17, T_{reg}, T_H1	IBD	(71),(72)

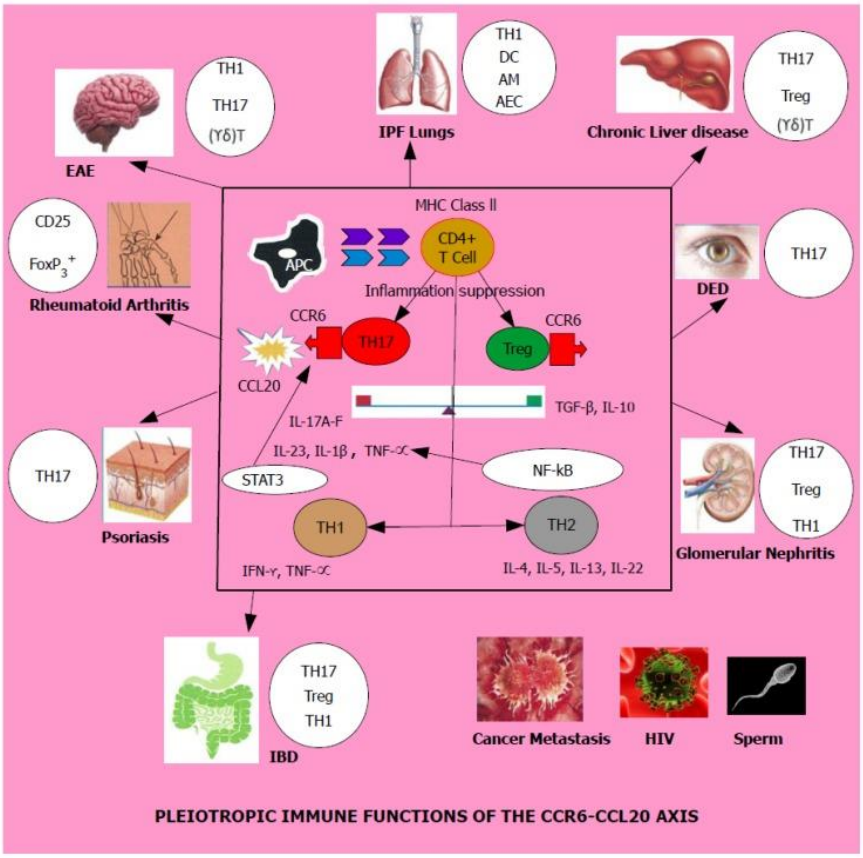

Figure 2. Schematic representation of the immunological impact of CCR6/CCL20 axis on multiple organs in the human body, with the cells involved in promoting disease given next to each organ. Experimental Autoimmune Encephalitis (EAE), Idiopathic Pulmonary Fibrotic (IPF) lungs, Chronic liver disease, Dry Eye Disease (DED), Rheumatoid arthritis, IBD, Psoriasis, Glomerular nephritis, HIV and Cancer metastasis are all diseases driven by the CCR6-CCL20 axis and disease progression leading to pathogenesis is promoted by T helper lymphocyte subsets, particularly TH17 and a decrease in Treg cells. The factors which tilt the TH17-Treg balance, influenced by transcription factors and cytokines in the tissue microenvironment are yet to be discovered. Legend for abbreviations: Experimental Autoimmune Encephalitis (EAE), Idiopathic pulmonary fibrosis (IPF) lungs, Dry Eye Disease (DED), IBD, Human Immunodeficiency Virus (HIV), APC—Antigen Presenting Cell, MHC Class II—Major Histocompatibility Complex Class II, AM—Alveolar

Macrophages, DC—Dendritic Cells, FB—Fibroblasts, AEC—Alveolar Epithelial Cells, CCR6—Chemokine receptor 6, CCL20—Chemokine ligand 20, IL—Interleukin, T helper lymphocyte 1, 2 and 17 (TH1, TH2, TH17), Treg—Regulatory Treg cells, (γδ) T cells—gamma delta T lymphocytes, NF-kB—nuclear factor kappa B, STAT3—signal transducer and activator of transcription 3. TNF-α—tumour necrosis factor-alpha. (42).

Sixteen tractable inhibitors of CCR6 and its sole ligand, CCL20 have already been identified (Table 50), (Figure 3) and some have even undergone clinical trials for the treatment of several autoimmune disorders such as experimental autoimmune encephalitis (EAE), rheumatoid arthritis (RA) and psoriasis (73). No such clinical trials have been performed with the existing inhibitors to date in IBD, which is also considered by some as an autoimmune disease.

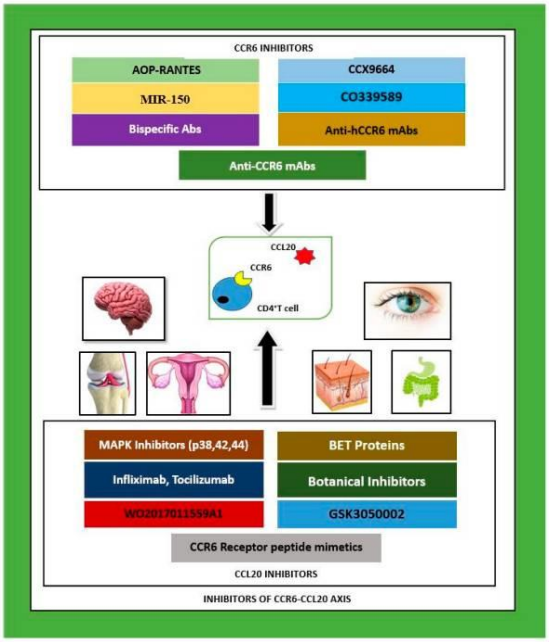

Figure 3. CCR6–CCL20 axis inhibitors investigated in pre-clinical and clinical studies to date *as* possible therapeutics for autoimmune and inflammatory diseases in multiple organ systems: nervous, skeletal, integumentary and gastrointestinal systems. CCR6 inhibitors are given above as a cluster, and CCL20 inhibitors are given below as a cluster. Legend: MAPK—mitogen activated protein kinase, p—protein,

CCL20—CC chemokine ligand 20, mAbs—monoclonal antibodies, CCR6—CC chemokine receptor 6, hCCR6—humanised CCR6, Abs—antibodies, IL—interleukin, BET—bromodomain extra-terminal proteins, R—receptor, MIR-150—micro ribonucleic acid-150, AOP-RANTES—amino oxypentane regulated on activation, normal T cell expressed and secreted (73).

1.3 Role of CCR6-CCL20 in Gut Immune Function

CCR6 plays an exclusive role in facilitating chronic colitis (42), (53), (74). It makes a significant contribution to T cell differentiation and helps to establish the TH1/TH2 and TH17/Regulatory T cells (Treg) imbalance paradigms in IBD (75). The principal mechanisms of adaptive immunity encompass $CD4^+$ T cells and its subsets in enforcing immune activation in the gut (76). Naïve TH0 helper cells are transformed into effector T helpers upon antigen - sampling by dendritic cells and / or macrophages in the mesenteric lymph nodes. The effector T helpers consist of four congenial immune subtypes: TH1, TH2, TH17, and regulatory Treg cells. Thus, recent interest has been focused on the two subgroups of TH17 and Treg cells in the immune induction of IBD (76).

These two subgroups of T helper lymphocytes have demonstrated distinctively opposing functional roles, primarily attributed to their different cytokine profiles, represented by inflammation-triggering - IL-17 and inflammation-dampening - IL-10, respectively (40). TH17 induces disease activation by releasing inflammatory cytokines leading to tissue damage, while Treg cells promote immune tolerance, induced by inflammation-suppressive cytokines which aid tissue restitution (77). The underlying mechanisms favouring these two opposing roles are not yet clear, but the expression of CCR6 is considered the cardinal determinant in their selective proliferation to maintain immune homeostasis (74). Immune homeostasis is maintaining the immune responsivity and the ability to overcome disease manifestation by sustaining the fine balance between both inflammation and resolution. This underpins the concordant, yet enigmatic role that CCR6–CCL20 axis

performs in primarily resolving the IBD immune mechanisms, also by promoting immune tolerance. Immune tolerance is the ability to suppress disease symptoms and defend against all the factors which promoted disease manifestation in the individual. The discovery of factors which skew the selection of TH17 and Treg cell polarization in the gut mucosa would be a significant breakthrough in IBD therapy (74).

Multiple cytokines and transcription factors serve to upregulate CCR6 expression on the TH17 cells (78). Transforming growth factor-beta sulphate (TGF-β), interleukin (IL) - 6, IL-17, IL-21 and IL-23, as well as the lineage-selective master transcription factors, retinoic-acid-receptor-related orphan nuclear receptor gamma t (RORγt) and retinoic-acid-receptor-related orphan nuclear receptor alpha (RORα), are important regulators in upholding the immune induction of CCR6, which is the hallmark of the TH17 cell cohort and they are strongly associated with autoimmune diseases (53). IBD invariably falls under the direct influence of the pro-inflammatory apparatus driven by CCR6, including the TH17 cell differentiation and proliferation (77). Well-documented studies report that neutralizing IL-17 as well as TH17 cells lacking CCR6 receptors, serve to markedly inhibit several autoimmune disorders (79). CCR6 is a double-edged sword because of its additional ability to mobilize the immune-suppressive T cell population consisting, the natural regulatory Treg cells induced by the transcription factor FoxP3. The Treg cells are highly effective in modulating autoimmune disease progression by actively suppressing pro-inflammatory T cell proliferation (80).

Concomitantly, CCR6 drives chemotactic recruitment of TH17and Treg cell subsets to sites of infection in a self-sustained feedback loop, because TH17 cells also could express CCL20, induced by the cytokines TGF-β and IL-6 and the transcription factor, STAT3 (81). Given the dubious role played by CCR6 in disease amelioration, there remain a repertoire of hitherto unidentified factors (82). They are chemokines, cytokines, adhesion and costimulatory molecules and a collection of innate immune induction factors which are associated with CCR6 immunity and contribute towards

the selective mobilization of TH17 cells versus Treg distribution, at the sites of inflammation (82). The most recently introduced immunological concepts about IBD links the deregulated TH17 and Treg axis as the pivotal point which decides the fate of IBD resolution (78).

Research from different groups have conferred opposing roles to TH17 and regulatory Treg cells in inflammatory disease (74). IL-23 - induced TH17 differentiation is known to promote inflammation and intriguingly, TH17 cells also release CCL20, the chemokine ligand of CCR6. With either an autocrine or paracrine secretion of CCL20, TH17 cells also trigger a self-perpetuating cycle at inflammatory locations in a positive feedback loop (74). The IL-17 production also induces TNF-α and IL-1β, pointing towards an inflammatory pathway involving the nuclear transcription factor, NF-kB (74). The $FoxP3^{+}$ bearing regulatory Treg cells are primarily disease suppressive in function and promote disease resolution by downregulating the pro-inflammatory T cell proliferation induced by TGF-β and IL-10 production (42).

CCL20 can be induced in several cell types by lipopolysaccharide (LPS) and could be stimulated and up-regulated by the inflammatory cytokines; interleukin 1 alpha (IL-1α) and tumour necrosis factor – alpha (TNFα) during acute inflammation (83). CCL20 expression is constitutively up-regulated by other inflammatory cytokines, namely, gamma interferon (IFN-γ), interleukin 1-beta (IL-1β), IL-17, IL-21 (84). In contrast, IL-10, which is anti-inflammatory, downplay the CCL20 expression which does not favour the accumulation of regulatory T cells, particularly at inflammatory locations (83). IL-4, IL-22 and surprisingly, IL-23 have reported insignificant stimulatory effects on CCL20 expression (83). CCR6 confers an antagonistic function in the TH17 and Treg cells, although it is unknown what other factors are responsible for tipping the balance in favour of disease progression (40). The CCR6-CCL20 axis remains the pivotal point which determines reciprocal generation of these two cell types (TH17 and Treg), but simultaneously highlights the importance of CCR6 in T cell migration (52).

A disrupted CCR6-CCL20 axis only leads to the development of inflammation because CCR6 is adequately expressed on regulatory T cell populations in the cure phenotypes (85). A study involving the transfer of "wild type" TH17 cells and CCR6 - deficient T cells into a "$Rag1^{-/-}$ severe combined immune deficient (SCID) mice" resulted in extreme intestinal inflammation and a subsequent reduction in TH17 and Treg populations occurring (85). CCR6 expression is deemed to be critical to Treg cells than to TH17 cells, because this subset suppresses pro-inflammatory T cell proliferation and promotes disease resolution (86). However, research documented so far has failed to identify the exact role played by CCR6 in inflammation and immune homeostasis (86).

1.3.1 Immunologic Pathways Linking CCR6-CCL20 Axis to IBD Pathogenesis

A person afflicted with one immune-mediated affliction, will also run a high risk of contracting another disease of the same type (87). This overlapping aetiology is attributed to common clinical and immunological parameters concomitantly shared by those disorders (87). It led us to a systematized examination of the various immune-activation pathways involving the chemokine receptor 6, as shown in Figure 4 as well as Table 2 that culminate in immune-mediated disease pathogenicity in IBD (53).

Table 2. Different CCR6-driven immune pathways, their mechanisms, and disease outcomes.

Pathway	Link to CCR6	Mechanism	Outcome	Ref
T_H1/T_H2	$CCR6^+$ T_H1 cells	Migration of $CCR6^+$ T_H1 cells to the intestine, attracted by CCL20 produced by the IEC and their release of proinflammatory cytokines induces inflammation in the intestine.	Inflammation	(87)

T_H1/T_H17	CCR6$^+$ T_H17 cells	Induced by IL-23, RORγt, and TGF-β, T_H17 cells, upon differentiation, release IL-17A–F, which drives CCR6$^+$ T_H17 cell recruitment towards the intestinal epithelium, attracted by CCL20 produced by the IEC.	Inflammation	(88) (89)
T_H17/T_{reg}	CCR6$^+$ T_{reg} cells	Induced by TGF-β and FoxP3, regulatory T_{reg} cells, after differentiation, release IL-10, which drives CCR6$^+$ T_{reg} cells towards the intestinal epithelium, attracted by CCL20 produced by the IEC.	Resolution	(90) (91)
IL-23/IL-17	CCR6$^+$ T_H17	IL-12, STAT3, and IL-23-induced CCR6$^+$ T_H17 cells migrate towards the intestinal epithelium, stimulated by IL-17A–F and attracted by CCL20 produced by the IEC.	Inflammation	(92) (90)
Akt/ERK-1/2	CCR6$^+$ T_H17/T_{reg}	CCL20 activates Akt/ERK-1/2 and SAPK/JNK MAP kinases to increase cell proliferation and cell mobilization in the intestinal epithelium.	Homeostasis	(93)
ILC	CCR6$^+$ NCR$^+$ ILC3	Induced by IL-22, CCR6$^+$ NCR$^+$ ILC3 release IL-12 and activate IFN-γ-producing ILC1 cells.	Inflammation	(94) (95)
		IL-23-producing ILC1 activate NCR$^+$ ILC3 to express MHC class II epitopes to initiate transformation of naïve T helper cells into effectors.	Inflammation/Resolution	
		Induced by IL-22, CCR6$^+$ ILC3 migrate to Peyer's patches, attracted by CCL20 produced by the IEC. Decrease in IL-22		

		results in loss of immune tolerance.		
T_H9/T_H2	$CCR6^+$ T_H9 cells	Induced by retinoic acid, TGF-β and IL-10 released by ILC3 effect differentiation of T_{reg} cells in the intestine.	Inflammation	(96) (97)
		Induction by IL-9 elicits antiparasitic or allergic immunity, evoking a T_H2-type immune response.		

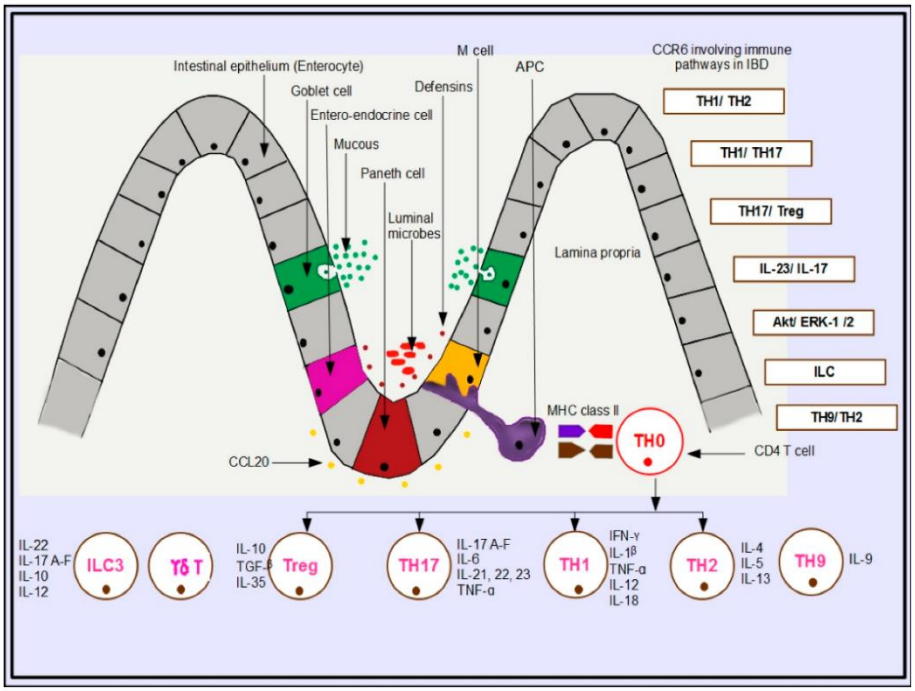

Figure 4. Schematic representation of the CCR6-involving immune pathways in IBD in the gut mucosa and priming of naïve CD4 T cells into effectors in mesenteric lymph nodes with their associated cytokines. Legend: APC—Antigen Presenting Cell; TH—T helper lymphocyte; M—Microfold Cell; Treg—Regulatory Treg Cell; ILC3—Innate Lymphoid Cell 3; MHC Class II—Major Histocompatibility Complex Class II; γδ T—Gamma delta T Cell. (53).

1.3.2 Specific Pathological Changes Caused by CCR6-Deficiency in Colitis

The small intestine is the primary site of inflammation as it is exposed to a significant load of bacterial antigens and nutrients (42). It is covered by a single layer of epithelium, containing epithelial cells, Paneth cells, entero-endocrine cells, microfold (M) cells, and mucous-secreting goblet cells (98). Most of the immune action takes place in Peyer's patches, where the follicle-associated epithelium (FAE) is crossed by antigen samplers, which stimulate naïve T and B cells to develop into effectors (98). Effector T and B lymphocytes are always found patrolling the mucosal surfaces in the gut during inflammation which helps the intestinal mucosa to maintain a healthy protective immune response to the numerous colonies of symbiotic microbes present within the gut (99).

Gut tolerance mainly occurs in Peyer's patches and isolated lymphoid follicles (40). Antigen uptake in the gut-associated lymphoid tissue (GALT) mostly occurs via M cells in the FAE in Peyer's patches by dendritic cells (100). The CCR6-bearing dendritic cells are attracted towards CCL20-producing epithelial cells and thus migrate towards the mucosa-associated connective tissue, the lamina propria (LP), to activate naïve T and B lymphocytes (101). Primed effector cells drain out of afferent lymphatics to the mesenteric lymph nodes, from where they enter the thoracic duct and then join the bloodstream and return through the network of vessels back to the intestinal mucosa (102). The activated T helper cells stimulate naïve B cells into antibody-producing plasma cells. The antigen-primed B lymphocytes are transformed into class-switching B plasma cells that secrete IgA in the gut mucosa upon antigen presentation and activation by dendritic cells (103).

The CCR6-deficient models have displayed an overall change in the architecture of the intestinal epithelium, with smaller Peyer's patches, a lesser number of subepithelial domes, absence of isolated lymphoid follicles, few intestinal M cells, and high resistance to bacteria which enter through M cell conduits (104). Other significant

IBD-relevant responses included, marked elevation in the number of TH17 cells in the spleen and lymph nodes, low preference for migration to inflamed sites, and less suppressive capabilities of Treg cells (74). The other evidence included [Dextran Sodium Sulphate (DSS) - and Trinitrobenzene Sulphonic Acid (TNBS)] - induced colitis producing moderate and severe disease, respectively, in CCR6-deficient mouse models and the reconstitution of $Rag2^{-/-}$ SCID mice with naïve T cells from healthy mice resulting in acute inflammation (105).

Typical histological changes induced by DSS in mouse models include; mucin and goblet cell depletion, epithelial erosion and ulceration (106). Further, DSS induced an influx of neutrophils into the lamina propria and submucosa. Chronic DSS colitis resulted in mononuclear leukocyte infiltration, crypt architecture disarray and a widening of the gap between the base of the crypt and muscularis with deep mucosal lymphocytosis (106). DSS-treated CCR6 knockout mice had remarkably reduced intestinal pathology (shortening of the long axis of intestine, thickening of intestinal wall) particularly as they showed recovery in between DSS-free periods (106). They also showed accumulation of TCR$\alpha\beta$ cells in the gut mucosa with a significant elevation of mRNA by many folds in $CD8^+$ T cells compared to $CD4^+$ at the beginning of DSS treatment (106). Interestingly, in DSS-treated $CCR6^{-/-}$ mice, there was no major difference in these T cell populations during the acute phase of colitis although in the WT the numbers decreased drastically. It points to CCR6 being needed for trafficking and limiting T cell populations into the intestinal mucosa during acute IBD. It is widely accepted that CCR6 plays a key role in the mobilization of T lymphocytes, highlighting the mobilization of pro-inflammatory cell types in the intestines. The accumulation of TCR$\alpha\beta$ lymphocytes in the gut during colitis reported by Varona *et al*., further supports this observation. However, WT mice otherwise resistant to TNBS - induced colitis became more susceptible to TNBS when CCR6 was deleted (106).

Mouse models of acute colonic inflammation, however, are conflicting in their results. In the TNBS model of colitis, $CCR6^{-/-}$ mice developed severe colitis compared to WT

mice (40). In a third widely used classical model of colitis induced by T cell transfer, naïve T cells from CCR6$^{-/-}$ mice transferred into *Rag2*$^{-/-}$mice caused a very severe colitis compared to CCR6$^{+/+}$ transferred T cells (40). In this model, CCR6$^{-/-}$ T reg cells displayed less suppressive capabilities and reduced migration to the site of inflammation compared to WT Treg cells. This indicates that the protection from colitis is offered by a novel colon-homing, IL-10-producing CCR6^{+} regulatory T cell population (40). Using a T cell-depletion model of colitis, it was demonstrated that TH17 cells accumulated in great numbers in the small intestine when a strong T cell receptor stimulus was present. More importantly, it was established that this TH17 accumulation was dependent on the CCL20-CCR6 axis and that these TH17 cells, interestingly, acquired an immunosuppressive phenotype in the gut, rather than the typical inflammatory phenotype associated with this cell subset (40). This was determined when the accumulated TH17 cells were able to suppress carboxyfluorescein succinimidyl ester (CFSE) - labelled responder T cells (CD4^{+}CD25^{-}) in an *in vitro* suppression assay and prevented the establishment of EAE in experimental transfer models (*in vivo*). The likely mechanism of these cells is through the secretion of the immunosuppressive cytokine IL-10 (40).

Chemokine-directed migration of leukocyte subsets are thought to contribute to the qualitative differences between systemic and mucosal immunity (40). An early study had demonstrated that in mice lacking CCR6, dendritic cells expressing CD11c and CD11b were absent from the subepithelial dome of Peyer's patches (49). These mice also had an impaired humoral immune response to orally administered antigen and to the enteropathy rotavirus (49). In addition, CCR6 (-/-) mice have a 2-fold to 15-fold increase in cells of certain selected T lymphocyte populations within the mucosa (49). By contrast, systemic immune responses to subcutaneous antigens in CCR6 (-/-) mice were normal. These findings demonstrate that CCR6 is a mucosa-specific regulator of humoral immunity and lymphocyte homeostasis in the intestinal mucosa (49).

1.4 Importance of Winnie as an Experimental Mouse Model

Around sixty six different animal models classified under different approaches have been used to date, to analyse and understand the complex mechanisms which cause pathogenesis in IBD as well as develop novel therapeutic regimes (107). Most of the IBD mouse models are genetically engineered to carry a deletion (Knockout – KO) or a mutation in the gene of interest (Knock in – KI) and are useful for investigating a targeted mechanism. However, most of their inflammatory phenotype had been generated either through single mutations, immunologic manipulations or with exposure to noxious substances which is not the case in humans where multiple genetic, microbial and environmental factors come into play. Therefore, there is a need for spontaneous animal models that resemble the multifactorial nature of the human disease (108).

Winnie mice display immune responses through a threefold increase of immune cells in the colon compared to WT mice, with a significant increase in mucosal cytokine secretion in the gut and produced disease like that of human UC (109). By crossing Winnie mice heterozygous for *Muc2* (m/+) and *Ccr6* (CCR6+/-), we have induced a mild, chronic colitis, which strongly resembled human UC in Winnie x *Ccr6*-/-, which was also homozygous recessive for *Muc2* and *Ccr6* (Figure 5). To begin with, we mated male Winnie m/m with *Ccr6* -/- Winnie females, to produce offspring having the genotype Winnie m/+ *Ccr6* +/- (which is heterozygous for Winnie and heterozygous for *Ccr6*). From mating these heterozygous Winnie mice, we obtained mice having the Winnie m/+ *Ccr6* -/- genotype. We then mated male Winnie m/+ *Ccr6* -/- with female Winnie m/+ *Ccr6* -/- which produced, Winnie m/m, *Ccr6* -/- mice. Thereafter the male Winnie m/m, *Ccr6* -/- were mated with female Winnie m/m *Ccr6* -/-, which produced Winnie m/m, *Ccr6* -/-, which is the experimental model, the double homozygous recessive (Winnie x *Ccr6*-/-).

Chronic colitis in Winnie is caused by a primary epithelial cell defect that is activated by a (point) missense mutation in the *Muc2* gene, which resulted in aberrant mucin-2

biosynthesis (110). This has led to endoplasmic reticulum stress in the intestinal goblet cells which had produced, a decrease in the secretion of mucus (111). Winnie mice display symptoms of diarrhoea, ulcerations, rectal bleeding and pain at different stages of colitis synonymous with human disease (112). Exhaustive studies conducted in Winnie have proven it to be the best available murine model to study human chronic colitis and its pathogenesis (111).

Winnie, our model of spontaneous colitis, produces chronic intestinal inflammation caused by endoplasmic reticulum (ER) stress evident by the reduced number of goblet cells, a depleted mucous layer, increased crypt proliferation and apoptosis (110). Intestinal permeability is thus increased, by enhanced susceptibility to luminal inflammation-inducing toxins (110). Disease severity increases with age and is more pronounced in the proximal colon, accompanied by activation of TH1 and TH2 cytokines, IFN-γ, TNF-α and IL-13 (109).

Winnie displays both innate and adaptive immune responses, with a threefold increase of colonic lamina propria mononuclear cells: CD4, CD8, T cells, B cells and CD11b and CD11c, compared to WT mice and also showed a significant increase in the mucosal cytokine secretion: IL-1β, IL-12/23 p40 and IL-17 (110). Winnie also provides evidence of the immune deviation from TH1/TH2 control towards enhanced IL23/Th17 by expressing increased mRNA for the TH17 signature genes: *Il-17a*, *Il-17f*, *tgfβ* and *Ccr6* (110). However, skewing the immune response towards IL-23/TH17 is a recently emerged pathway in IBD with the concordant contribution of TH17 cells to enhance inflammation and produce disease like human UC (113). This study has therefore become highly clinically relevant in most aspects.

In summary, the typical functions of the chemokine receptor CCR6 include immune regulation by manoeuvring cell chemotaxis and selective delimiting of the pro-inflammatory T_H17 and regulatory T_{reg} subsets during chronic or acute systemic inflammation (73). Inhibition of CCR6 is proposed to attenuate disease symptoms and promote recuperation of multiple inflammatory and autoimmune disorders (73). The

development of *Ccr6*-inhibition therapeutics is still at an early experimental stage and has mostly involved the utilization of pre-clinical models and neutralizing mono or polyclonal antibodies against either partner (CCR6 or CCL20) (73). Other methods include the constitutive use of small molecules as peptide inhibitors or small interfering ribonucleic acid (siRNA) to interfere with transcription at the nuclear level (114). A multitude of antibody preparations are already available in the current pharmaceutical market as patented treatments for diseases in which the CCR6–CCL20 axis is operative, yet they must be used only as supplements with existing routinely prescribed medication as they collectively produce adverse side effects (115). Novel inhibitors are needed to evaluate this invaluable therapeutic target which holds much promise in the research and development of appropriate remedies for inflammatory diseases.

CCR6, is a chemokine receptor that is abundantly expressed by a variety of immune and non-immune cells (39). CCR6 binds CCL20, although members of the β defensin family also bind CCR6 with a lower affinity (57). In addition to the gut, CCR6 positive cells, and the chemokines, CCR6 and CCL20, have been detected in numerous organs, especially the secondary lymphoid organs (42). CCL20 is selectively made by the follicle-associated epithelium (FAE) overlying Peyer's Patches (PPs) and isolated lymphoid follicles (ILFs) (47). CCL20 contributes to the recruitment of CCR6-expressing cells to these structures (47). In humans, CCR6 and/or CCL20 have been implicated in the pathogenesis of inflammatory bowel disease and a wide spectrum of disorders involving many organ systems (42). It suggests that CCL20 and CCR6 have a role in inflammatory diseases, by recruiting TH1, TH2, TH17 and Treg cells to target tissues and the manifestation of IBD (65).

1.5 The Reasons for Undertaking this Study

1.5.1 Aims of this Study

Aim 1: Understand the functional role of *Ccr6* in spontaneous IBD by assessing its impact on multi system pathophysiology.

Aim 2: Understand the functional role of *Ccr6* in the immunology of spontaneous IBD.

Aim 3: Understand the functional role of *Ccr6* in relation to molecular signalling in spontaneous IBD.

1.5.2 Rationale of this Study

The impact of CCR6 in IBD has not been comprehensively studied and its exact immunological behaviour has not been elucidated. Therefore, we have investigated the effect of *Ccr6* gene ablation in a model of spontaneous colitis to evaluate the murine immune profile, which will indicate: (i) reduced leukocyte migration to inflammatory locations and hence, (ii) reduced release of pro-inflammatory mediators at the sites of inflammation, which is expected to produce (iii) reduced mucosal inflammation leading to subsequent disease amelioration. CCR6 plays an exclusive role in facilitating chronic colitis (111). It makes a significant contribution to T cell differentiation and helps to establish TH1/TH2 and TH17/Treg cell imbalance paradigms (111).

1.5.3 Hypothesis

The central hypothesis of this study was that the loss of CCR6 will ameliorate inflammation in the murine model of spontaneous colitis, Winnie x *Ccr6*-/-. This study was conducted to investigate the therapeutic potential of CCR6 in this model, where our results showed a considerable reduction in colitis.

The usefulness of this study is threefold; as the Winnie mouse model is a spontaneous colitis model which mimics human UC, the genetic deletion of *Ccr6* is expected to

ameliorate disease symptoms by reducing inflammation in the colon. Hence, CCR6 provides us with a possible manipulative therapeutic target in IBD.

1.5.4 Anticipated Benefits

The anticipated benefits of this study are the existing compelling evidence that CCR6 has multiple immune functions in many organ systems of humans and is considered a valuable therapeutic target (Figure 2, 3) (42) (73). From preclinical studies, it is hoped that the immune cell triggers or pathways that arise from CCR6 activation could be identified (53). These results could then be translated into clinical trials which target the neutralization of CCR6 or its associated cytokines/ products /mediators in human colitis.

Winnie, a tested and proven model of murine spontaneous colitis which closely resembles human UC, was used in which the *Ccr6* gene was knocked out. We determined clinical, histological and immunological parameters at two timepoints (8 weeks of age and between 16-22 weeks of age), which delineates the impact of CCR6 - deficiency in terms of its potential to become a proactive drug target.

Additionally, we have investigated the sequel of CCR6 deficiency in multi-system pathophysiology with the spleen, liver and kidneys, to identify a link between the gut and other organs which may become inflamed due to microbial dysbiosis that most commonly, stems within the enteric system. We have also quantified the percentage expression of three biomolecules (CCL20, phosphorylated PI3K and phosphorylated Akt) which are downstream targets in the CCR6-related immune signalling pathways (116). These preliminary findings are expected to open avenues to a more detailed examination of CCR6 immunobiology and physiology in order to evaluate the impact of CCR6 inhibition as a treatment option for IBD.

2.0 Materials and Methods

2.1 Experimental Mice

The mice used in this research project were imported from the Jackson Immuno Research Laboratories, Inc. PA, USA and obtained through the Animal Resource Centre (ARC) and bred directly at the Cambridge Farm Facility (CFF) of the University of Tasmania (UTAS). The mice were re-derived and bred at a specific pathogen-free facility at the CFF and transported to the Menzies Institute for Medical Research, Hobart, affiliated to UTAS which has a PC2 animal facility. Mice utilised were all aged between 8- 22 weeks and were genotyped by the Transnetyx, Automated Genotyping PCR services (www.transnetyx.com). The experimental mice genotypes are listed in Table 3. All animal procedures were approved by the Animal Ethics Committee of the University of Tasmania (Ethics Permit A 17451) and were conducted in accordance with the Australian code for the care and use of animals for scientific purposes 8th edition of 2013 guidelines set out by the National Health and Medical Research Council of Australia.

The breeding strategy was begun with two main mouse groups, namely, the Winnie mouse group and the CCR6 mice group. They were bred and maintained on a C57BL/6J background. C57BL/6J is a mouse strain and both the Winnie mice and the CCR6 mice were bred up to ten generations on this parental strain to eliminate genetic drift, before our experiments started.

C57BL/6J-derived Winnie, homozygous recessive for *Muc2* indicated by (m/m) but homozygous dominant for CCR6 indicated by (*Ccr6*+/+) was crossed with C57BL/6J-derived CCR6 mice, homozygous recessive for CCR6 (*Ccr6*-/-) but homozygous dominant for Winnie (+/+), produced Winnie heterozygous (het) mice, which were (*m*/+) (*Ccr6*+/-), then crossed to obtain Winnie (m/m, *Ccr6*-/-) males and females from which the Winnie x *Ccr6*-/- (m/m, *Ccr6*-/-), the double knockout model was obtained (Figure 5).

However, the mice utilised in this study were obtained from several litters although some mice in each of the four groups were littermates. The reason is, that from mating a breeding pair, most often the offspring produced are few in number such as 5-6 pups, which do not suffice for this research study. Therefore, we had to include mice produced from other similar breeding pairs as well. Since these mice were housed in the same aseptic environment and were fed with the same diet, we did not expect them to carry vastly different colonies of microbiota in their gut. Another fact which is worth mentioning is that when the parents of the experimental model are crossed, the chance of getting this genotype is rare.

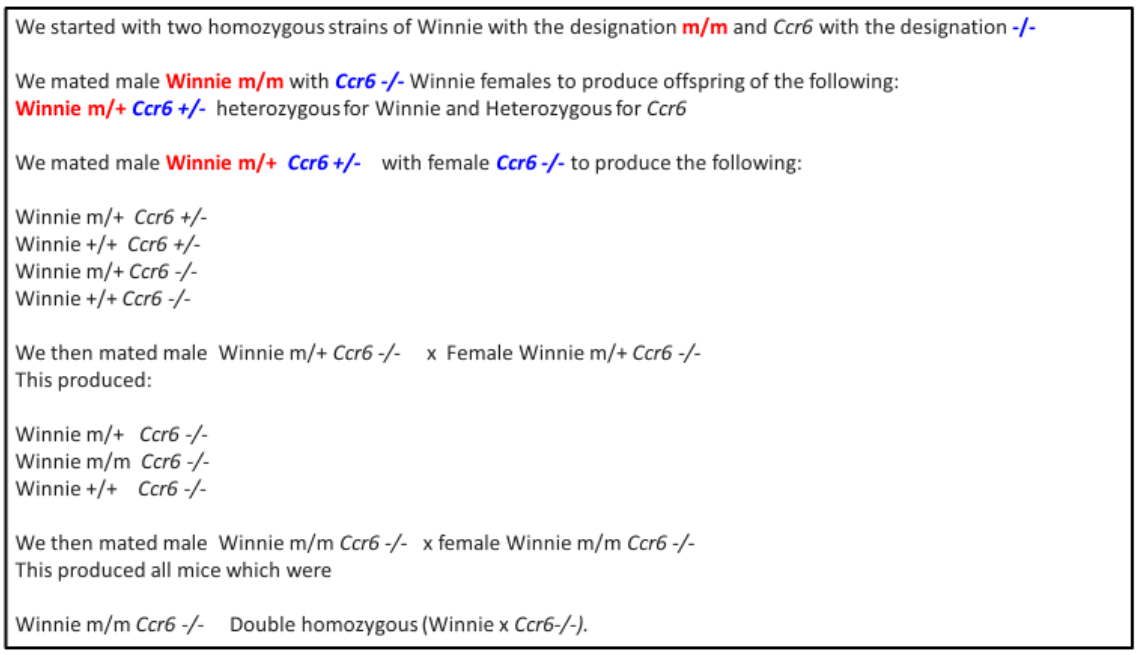

Figure 5. The breeding strategy of the experimental mouse model, Winnie x *Ccr6*-/-.

Table 3. The mice genotypes utilised with a description of the phenotype, numbers culled and their role in the research project. Tissues were harvested for analysis at 8 weeks and 16-22 weeks of age, respectively.

Mice genotype (Winnie / *Ccr6*)	**Age**	**Phenotype**	**Number**
C57BL/6J (WT) *(+/+, +/+)*	8-22 weeks	Healthy control	16
Ccr6-/- *(+/+, -/-)*	8-22 weeks	Targeted knockout	16
Winnie (m/m, +/+)	8-22 weeks	*Muc2* mutation	16
Winnie x *Ccr6-/-* (m/m, *-/-)*	8-22 weeks	*Muc2* mutation and targeted knockout for *Ccr6*	16

2.2 Data Collection

The phenotype was assessed using pre-clinical parameters of each group of mice. The body weight was recorded prior to culling and after comparing the mouse number and the ear-clip description. The mice were culled using carbon dioxide euthanasia for 6 minutes at 0.4 foot-pound (foot-lb). Having determined the mouse was dead by testing for corneal reflex, tail and toe pinch and rolling reflexes, the mice were dissected under sterile conditions. The spleen, kidneys and liver were harvested and weight of each was recorded. Both the kidneys were weighed together. Spleen was

stored in 10 mL of ice-cold phosphate buffered saline (PBS; pH 7.4- Dulbecco's, 10 x L, Gibco, Life Technologies Pty Ltd, Victoria, Australia) on ice for 2 hours after which it was processed for analysis by flow cytometry. Spleen, liver and kidneys were stored in 10% neutral buffered formalin and transferred into 70% ethanol after 48 hours. Mesenteric lymph nodes were harvested and stored in ice-cold RPMI 1640 culture medium (Life Technologies Pty Ltd, Victoria, Australia). The large intestine was separated at the ileo-caecal junction and the anus and placed on a non-absorbent surface. The length of the colon was measured from the caeco-colic junction to the anus and was recorded. The whole colon was cut open along the longitudinal axis, faecal matter removed, and weight was recorded. One half of the colon cut length wise was rolled around a sterile toothpick from the proximal colon to the distal colon end and made into a Swiss roll, fixed to a small piece of regiform and preserved in 40 mL of 10% neutral buffered formalin. It was transferred into 70% ethanol after 3 days. The other half of the colon was cut in the middle into proximal and distal colon and each was cut into half again. Pieces of fresh colon tissue were immediately frozen in a DNase and RNase-free Eppendorf tube at minus 20 degrees centigrade and later transferred to minus 80 degrees centigrade for RNA extraction for analysis by real-time polymerase chain reaction (RT-PCR).

2.3 Flow cytometry

Mouse spleen and MLN were macerated using the end of a 10cc syringe plunger with ice-cold PBS and passed through a 70 μ corning cell strainer (Catalogue No. 08-771-2, Thermo Fisher Scientific Pty Ltd, Victoria, Australia) to prepare a homogenous suspension of 20 mL which was centrifuged at 500g for 10 minutes at 4°C (Allegra X15R Beckman Coulter, USA) to obtain a cell pellet. The red blood cells (RBC) were removed from splenocyte suspensions by adding 1 mL of x 1 RBC lysis buffer (Catalogue No. 420301, Australian Biosearch Pty Ltd, Wangarra, WA, Australia) for 2 minutes at 25°C in the dark, after discarding the supernatant. Ice-cold PBS was added up to 25 mL to inactivate the RBC lysis buffer and centrifuged at 500g for 7 minutes at

4°C. 10 mL of FACS buffer (Table 4) was added to the RBC-free splenocyte samples, vortexed to mix and kept on ice. 10 µl of the suspension was mixed with 10 µl of trypan blue and the number of cells were enumerated using a haemocytometer taking the average cell count by counting the cells in the 4 corners and centre squares of the grid. Around 2 x10^7 cells per mL was adjusted by adding FACS buffer. 1 mL of this prepared sample was centrifuged at 500g for 7 minutes in a microcentrifuge to obtain a cell pellet. The supernatant was discarded and 40 µl of fluorescent conjugated antibody (Table 5) was added and vortexed briefly to mix and incubated on ice in the dark for 30 minutes. The cells were washed in 0.5 mL of PBS at 500g for 7 minutes. The supernatant was discarded and 300 µl of FACS buffer was added, vortexed and flow cytometric data was obtained using a BD FACS CANTO™ flow cytometer (BD Biosciences, USA) and analysed using FCS Express version 6.06.0014 (De Novo Software, USA) for windows. Mesenteric lymph node suspensions were processed in the same way, without the addition of RBC lysis buffer.

Table 4. Composition of FACS Buffer used in flow cytometry assays.

	1000 mL PBS X1
FACS Buffer	10% BSA
	0.1% Sodium Azide

Table 5. List of flow cytometry antibodies used.

Antibody	Manufacturer	Catalogue Number	Fluorescent conjugate	Dilution
CD4	Australian Biosearch	100443	Brilliant Violet 421	1:200
CD8	Australian Biosearch	100723	Alexa flour 488	1:200
CD19	Australian Biosearch	152408	PE	1:200
Live/Dead Cell Stain	Invitrogen	L-34975	IR 633-635	1:50

2.4 Real Time Polymerase Chain Reaction (RT-PCR)

2.4.1 RNA Extraction

Colon tissue less than 30 mg in weight was crushed and homogenized using a plastic disposable tip and RNA was extracted using Qiagen RNeasy mini kit (50) (Catalogue No. 74104) following the manufacturer's protocol. 100 µl of RNA was eluted using a spin column and purity of eluted RNA was determined using the ratio of absorbance at 260nm/280nm using an Eppendorf Bio Photometer (Eppendorf). Samples above 2 were utilised for RT-PCR.

2.4.2 Complementary DNA (cDNA) synthesis from RNA

Complementary DNA (cDNA) was synthesized from RNA samples using a High Capacity cDNA Reverse Transcription Kit (Catalogue No. 4368814, Thermo Fisher Scientific Australia Pty Ltd, Victoria, Australia) using the reaction conditions (Table 6 and 7) suggested by the manufacturer. 100 ng of cDNA from each sample was added to a PCR reaction including TaqMan Fast Master Mix (Catalogue No. 4444557, Thermo

Fisher Scientific Australia Pty Ltd, Victoria, Australia) and a single gene-specific primer set supplied in the kit.

Table 6. Recipe for the cDNA Master Mix and per reaction.

Ingredients	**Volume /Reaction (µl)**
10X RT Buffer	2.0
25X dNTP Mix (100mM)	0.8
10X RT Random Primers	2.0
Multiscribe Reverse Transcriptase	1.0
Nuclease free water	4.2
Final Volume	10.0
Volume of cDNA Master Mix per reaction	5.0
Volume of RNA	5.0
Final volume per reaction	10.0

Table 7. Thermal cycling conditions for synthesizing cDNA.

Temperature (°C)	**Time (min)**
25	10
37	120
85	5
4	Infinite Hold
Number of cycles	1

2.4.3 The PCR Assay

Fast SYBR™ Green Master Mix (Catalogue No. 4385612 – Thermo Fisher Scientific Pty Ltd, Victoria, Australia) was used with the cDNA template, forward and reverse DNA primers in a reaction volume of 20 µl, in pre-determined volumes as per manufacturer's protocol (Table 8). The PCR plate was run (Table 9) on Applied Biosystems StepOnePlus ™ Real-Time PCR systems (version 2.2.3). The samples were run in duplicate and an average CT (Cycle Threshold) value was calculated. The CT value for the housekeeping gene *Gapdh* was subtracted from the CT value of the gene under investigation. Gene expression was quantified using the comparative (ΔΔCT) method where the threshold cycle (CT) for each gene was normalised to reference gene *Gapdh*. Relative gene expression in the animals was presented as $2^{-\Delta CT}$.

Table 8. Recipe for the PCR Reaction Mix.

Ingredient	**Volume (µl) x1**
SYBR Green Master Mix	10
Forward Primer (25ng/reaction)	2
Reverse Primer (25 ng/reaction)	2
cDNA template (10-20 ng/reaction)	4
RNase-free water	2
Total reaction	20

Table 9. Thermal Cycling Conditions for PCR.

Temperature (°C)		**Duration (sec)**
95 Hold		20 sec
95 Denature	x40	03 sec
60 Extension	x40	30 sec
4 Hold		10 min

2.5 Histopathology

Colon tissue which was cut into one half along the longitudinal axis was rolled around a sterile toothpick into a Swiss roll, and spleen, liver and both kidneys were placed in 50 mL of 10% neutral buffered formalin for fixation for 2-3 days. The tissue was then transferred into 70% ethanol until chemical processing and embedded in paraffin and sections cut to a thickness of 5 μm by a rotary microtome and were stained with Gill's haematoxylin and eosin (H&E). The H&E stained sections were imaged using an Olympus DP72 microscope. The tissue sections of colon, spleen, liver and kidneys, from all animals were scored in a blinded manner after grading for colitis (Table 20, 22, 24 and 26) by the histopathologist involved in this study at the Launceston General Hospital. Cell counting was performed manually in 10 random microscopic fields at magnifications of x100 and x200.

2.6 Immunohistochemistry

Colon tissue sections were fixed in 10% neutral buffered formalin for 2-3 days and transferred to 70% ethanol, processed, embedded in paraffin, and 5 μm thick sections were cut using a microtome. Wax tissue sections were marked using a silicon pencil and left in an oven at 60°C for 10 minutes and the dewaxing process begun. The tissue was processed for 2 minutes in xylene, rehydrated in a series of ethanol from 100%, 100%, 95%, 95%, 70%, 70% after which two washes performed in distilled water. Antigen retrieval was carried out in 0.1M citrate buffer (pH 6.0) (Table 10) at maximum pressure for 6 minutes using a decloaking chamber, allowed to cool under running water and rinsed twice in distilled water. 1:10 hydrogen peroxide incubation was performed for 10 minutes followed by protein blocking for 30 minutes using the Rabbit specific HRP/DAB (ABC) detection IHC kit (Catalogue No. 64261, Abcam, UK) following the manufacturer's protocol. Slides were washed under running water for 5 minutes and rinsed twice in PBS (Dulbecco's, Invitrogen, Australia) after each treatment. 200 μl of primary antibody (Table 11) diluted 1:100 in supplied antibody diluting solution was added and incubated for 1 hour in the dark inside a humidified

chamber at room temperature. Rinsed in PBS 3 times and 3 drops of the secondary antibody added and incubated for 30 minutes at room temperature. After rinsing 3 times in PBS, DAB chromogen + substrate buffer (1 drop of DAB chromogen diluted in 1 mL substrate buffer) was added to the tissue sections for 10 minutes and washed under running water for 5 minutes, and counterstained with strong liquid Mayer's haematoxylin for 30 seconds, dipped in ammonia water for 1-2 minutes and dehydrated in ethanol (70%, 70%, 95%, 95%, 100%, 100%, xylene, xylene), after which a mounting medium was added and a coverslip placed on top.

Table 10. Composition of Citrate Buffer.

	3.5 mL 0.1M Sodium Citrate
Citrate Buffer	46.5 mL Citric Acid
	Up to 100 mL Distilled Water
	pH adjusted with 0.1M NaOH

Table 11. Primary antibodies used for IHC.

Antibody	**Catalogue Number**	**Manufacturer**	**Dilution**
CCL20	9829	Abcam, UK	1:200
$PI3K^{P}$	78429	Abcam, UK	1:200
Akt^{P}	227100	Abcam, UK	1:500

2.7 Alcian Blue staining of mucus producing goblet cells

Slides were deparaffinized and rehydrated in a series of alcohol. Stained with Alcian blue pH 2.5 for 30 minutes, washed in running water for 2 minutes, rinsed in distilled water, counterstained with safranin for 1 hour, washed and dehydrated in alcohol,

cleared in xylene and mounted. Acid mucins were stained blue and the nuclei were stained in pink (Figure 14).

2.8 Statistical Data Analysis

The data were analysed using Graph Pad Prism version 8.4.2 (Graph Pad Software Inc., USA). All data were expressed as mean $\pm$ standard error of mean (SEM) and the data were evaluated by one - way analysis of variance (ANOVA) and Tukey's multiple comparison test to compare the mean values between groups. The data was considered significant when $p \leq 0.05$.

3.0 Results

3.1 A Brief Overview of the Genotypes

This study involved a preliminary investigation of multi-system pathophysiology produced by CCR6-deficiency in a novel murine model of colitis with the view to phenotype and evaluate its potential to ameliorate UC. Table 12 describes the different groups of mice utilised in this study and the reasons for selecting these groups and why they were compared.

Table 12: The investigated genotypes and their ensuing phenotypes.

Model	**Genotype** **Winnie / *Ccr6***	**Description**
C57BL/6J (WT)	+/+, +/+	Normal for mucin 2 and normal for CCR6
Ccr6 -/-	+/+, -/-	Normal for mucin 2 but no CCR6
Winnie	m/m, +/+	No mucin 2 but normal for CCR6
Winnie x *Ccr6*-/-	m/m, -/-	No mucin 2 nor CCR6

The reasons for selecting the C57BL/6J as the WT was because it is a healthy control which had no mutations as well as did not develop the disease. We have compared

the WT against Winnie, which carried a mutation in *Muc2* gene and hence developed colitis. It is already established that the defect in *Muc2* produces colitis (111). By doing so, we were directly comparing the healthy control with the diseased phenotype, using mice generated from the same background strain. Between these two groups, we hypothesised that the CCR6 chemokine receptor-ligand activity remained the same but produced different outcomes. The *Ccr6*-/- mice were used to demonstrate the influence of the CCR6 receptor activity by comparing the healthy WT control with the loss of chemokine CCR6 activity in the WT. We induced the *Muc2* mutation in Winnie x *Ccr6*-/- mice (the experimental model) to produce spontaneous colitis in these mice and knocked out the *Ccr6* gene to investigate the clinical and immunological effects arising from the loss of CCR6 activity in the colitis model, which was Winnie. Since it is also known that the chemokine receptor CCR6 upregulates certain autoimmune diseases (42) as well as certain CCR6-inhibitors had produced attenuation of several autoimmune diseases (73), we hypothesised that the absence of CCR6 in a colitis mouse model would also contribute towards attenuating the disease. A comparison of Winnie x *Ccr6*-/- and *Ccr6*-/- was made to see whether the loss of CCR6 activity in the WT and Winnie mice were similar or were vastly different. Since the WT and Winnie were generated from the same background strain, the comparison was deemed to be valid.

3.1.1 C57BL/6J control mice [WT (Winnie +/+, *Ccr6*+/+)]

These mice were purchased from the Jackson Laboratories in the USA and obtained via the Animal Resource Centre (ARC). The colony is refreshed every 10 generations to prevent genetic drift. It is a tolerant background for the expression of many mutations. The C57BL/6J has no gene manipulations. Therefore, with regards to the genotype concerning *Muc2* and *Ccr6* loci, they are homozygous dominant and could be described as +/+ for Winnie which means the dominant form of m/m and +/+ for *Ccr6*. It means that these mice are healthy and have normal mucin production and as a result, do not develop the disease although they carry the CCR6 chemokine receptor.

3.1.2 Winnie mice (m/m, *Ccr6*+/+)

These mice are on the C57BL/6J parental background carrying a missense mutation in *Muc2*. The signage for a mutation is m. Homozygous mice designated m/m show symptoms closely resembling inflammatory bowel disease. The colony is normally maintained as heterozygous m/+ x m/+. The Winnie mouse model was utilized because the gene deficiency in *Muc2* causes the depletion of the mucin glycoprotein that forms a thick protective layer over the colonic epithelium and renders the mice susceptible to pathogenic microbial penetration into the colonic mucosal system. Pathogenic microbial assault and the influence of the CCR6-CCL20 axis in the intestines are regarded as substantial causes of developing chronic colitis in mouse models (40). Winnie mice develop chronic spontaneous colitis by 6 weeks of age (and mimics clinical UC), and the disease pathology advances with age.

3.1.3 *Ccr6* -/- mice (Winnie +/+, *Ccr6*-/-)

These mice are on the C57BL/6J parental background in which the *Ccr6* gene has been knocked out. The genotype is *Ccr6* -/-. The signage -/- designates a knockout. This is a homozygous strain and has been maintained in the facility as a homozygous colony. CCR6 -/- males are mated with CCR6 -/- females to produce the CCR6 -/- offspring. These mice do not carry the Winnie mutation. These mice are deficient for *Ccr6* and yet, do not display any gut-associated clinical symptoms. These mice have normal *Muc2* expression and were deficient in the CCR6 protein. This group of mice were denoted by the Winnie +/+, *Ccr6*-/- genotype.

3.1.4 Winnie x *Ccr6*-/- mice (m/m, *Ccr6*-/-)

The experimental model, derived from Winnie and CCR6 mice (Figure 5), thus named Winnie x *Ccr6*-/-, develops the disease (spontaneous colitis) due to the absence of mucin and because it was also CCR6 deficient, we hypothesised these mice to have the ability to resist chronic intestinal inflammation and perhaps promote its resolution.

3.2 Pre-clinical parameters indicate that *Ccr6*-deficiency reduces inflammation in the colon.

3.2.1 Colon length

Table 13. The mean colon length (cm) in the genotypes at both timepoints.

	WT **Mean ± SEM**	***Ccr6*-/-** **Mean ± SEM**	**Winnie x *Ccr6*-/-** **Mean ± SEM**	**Winnie** **Mean ± SEM**
8 weeks	8.4 ± 0.14 cm	8.4 ± 0.25 cm	8.2 ± 0.25 cm	8.6 ± 0.25 cm
16-22 weeks	8.0 ± 0.11 cm	8.6 ± 0.27 cm	9.3 ± 0.15 cm	9.7 ± 0.25 cm

A significant difference in colon length exists between WT and Winnie (***p<0.001) as well as WT and Winnie x *Ccr6*-/- (**p ≤ 0.01) at the second timepoint (Table 13, Figure 6).

A **B**

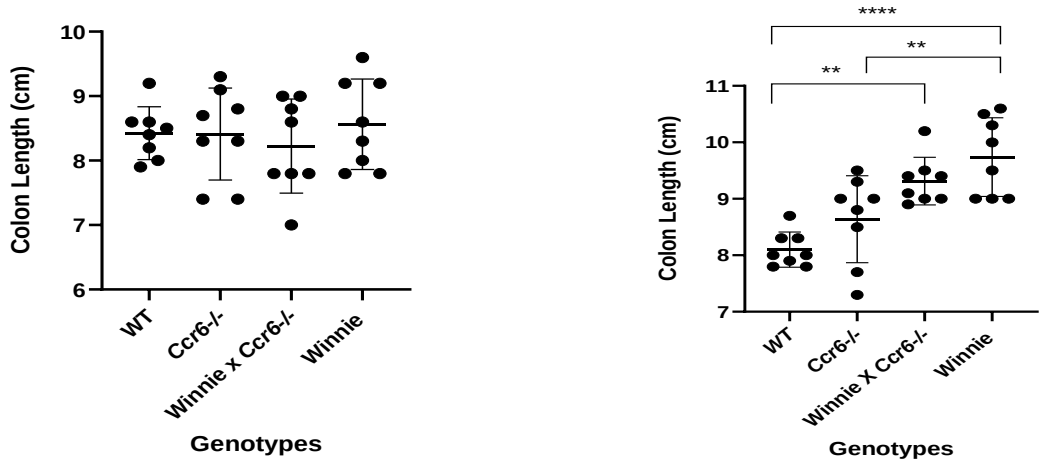

Figure 6. Comparison of the lengths of freshly removed colons measured from the ileo-caecal junction to the anus in the four genotypes. Data expressed as mean ± SEM by one-way analysis of variance (ANOVA) and Tukey's multiple comparison test, n=8, (A) at 8 weeks of age (B) at 16-22 weeks of age.

3.2.2 Colon weight

Table 14. The mean colon weight (g) in the genotypes at both timepoints.

	WT **Mean ± SEM**	***Ccr6*-/-** **Mean ± SEM**	**Winnie x *Ccr6*-/-** **Mean ± SEM**	**Winnie** **Mean ± SEM**
8 weeks	0.15 ± 0.01 g	0.15 ± 0.01 g	0.29 ± 0.03 g	0.36 ± 0.01 g
16-22 weeks	0.1 3± 0.01 g	0.65 ± 0.03 g	0.53 ± 0.03 g	0.55 ± 0.1 g

A significant difference in the colon weight was observed between Winnie x *Ccr6*-/- and Winnie (*p< 0.05) at the first timepoint and between WT and Winnie x *Ccr6*-/- (****p< 0.0001) and between WT and Winnie (****p< 0.0001) at both timepoints (Table 14, Figure 7).

A **B**

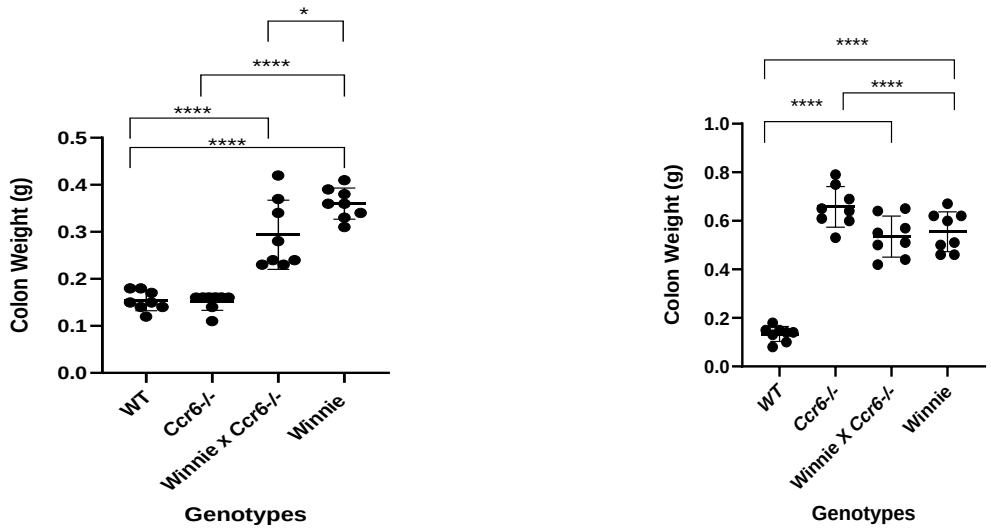

Figure 7. Comparison of wet colon weight after removing the luminal contents in the four genotypes. Data expressed as mean ± SEM by one-way analysis of variance (ANOVA) and Tukey's multiple comparison test, n=8. (A) at 8 weeks of age (B) at 16-22 weeks of age.

3.2.3 Colon Weight /Colon Length Ratio

Table 15. The mean colon weight/ length (g/cm) ratio in the genotypes at both timepoints.

	WT **Mean ± SEM**	***Ccr6-/-*** **Mean ± SEM**	**Winnie x *Ccr6-/-*** **Mean ± SEM**	**Winnie** **Mean ± SEM**
8 weeks	0.018 ± 0.003	0.018 ± 0.002	0.036 ± 0.01	0.041 ± 0.004
16-22 weeks	0.01 ± 0.003	0.07 ± 0.01	0.05 ± 0.01	0.06 ± 0.01

The colon weight/colon length ratio was significantly increased between WT and Winnie x *Ccr6-/-* (****p<0.0001) and between WT and Winnie (****p<0.0001) at both timepoints (Table 15, Figure 8).

A **B**

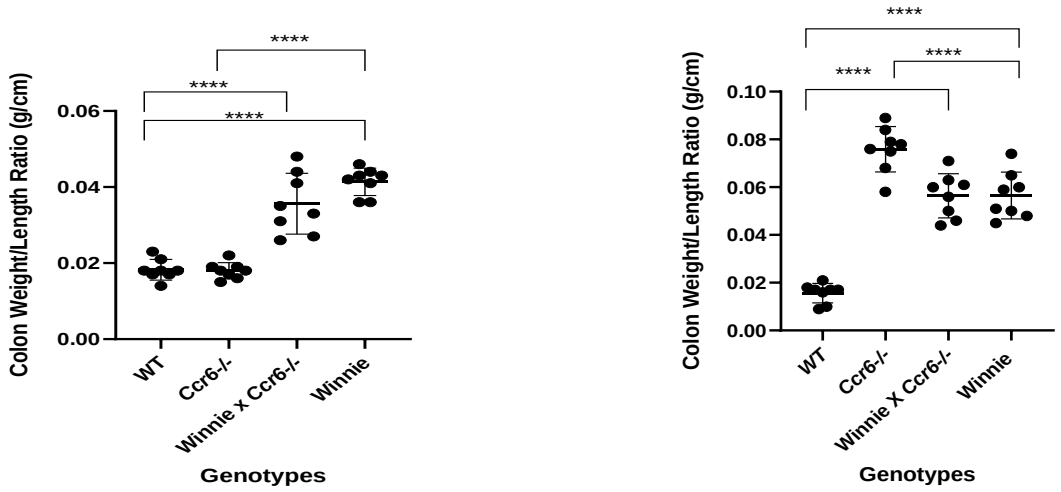

Figure 8. Comparison of the colon weight/length ratio in the four genotypes. Data expressed as mean ± SEM by one-way analysis of variance (ANOVA) and Tukey's multiple comparison test, n=8. (A) at 8 weeks of age (B) at 16-22 weeks of age.

3.2.4 Body Weight

Table 16. The mean body weight (g) in the genotypes at both timepoints.

	WT **Mean ± SEM**	***Ccr6*-/-** **Mean ± SEM**	**Winnie x *Ccr6*-/-** **Mean ± SEM**	**Winnie** **Mean ± SEM**
8 weeks	26.2 ± 0.35	20.46 ± 0.6	20.15 ± 0.68	16.95 ± 0.82
16-22 weeks	24.64 ± 0.33	22.35 ± 0.2	24.60 ± 0.17	19.97 ± 0.04

A significant difference was evident in the mean body weight between the WT and Winnie (****p<0.0001) and between WT and Winnie x *Ccr6*-/- (****p<0.0001) at both timepoints and between Winnie x *Ccr6*-/- and Winnie (****p<0.0001) at the second timepoint (Table 16, Figure 9).

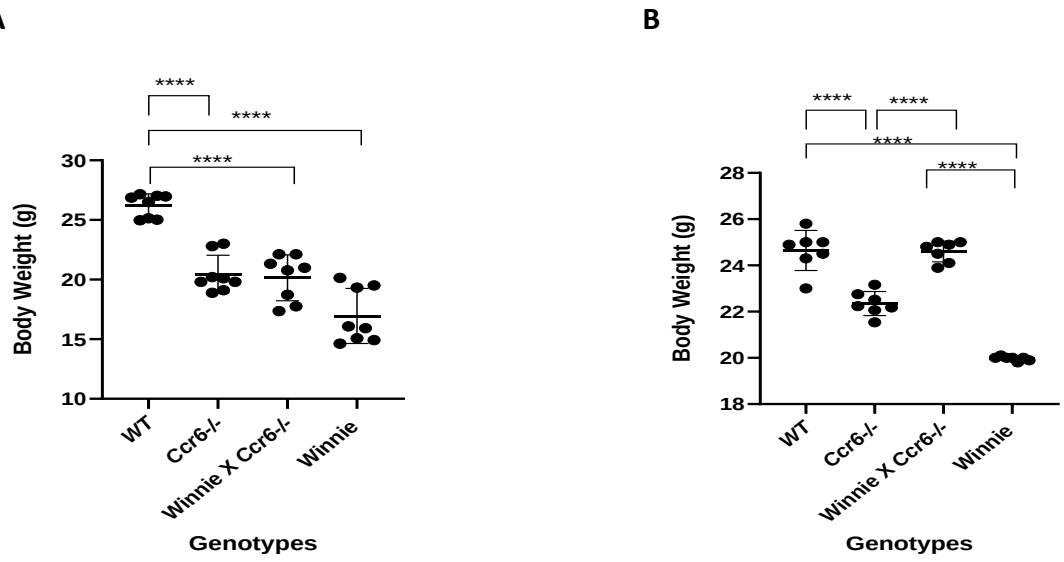

Figure 9. Comparison of body weight in the four genotypes. Data expressed as mean ± SEM by one-way analysis of variance (ANOVA) and Tukey's multiple comparison test, n=8. (A) at 8 weeks of age (B) at 16-22 weeks of age.

3.2.5 Colon Weight/Body Weight Ratio

Table 17. The colon weight/body weight in the genotypes at both timepoints.

	WT **Mean ± SEM**	***Ccr6*-/-** **Mean ± SEM**	**Winnie x *Ccr6*-/-** **Mean ± SEM**	**Winnie** **Mean ± SEM**
8 weeks	0.006 ± 0.001	0.007 ± 0.001	0.017 ± 0.005	0.018 ± 0.002
16-22 weeks	0.007 ± 0.001	0.026 ± 0.003	0.023 ± 0.005	0.03 ± 0.004

A significant difference was evident in the colon weight /body weight ratio between the WT and Winnie (****p<0.0001) and between WT and Winnie x *Ccr6*-/- (****p<0.0001) at both timepoints (Table 17, Figure 10).

A **B**

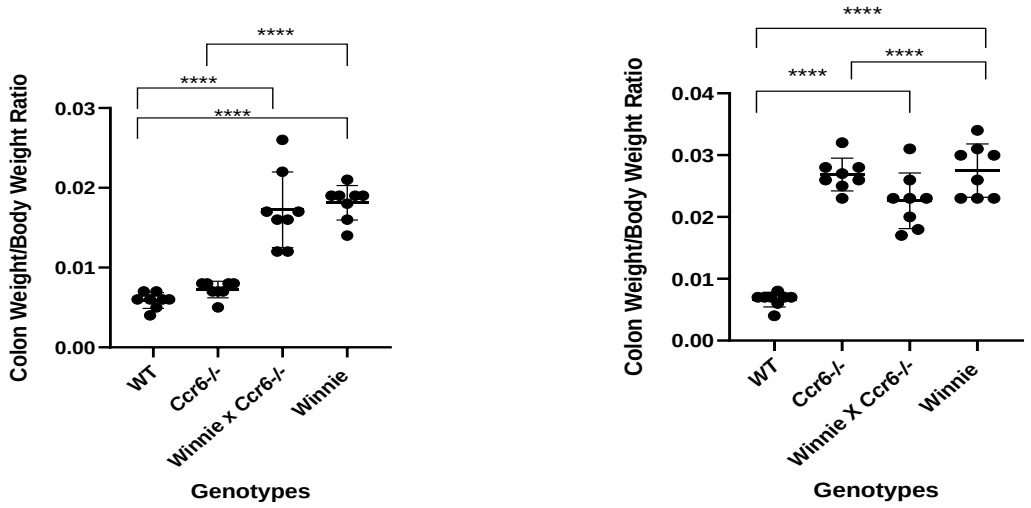

Figure 10. Comparison of colon weight/body weight ratio in the four genotypes. Data expressed as mean ± SEM by one-way analysis of variance (ANOVA) and Tukey's multiple comparison test, n=8. (A) at 8 weeks of age (B) at 16-22 weeks of age.

3.2.6 Gross Colon Morphology

Table 18. Gross colonic morphological features after the removal of the colon.

Genotype	Observation
WT	Faecal pellets were well -formed, solid and hard with no symptoms of inflammation, narrow short colon with thin bowel wall (Table 18, Figure 11 A, B).
Ccr6-/-	Semi-solid faeces in the proximal colon, faecal pellets formed in the distal colon, mild inflammation, slightly oedematous bowel wall (Table 18, Figure 11, C, D).
Winnie x *Ccr6-/-*	Semi-solid faeces in the proximal colon, faecal pellets formed in distal colon, mild inflammation, mildly thickened bowel wall (Table 18, Figure 11 E, F).
Winnie	Watery stools, faecal pellets not formed, high inflammation, thickened, reddened and oedematous bowel wall (Table 18, Figure 11 G, H).

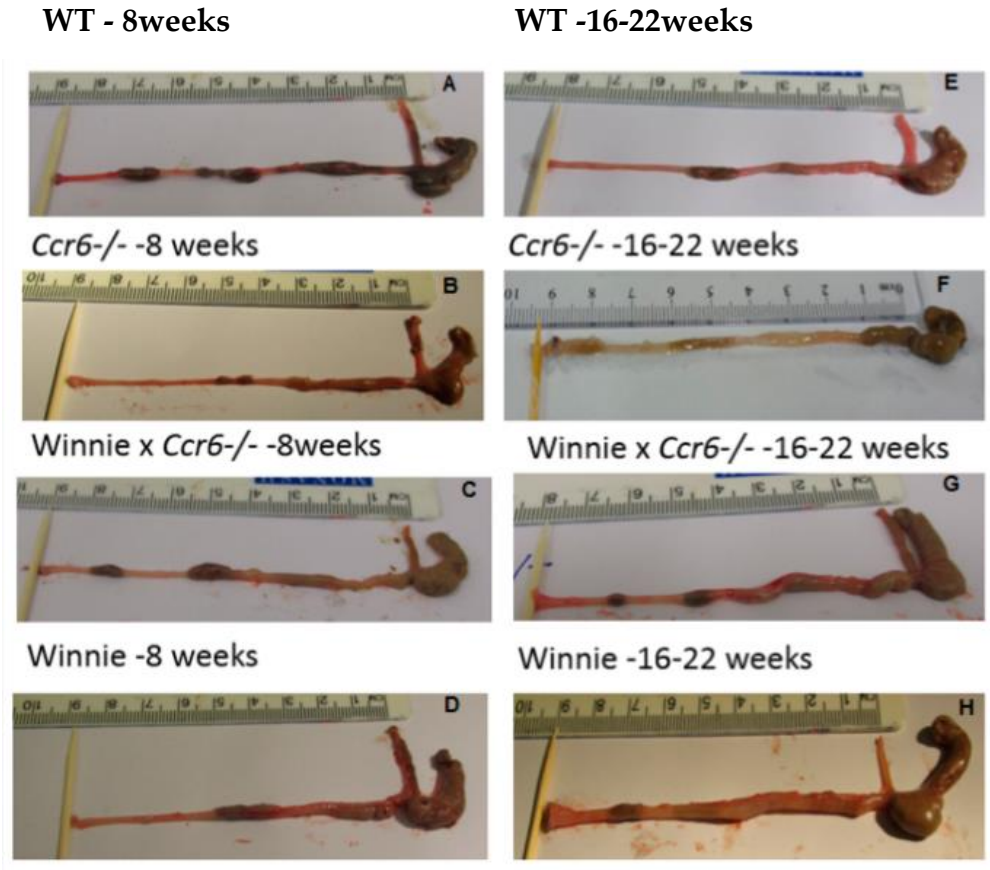

Figure 11. Comparison of gross colon morphology. Freshly removed colons measured from the ileo-caecal junction to the anus in the four genotypes at 8 weeks of age (A-D) and 16-22 weeks of age (E-H). Magnification x1.

3.2.7 Disease Activity Index

The disease activity index (DAI) in the four genotypes was assessed as per the criteria given in Table 19.

Table 19. The DAI score in the genotypes at both timepoints.

Genotype	Body Weight (g)	Diarrhoea	Bloody faeces	Rectal Prolapse	DAI Score
WT	Normal (25 g)	Absent	Absent	Absent	0 – No inflammation
***Ccr6*-/-**	Loss of body weight (moderate)	Absent	Absent	Absent	1-Mild inflammation
Winnie x *Ccr6*-/-	Loss of body weight (Moderate)	Absent	Absent	Absent	2-Moderate inflammation
Winnie	Loss of body weight (Severe)	Present	Absent	Present	3- High inflammation

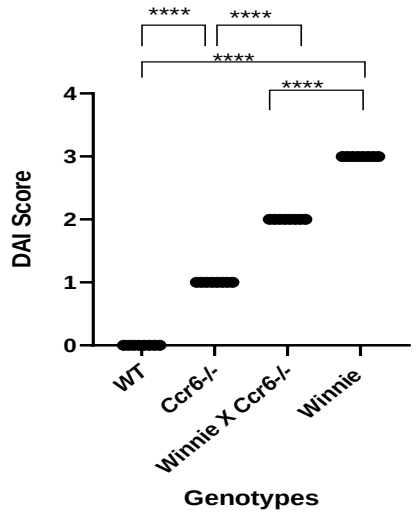

Figure 12. The overall mean DAI score in the four genotypes tested. Data expressed as mean ± SEM by one-way analysis of variance (ANOVA) and Tukey's multiple comparison test, n=8.

3.3 *Ccr6*-deficiency displayed attenuated inflammation in multi-system pathology concomitant with colitis.

3.3.1 Colon Histology

Table 20. Grading of colitis and scoring sheet for H&E sections (117)**.**

Criterion	**WT**	***Ccr6-/-***	**Winnie x *Ccr6-/-***	**Winnie**
Distribution of inflammation	0	0	1	2
0=None				
1=Focal				
2=Multifocal				
Depth of inflammation	0	0	1	3
1=Mucosal				
2=Submucosal				
3=Transmural				
Lamina propria neutrophils				
0=None	0	1	3	3
1=1-10				
2=11-20				
3=>20				
Cryptitis	0	0	1	1
0=No cryptitis				
1=Cryptitis				
Crypt abscess	0	0	1	3

0=None				
1=1-5				
2=6-10				
3=>10				
Goblet cell loss	0	0	1	3
0=Normal or <10%loss				
1=10-25%				
2=25-50%				
3=>50%				
Crypt architecture	0	1	1	3
0=Normal				
1=Mildly irregular				
2=Moderate				
3=severe				
Ulceration	0	0	1	2
0=None				
1=Superficial				
2=Deep				
Overall mean score	0	2	10	20

(a)

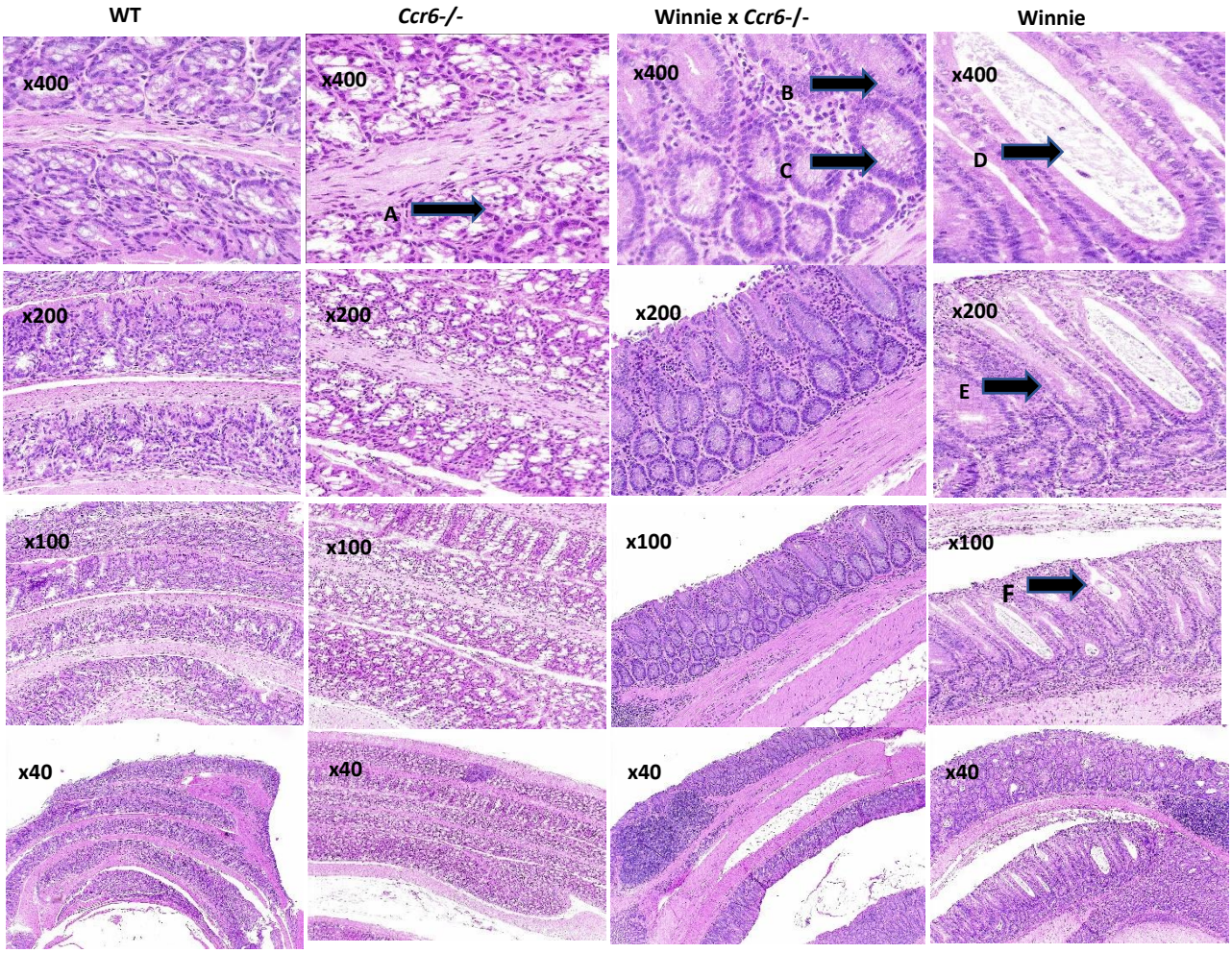
WT
Ccr6-/-
Winnie x Ccr6-/-
Winnie
x400
x200
x100
x40
A
B
C
D
E
F

(b)

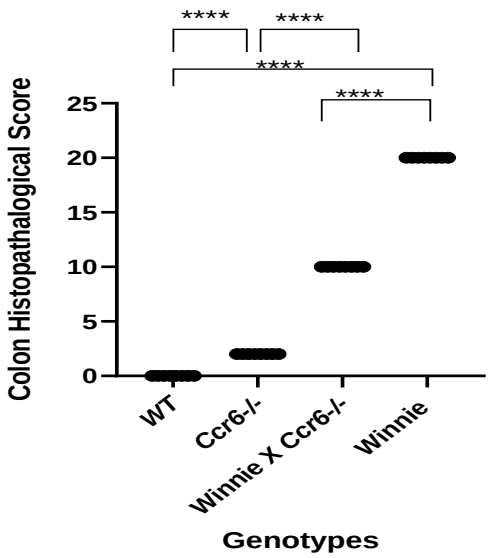
****
****
****
****
Colon Histopathalogical Score
25
20
15
10
5
0
WT
Ccr6-/-
Winnie X Ccr6-/-
Winnie
Genotypes

Figure 13. (a) Representative images of H&E colon histomorphology in the genotypes at 16-22 weeks of age. Arrows indicate (A) mucus filled goblet cells inside short crypts in *Ccr6*-/-, (B) moderately elongated crypts in Winnie x *Ccr6*-/-, (C) mucus filled goblet cells in Winnie x *Ccr6*-/-, (D) crypt abscess in Winnie, (E) highly elongated crypts in Winnie, (F) mucosal ulcerations in Winnie. No inflammation in WT and *Ccr6*-/- while moderate inflammation existed in Winnie x *Ccr6*-/-. Severe inflammation was evident in Winnie. Magnification x40, x100, x200 and x400. **(b)** Quantification of inflammation in the colon in the four genotypes at 16-22 weeks of age using the histopathological score given in Table 20. Data expressed as mean ± SEM by one-way analysis of variance (ANOVA) and Tukey's multiple comparison test, n=8.

3.3.2 Validation of mucin production by goblet cells in the colonic epithelium

(a) **(b)**

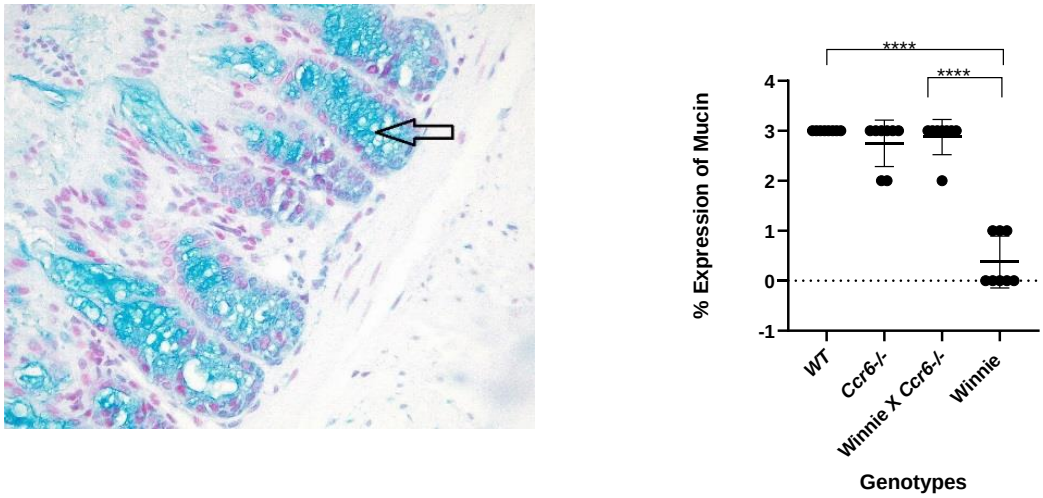

Figure 14. (a) The validation of mucin produced by the goblet cells within the colonic epithelium which makes the gut mucosa inaccessible to infectious microbes. Arrow points to a representative image of mucin stained with Alcian blue within the colonic epithelium of Winnie x *Ccr6*-/-. (x200), **(b)** the mean percentage (%) expression of mucin glycoprotein quantified by Fiji image J software. Percentage expression of intensity was calculated by the formula; optical density (OD) = log

(maximum intensity/mean intensity), where max intensity = 255 for 8-bit images using Fiji Image J Version 1.64 software for windows 7 (Scijava Software Inc, USA). Data expressed as mean ± SEM by one-way analysis of variance (ANOVA) and Tukey's multiple comparison test, n=8.

3.3.3 Spleen weight

Table 21. The mean spleen weight (g) in the genotypes at both timepoints.

	WT Mean ± SEM	***Ccr6*-/- Mean ± SEM**	**Winnie x *Ccr6*-/- Mean ± SEM**	**Winnie Mean ± SEM**
8 weeks	0.07 g ± 0.004	0.066 g ± 0.002	0.082 g ± 0.01	0.09 g ± 0.01
16-22 weeks	0.09 g ± 0.01	0.11 g ± 0.003	0.12 g ± 0.01	0.14 g ± 0.01

A significant difference in mean spleen weight existed between WT and Winnie (*p<0.05) and between WT and Winnie x *Ccr6*-/- (*p<0.05) at the first timepoint. At the second time point, there were significant differences between WT and Winnie (****p<0.0001), WT and Winnie x *Ccr6*-/- (*p<0.05) and Winnie x *Ccr6*-/- and Winnie (*p<0.05) (Table 21, Figure 15).

A **B**

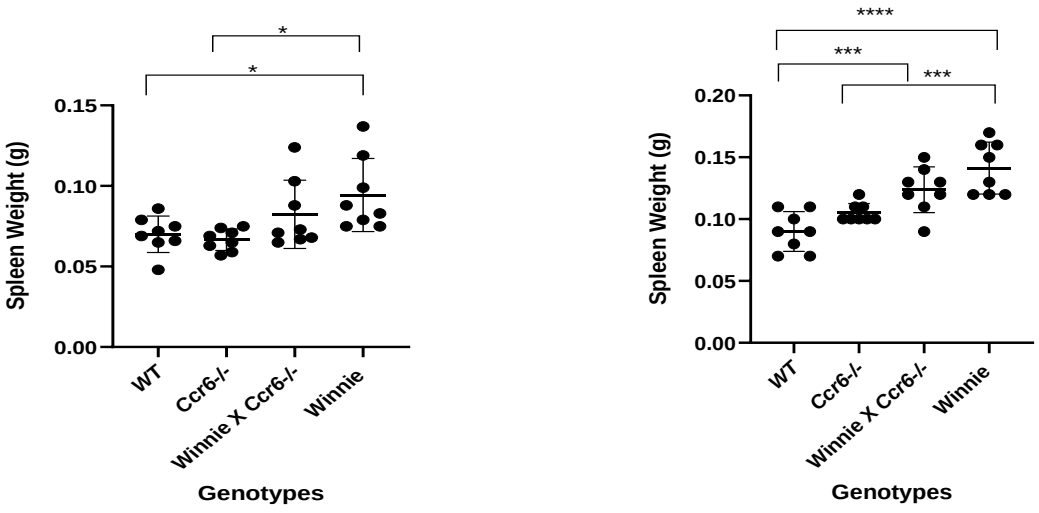

Figure 15. Comparison of the mean splenic weight in the 4 genotypes. Data expressed as mean ± SEM by one-way analysis of variance (ANOVA) and Tukey's multiple comparison test, n=8. (A) at 8 weeks of age (B) at 16-22 weeks of age.

3.3.4 Spleen Histology

Table 22. Spleen Histology Scoring System (118)**.**

Criterion	**WT**	***Ccr6-/-***	**Winnie x *Ccr6-/-***	**Winnie**
Distorted Lymphoid Architecture	Absent	Absent	Absent	Absent
Minimized Lymphoid Follicles	Absent	Absent	Absent	Absent
Diffuse White Pulp	Absent	Absent	Absent	Absent
Presence of Granular Leukocytes	Absent	Absent	Absent	Absent
Giant Macrophages	Absent	Absent	Absent	Absent
Infiltration of Inflammatory Cells	Absent	Present	Present	Present
Histology Inflammation Score	**Normal=0**	**Mild=1**	**Moderate=2**	**Severe=3**

(a)

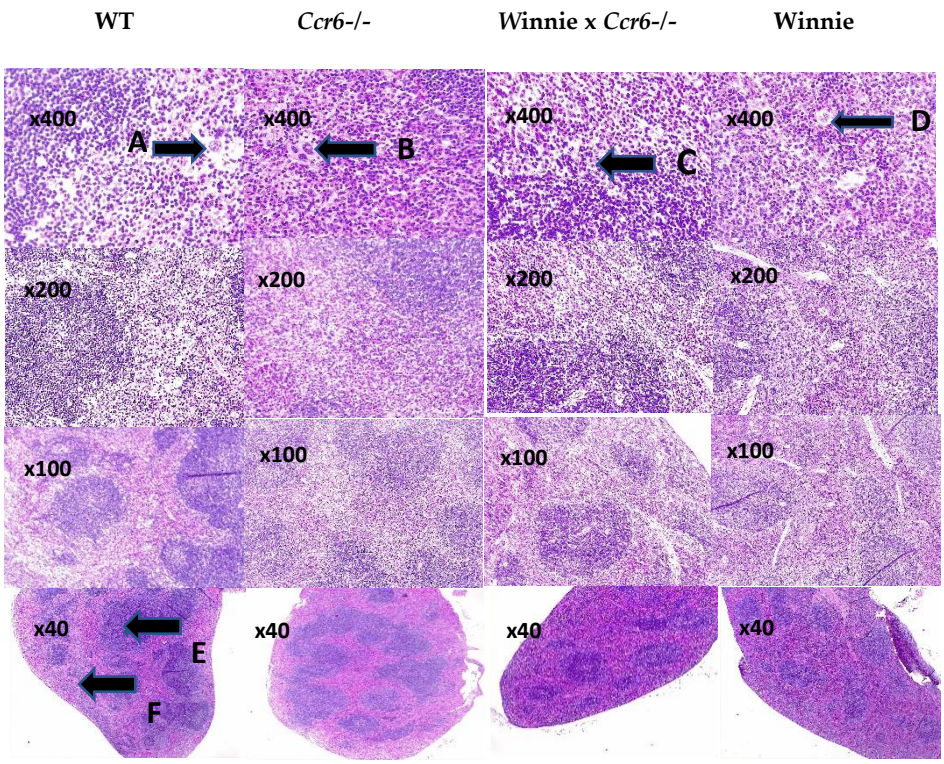

(b)

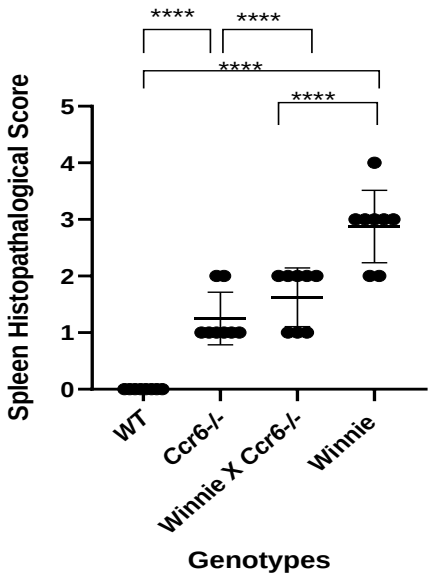

Figure 16. ***(a)*** **Representative images of H&E spleen histology in the four genotypes at 16-22 weeks of age**. Paraffin embedded haematoxylin and eosin (H&E) stained sections at x40, x100, x200 and x400 magnification. Arrows indicate (A) megakaryocyte, (B) neutrophils in *Ccr6-/-*, (C) neutrophils in Winnie x *Ccr6-/-*, (D)

neutrophils in Winnie, (E) red pulp, (F) white pulp. **(b)** Quantification of inflammation in the spleen in the four genotypes at 16-22 weeks of age using the histopathological score given in Table 22. n=8.

Inflammation was quantified in the genotypes by counting the numbers of immune cell infiltrations in 3 similar areas on the slides and comparing the mean value using a scoring index from 0 – 3, from no inflammation (score of 0) to severe neutrophil infiltration (score of 3), where WT was zero, *Ccr6*-/- was 1, Winnie x *Ccr6*-/- was a moderate 2 and Winnie had a score of 3.

3.3.5 Liver Weight

Table 23. The mean liver weight (g) in the genotypes at both timepoints.

	WT **Mean ± SEM**	***Ccr6*-/-** **Mean ± SEM**	**Winnie x *Ccr6*-/-** **Mean ± SEM**	**Winnie** **Mean ± SEM**
8 weeks	1.275 ± 0.04 g	1.115 ± 0.1 g	0.962 ± 0.1 g	1.21 ±0.1 g
16-22 weeks	0.986 ± 0.03 g	1.196 ± 0.1 g	1.48 ± 0.1 g	1.53 ± 0.1 g

The differences in the mean liver weight among the genotypes at the first time point were not significant [Table 23, Figure 17 (A)]. Significant differences existed between WT and Winnie x *Ccr6*-/- (****p< 0.0001), WT and Winnie (****p < 0.0001), and *Ccr6*-/- and Winnie (****p < 0.0001) at the second timepoint [Table 23, Figure 17 (B)].

A

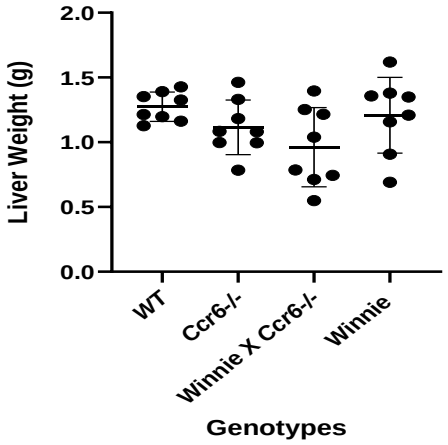

B

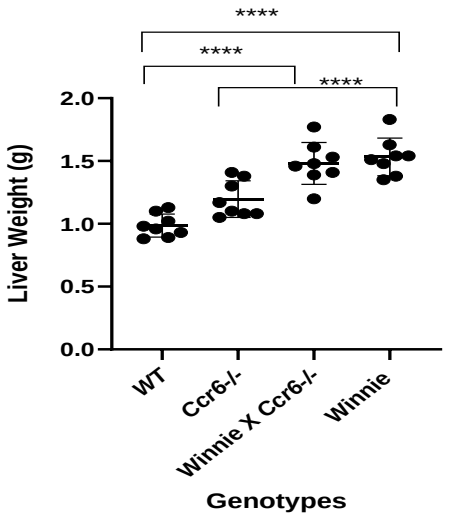

Figure 17. Comparison of liver weight in the four genotypes. Data expressed as mean ± SEM by one-way analysis of variance (ANOVA) and Tukey's multiple comparison test, n=8. (A) at 8 weeks of age (B) at 16-22 weeks of age.

3.3.6 Liver Histology

Table 24. Liver Histology Scoring System (118)**.**

Criterion	**WT**	***Ccr6-/-***	**Winnie x *Ccr6-/-***	**Winnie**
Steatosis	Absent	Absent	Absent	Absent
Micro and Macro vesicles	Absent	Absent	Absent	Absent
Cytoplasmic degeneration	Absent	Absent	Absent	Absent
Necrotic foci	Absent	Absent	Absent	Absent
Kupffer Cell activation	Absent	Absent	Absent	Absent
Haemorrhage	Absent	Absent	Absent	Absent

Infiltration of Inflammatory cells	Absent	Present	Present	Present
Hepatic Fibrosis	Absent	Absent	Absent	Absent
Hepatic Cirrhosis	Absent	Absent	Absent	Absent
Histology Inflammation Score	**Normal=0**	**Mild=1**	**Moderate=2**	**Severe=3**

(a)

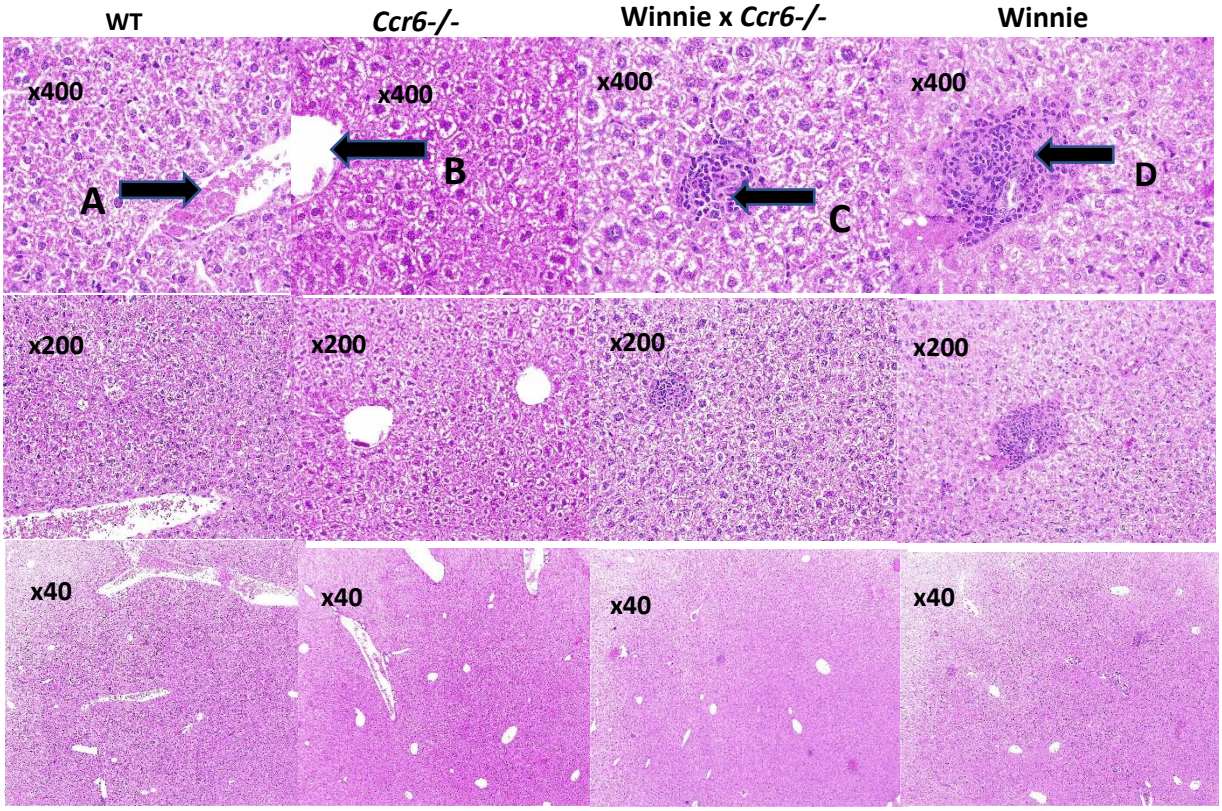

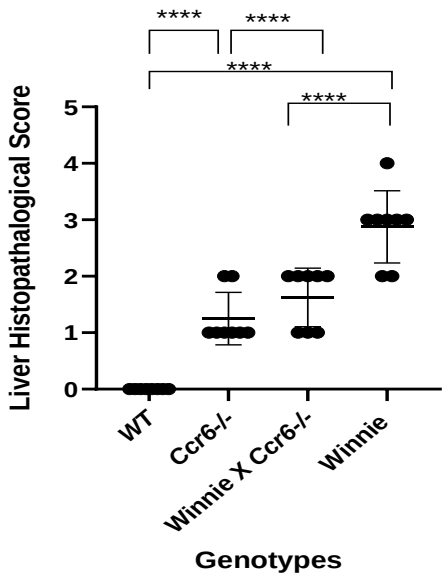

Figure 18. (a) Representative images of H&E in liver histology in the four genotypes at 16-22 weeks of age. Arrows indicate (A) portal tract, (B) central canal, (C) immune cell infiltration indicative of focal lobular inflammation in Winnie x *Ccr6-/-,* (D) severe focal lobular inflammation in Winnie at 16-22 weeks of age. (A) at 8 weeks of age (B) at 16-22 weeks of age. Inflammation was quantified in the genotypes by counting the numbers of immune cell infiltrations which indicate sporadic focal lobular inflammation in 3 similar areas on the slides and comparing the mean value using a scoring index from 0 – 3, from no inflammation to severe neutrophil infiltration, where WT was zero, *Ccr6-/-* was 1, Winnie x *Ccr6-/-* was a moderate 2 and Winnie had a score of 3. **(b)** Quantification of inflammation in the liver in the four genotypes at 16-22 weeks of age using the overall mean histopathological score given in Table 24. Data expressed as mean $\pm$ SEM by one-way analysis of variance (ANOVA) and Tukey's multiple comparison test, n=8.

3.3.7 Kidney Weight

Table 25. The mean kidney weight (of both kidneys together) (g) in the genotypes at both timepoints.

	WT **Mean ± SEM**	***Ccr6*-/-** **Mean ± SEM**	**Winnie x *Ccr6*-/-** **Mean ± SEM**	**Winnie** **Mean ± SEM**
8 weeks	0.362 ± 0.01 g	0.294 ± 0.02 g	0.275 ± 0.03 g	0.4 ± 0.01 g
16-22 weeks	0.29 ± 0.01 g	0.34 ± 0.02 g	0.36 ± 0.02 g	0.42 ± 0.03 g

A significant difference existed in the mean kidney weight between *Ccr6*-/- and Winnie (**p < 0.01), Winnie x *Ccr6*-/- and Winnie (***p < 0.001) and WT and Winnie x *Ccr6*-/- (***p < 0.001) at the first timepoint [Table 25, Figure 19 (A)]. A significant difference also existed between WT and Winnie (***p <0.001) at the second timepoint [Table 25, Figure 19 (B)].

A

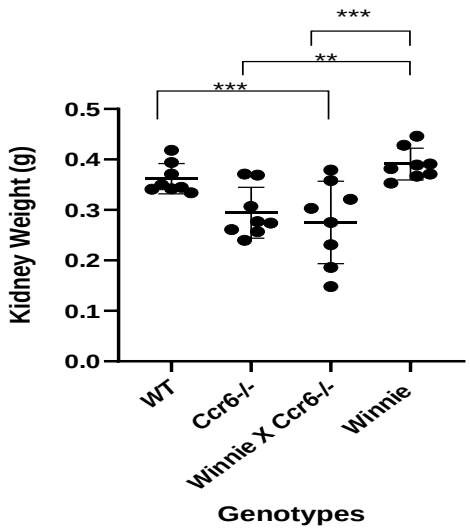

B

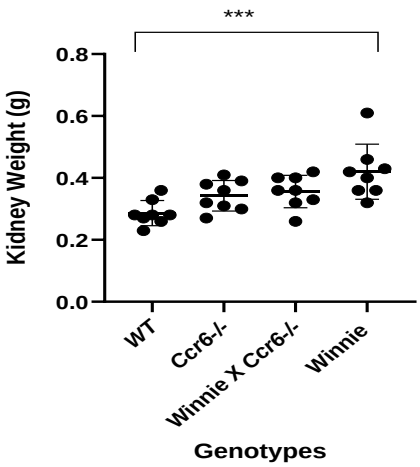

Figure 19. Comparison of kidney weight in the four genotypes. Data expressed as mean ± SEM by one-way analysis of variance (ANOVA) and Tukey's multiple comparison test, n=8. (A) at 8 weeks of age (B) at 16-22 weeks of age.

3.3.8 Kidney Histology

Table 26. Kidney Histology Scoring System (118).

Criterion	**WT**	***Ccr6*-/-**	**Winnie x *Ccr6*-/-**	**Winnie**
Diminished/Distorted Glomeruli	Absent	Absent	Absent	Absent
Dilated Tubules	Absent	Absent	Absent	Absent
Oedema Exudate	Absent	Absent	Absent	Absent
Mild Necrosis	Absent	Absent	Absent	Absent
Infiltration of Inflammatory Cells	Absent	Absent	Absent	Absent
Histology Inflammation Score	**Normal=0**	**Normal=0**	**Normal=0**	**Normal=0**

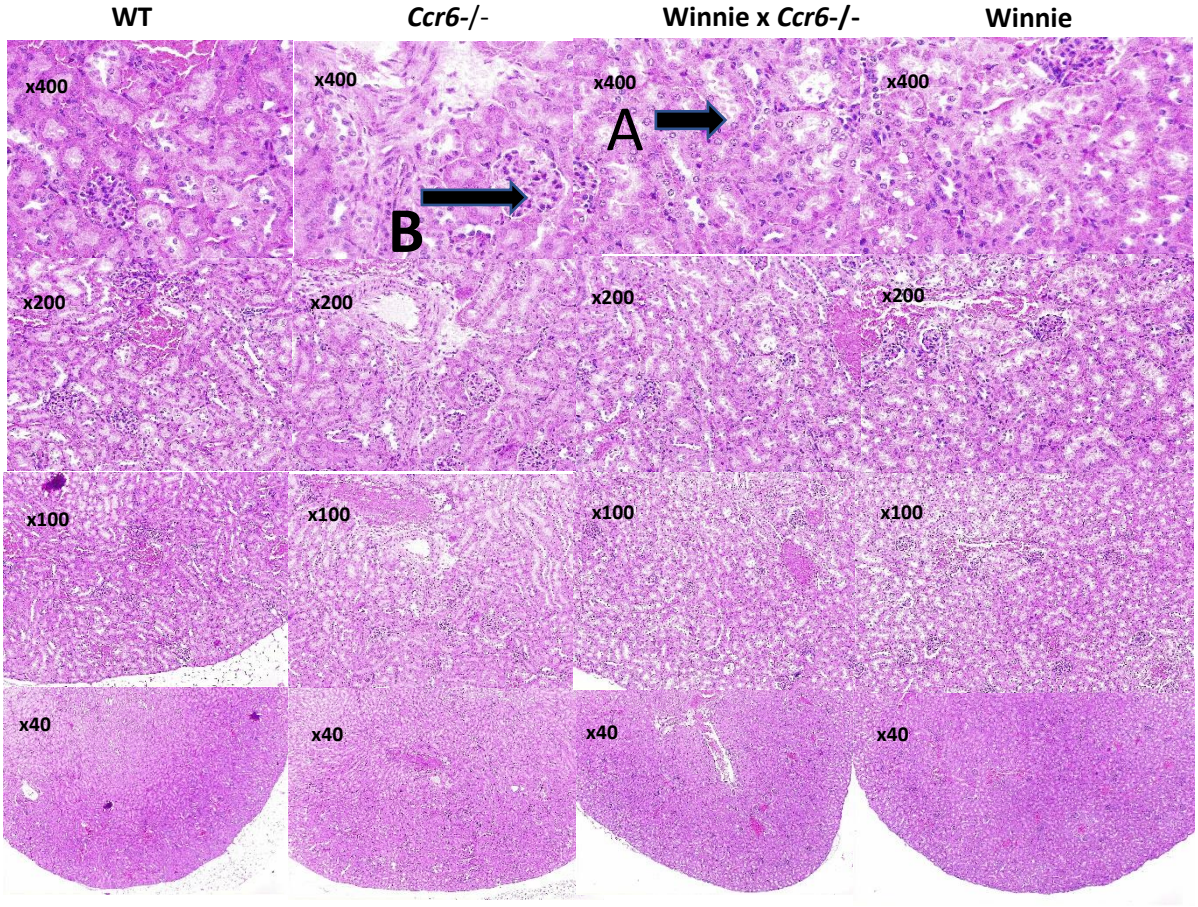

Figure 20. Representative images of H&E stained renal histology of the four genotypes, at magnification x40, x100, x200 and x400. No renal pathology was detected as per criteria in Table 26. Quantification of inflammation in both kidneys in the four genotypes at 16-22 weeks of age was made using the histopathological score given in Table 26 which yielded zero inflammation in all the genotypes tested. (A) Kidney tubule (B) Glomerulus. Data expressed as mean ± SEM by one-way analysis of variance (ANOVA) and Tukey's multiple comparison test, n=8.

3.4 *Ccr6*-deficiency reduces the lymphocyte distribution in the Spleen and MLN during colitis.

3.4.1 Gating Strategy

The gating strategy and dot plots used to quantify the lymphocyte percentages in the four genotypes in the spleen is displayed in Figure 21. In order to investigate the

relative distribution of T and B lymphocytes in the spleen, the percentages of the major surface markers ($CD4^+$, $CD8^+$ and $CD19^+$), were quantified by flow cytometry.

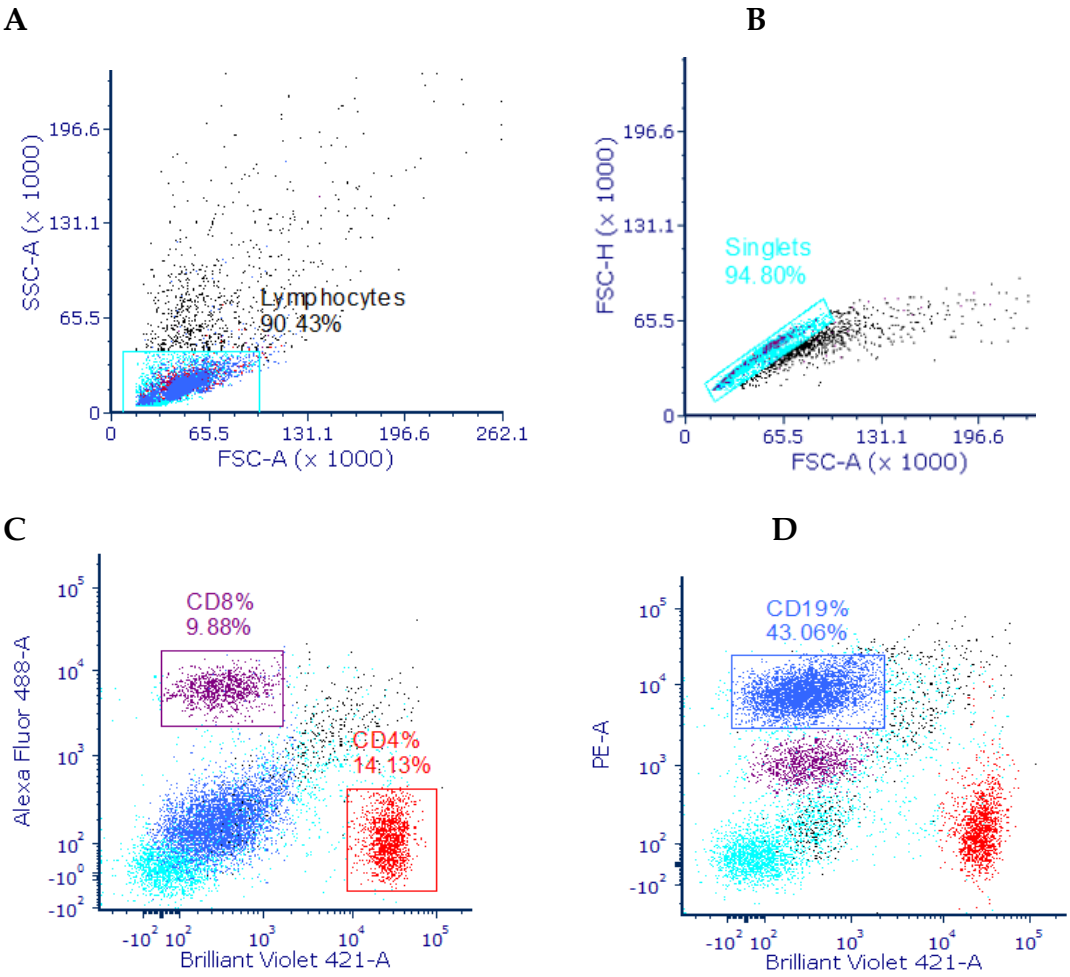

Figure 21. Flow cytometry evidence showing the gating strategy and the dot plots for obtaining the surface marker percentages. Quantification of $CD4^+$, $CD8^+$, $CD19^+$ percentage in 1 mL of splenocytes and MLN in the four genotypes at 8 and 16-22 weeks of age. (A) after gating the lymphocytes on FSC-A vs SSC-A axes (B) singlet cell population on FSC-H vs FSC-A axes, to discriminate against the doublets, (C) $CD4^+$% gated in red, $CD8^+$ % gated in maroon, and (D) $CD19^+$ % gated in blue. Over 95% of the cell population remained viable at the point of analysis.

3.4.2 T ($CD4^+$ & $CD8^+$) and B ($CD19^+$) Lymphocyte Distribution in the Spleen

Table 27. $CD4^+$ T lymphocyte mean percentage in the spleen.

	WT **Mean ± SEM**	***Ccr6-/-*** **Mean ± SEM**	**Winnie x *Ccr6-/-*** **Mean ± SEM**	**Winnie** **Mean ± SEM**
8 weeks	12.3 ± 0.8	13.55 ± 0.7	11.87 ± 0.5	12.7 ± 1.1
16-22 weeks	10.72 ± 0.6	10.86 ± 0.6	9.21 ± 0.6	8.6 ± 0.7

The differences between the splenic $CD4^+$ mean percentages were not significant at both timepoints (Table 27, Figure 21-22).

Table 28. $CD8^+$ T lymphocyte mean percentage in the spleen.

	WT **Mean ± SEM**	***Ccr6-/-*** **Mean ± SEM**	**Winnie x *Ccr6-/-*** **Mean ± SEM**	**Winnie** **Mean ± SEM**
8 weeks	7.93 ± 0.7	8.63 ± 0.53	6.83 ± 0.8	7.98 ± 0.8
16-22 weeks	6.24 ± 0.3	6.38 ± 0.17	4.1 ± 0.22	4.22 ± 0.6

The differences in splenic $CD8^+$ mean percentages between the genotypes tested were not significant at the first timepoint. There were significant differences between WT and Winnie (***p <0.001) and WT and Winnie x *Ccr6-/-* (***p <0.001) at the second timepoint (Table 28, Figure 21-22).

Table 29. CD19⁺ (B lymphocyte) mean percentages in the spleen.

	WT **Mean ± SEM**	***Ccr6*-/-** **Mean ± SEM**	**Winnie x *Ccr6*-/-** **Mean ± SEM**	**Winnie** **Mean ± SEM**
8 weeks	37.87 ± 2.98	47.33 ± 2.0	43.51 ± 1.75	34.97 ± 2.37
16-22 weeks	35.83 ± 1.4	51.42 ± 1.17	26.97 ± 1.7	28.0 ± 2.0

The differences in the splenic CD19⁺ mean percentages between the genotypes were significant between WT and *Ccr6*-/- (*p < 0.05) and *Ccr6*-/- and Winnie (**p < 0.01) at the first timepoint. There were significant differences between WT and *Ccr6*-/- (****p <0.0001), *Ccr6*-/- and Winnie x *Ccr6*-/- (****p <0.0001), WT and Winnie (**p < 0.01) and *Ccr6*-/- and Winnie (****p < 0.0001) at the second timepoint (Table 29, Figure 21-22).

(A)(i)

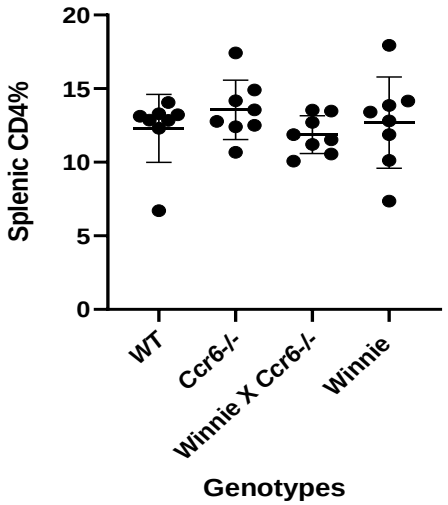

(B)(i)

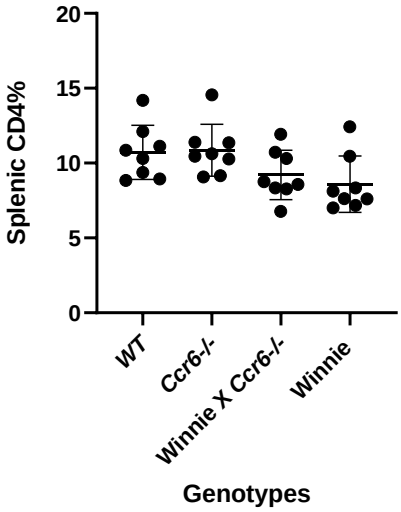

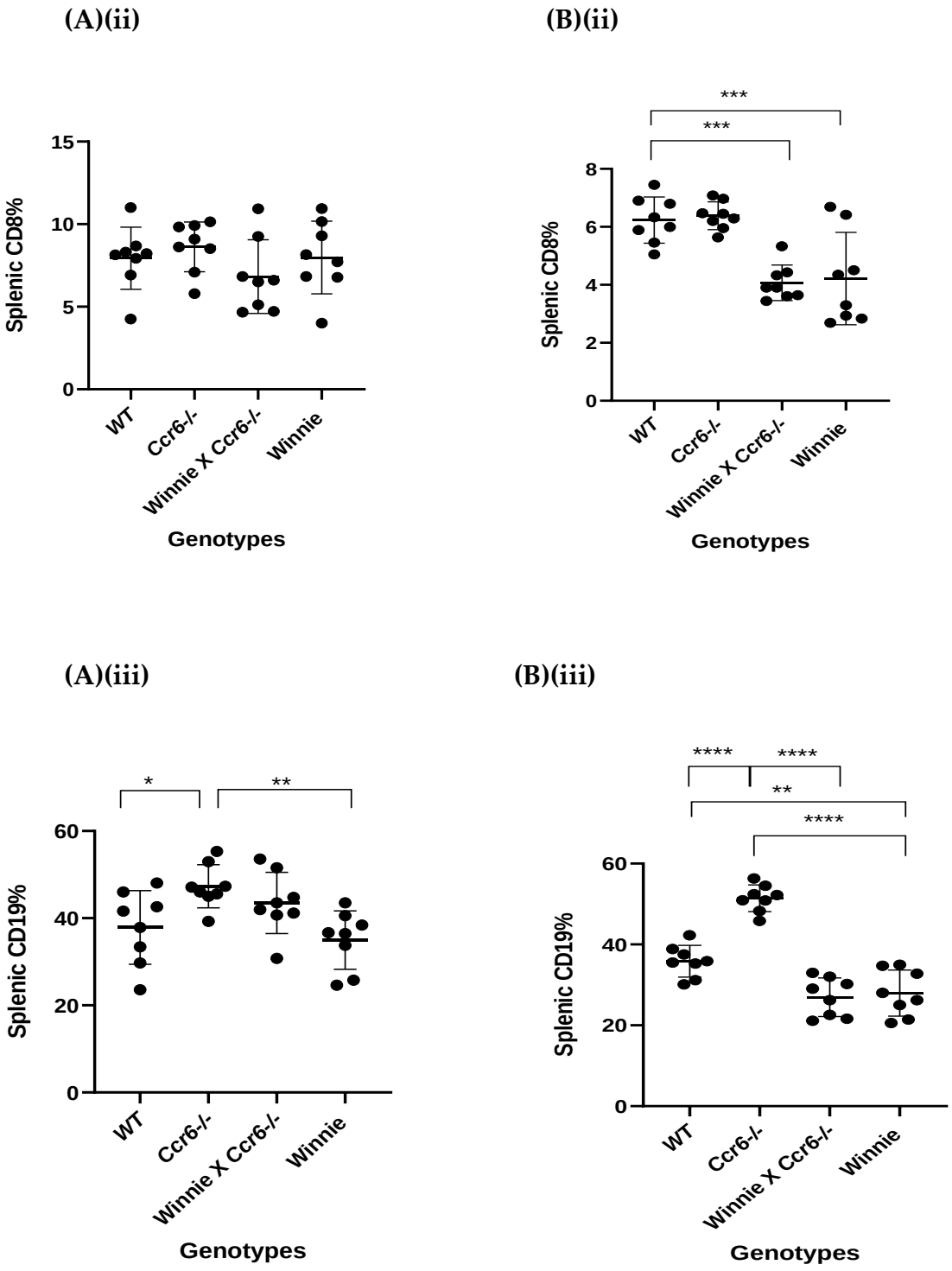

Figure 22. Quantification of splenic CD4⁺, CD8⁺ and CD19⁺ mean percentages in the four genotypes at 8 weeks of age [(A)(i), (A)(ii), (A)(iii) and at 16-22 weeks of age (B)(i), (B)(ii), (B)(iii). Spleens harvested in ice-cold PBS, RBC lysis buffer added to cell suspension, washed and suspended in FACS staining buffer. 2 x 10^7 cells per x1 mL

was stained with fluorescent-conjugated antibodies (CD4 – Brilliant violet 421, CD8 – Alexa fluor 488, CD19- PE and live/dead cell marker -IR 638) for 30 minutes on ice in the dark, washed and suspended in 200 µl of FACS buffer and analysed in a BD Canto FACS analyser with compensation and fluorescent minus one (FMO) controls. After gating the singlet cell population on FSC-H vs FSC-A axes, CD4% gated in red, CD8 % gated in maroon and CD19% gated in blue were quantified to discriminate against doublets. Over 95% of the cell population remained viable at point of analysis. Data expressed as mean ± SEM by one-way analysis of variance (ANOVA) and Tukey's multiple comparison test, n=8. (* $p< 0.05$, ** $p<0.01$, *** $p<0.001$, **** $p< 0.0001$).

3.4.3 T ($CD4^+$ & $CD8^+$) and B ($CD19^+$) Lymphocyte Distribution in the Mesenteric Lymph Nodes (MLN)

Table 30. $CD4^+$ (T lymphocyte) mean percentages in the MLN.

	WT **Mean ± SEM**	***Ccr6-/-*** **Mean ± SEM**	**Winnie x *Ccr6-/-*** **Mean ± SEM**	**Winnie** **Mean ± SEM**
8 weeks	10.7 ± 0.24	14.04 ± 0.1	6.56 ± 0.23	16.3 ± 0.4
16-22 weeks	4.66 ± 0.04	30.77 ± 0.44	22.19 ± 1.1	22.94 ± 0.1

The differences in the MLN $CD4^+$ mean percentages between the genotypes were significant between WT and Winnie x *Ccr6-/-* (*$p < 0.0001$) and *Ccr6-/-* and Winnie (**$p < 0.001$) at the first timepoint. There were significant differences between WT and *Ccr6-/-* (****$p < 0.0001$), WT and Winnie x *Ccr6-/-* (****$p <0.0001$), WT and Winnie (**$p < 0.0001$) and *Ccr6-/-* and Winnie (****$p < 0.0001$) at the second timepoint (Table 30, Figure 21,23).

Table 31. CD8⁺ (T lymphocyte) mean percentages in the MLN.

	WT **Mean ± SEM**	***Ccr6-/-*** **Mean ± SEM**	**Winnie x *Ccr6-/-*** **Mean ± SEM**	**Winnie** **Mean ± SEM**
8 weeks	13.23 ± 0.2	6.85 ± 0.13	5.35 ± 0.4	15.8 ± 0.3
16-22 weeks	3.65 ± 0.02	15.74 ± 0.6	14.87 ± 0.4	18.38 ± 0.5

The differences in the MLN CD8⁺ mean percentages between the genotypes were significant between WT and Winnie x *Ccr6-/-* (****p < 0.0001) and *Ccr6-/-* and Winnie (****p < 0.001) and Winnie x *Ccr6-/-* and Winnie (****p <0.0001). There were significant differences between WT and Winnie x *Ccr6-/-* (****p <0.0001), WT and Winnie (**p < 0.0001) and Winnie x *Ccr6-/-* and Winnie (**p < 0.001) at the second timepoint (Table 31, Figure 21,23).

Table 32. CD19⁺ (B lymphocyte) mean percentages in the MLN.

	WT **Mean ± SEM**	***Ccr6-/-*** **Mean ± SEM**	**Winnie x *Ccr6-/-*** **Mean ± SEM**	**Winnie** **Mean ± SEM**
8 weeks	13.2 ± 0.25	17.1 ± 0.35	7.0 ± 0.36	17.92 ± 0.36
16-22 weeks	4.31 ± 0.12	34.18 ± 0.12	37.69 ± 0.9	39.65 ± 0.75

The differences in the MLN CD19⁺ mean percentages between the genotypes were significant between WT and Winnie x *Ccr6-/-* (*p < 0.0001), WT and Winnie (*p < 0.0001) at the first timepoint. There were significant differences between WT and *Ccr6-/-* (****p < 0.0001), WT and Winnie x *Ccr6-/-* (****p <0.0001), WT and Winnie (**p < 0.0001) and *Ccr6-/-* and Winnie (****p < 0.0001) at the second timepoint (Table 32, Figure 21,23).

(A)(i)

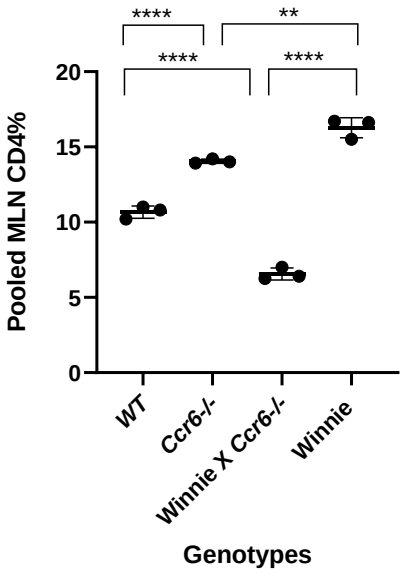
****
**
****
****
Pooled MLN CD4%
20
15
10
5
0
WT
Ccr6-/-
Winnie X Ccr6-/-
Winnie
Genotypes

(B)(i)

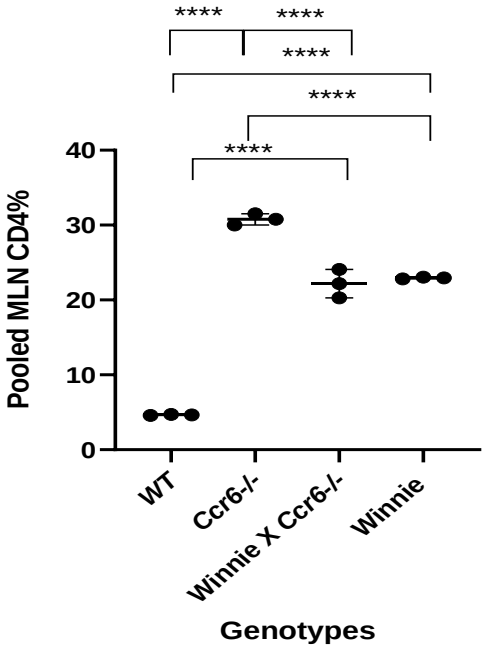
****
****
****
****
****
Pooled MLN CD4%
40
30
20
10
0
WT
Ccr6-/-
Winnie X Ccr6-/-
Winnie
Genotypes

(A)(ii)

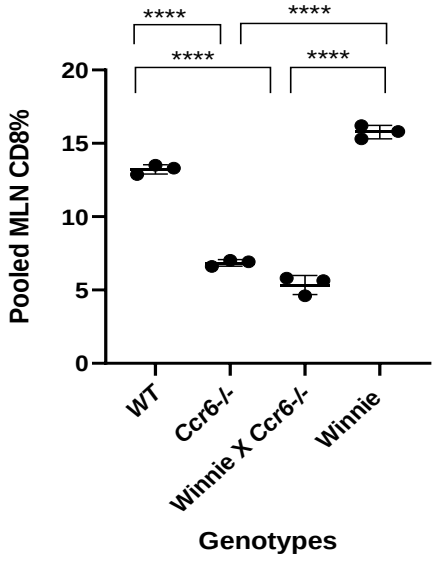
****
****
****
****
Pooled MLN CD8%
20
15
10
5
0
WT
Ccr6-/-
Winnie X Ccr6-/-
Winnie
Genotypes

(B)(ii)

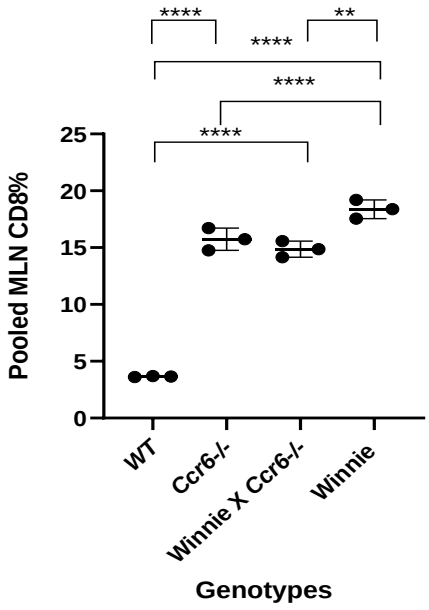
****
**
****
****
****
Pooled MLN CD8%
25
20
15
10
5
0
WT
Ccr6-/-
Winnie X Ccr6-/-
Winnie
Genotypes

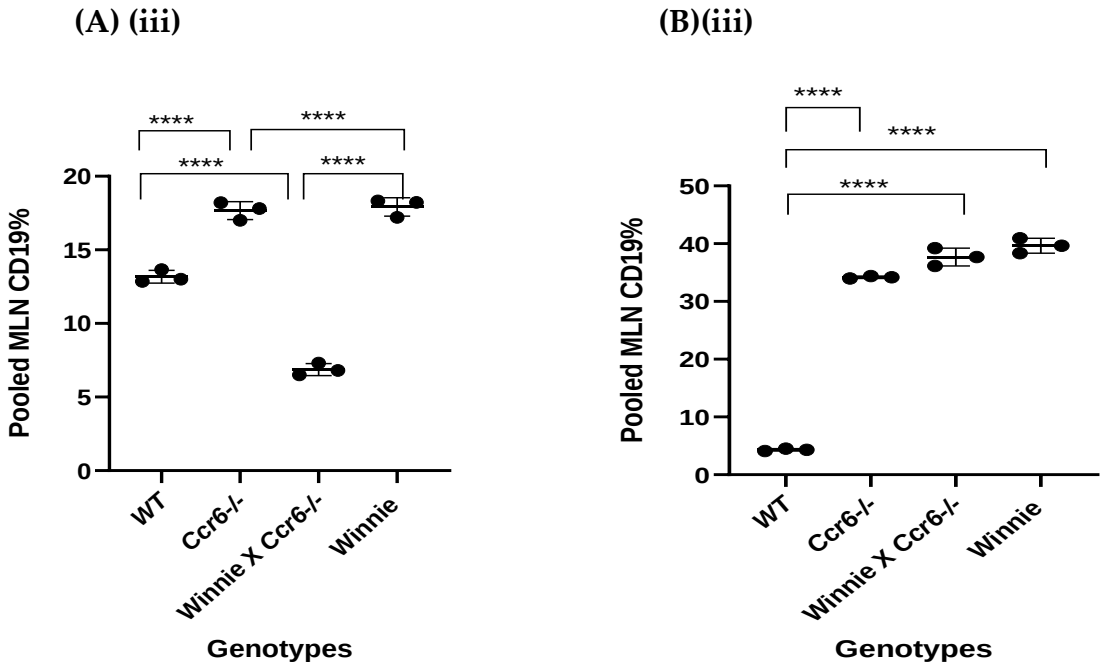

Figure 23. Quantification of MLN CD4⁺, CD8⁺ and CD19⁺ mean percentages in the four genotypes at 8 weeks of age [(A)(i), (A)(ii), (A)(iii) and at 16-22 weeks of age (B)(i), (B)(ii), (B)(iii). Pooled MLN were harvested and stored in ice-cold RPMI 1640 culture medium (Life Technologies Pty Ltd, Victoria, Australia), washed and suspended in FACS staining buffer. 2 x 10^7 cells per x1 mL was stained with fluorescent-conjugated antibodies (CD4 – Brilliant violet 421, CD8 – Alexa fluor 488, CD19- PE and live/dead cell marker -IR 638) for 30 minutes on ice in the dark, washed and suspended in 200 µl of FACS buffer and analysed in a BD Canto FACS analyser with compensation and fluorescent minus one (FMO) controls. After gating the singlet cell population on FSC-H vs FSC-A axes, CD4⁺ % gated in red, CD8⁺ % gated in maroon and CD19⁺ % gated in blue were quantified to discriminate against doublets. Over 95% of the cell population remained viable at point of analysis, (n=3 independent experiments in duplicate for MLN). Data expressed as mean ± SEM by one-way analysis of variance (ANOVA) and Tukey's multiple comparison test. (* $p< 0.05$, **$p<0.01$, ***$p<0.001$, ****$p< 0.0001$).

3.5 *Ccr6*-deficiency downregulates CCL20 and PI3K^{P}, upregulates Akt^{P} in the colon.

3.5.1 CCL20 expression pattern in the colon.

Table 33. CCL20 percentage expression in the colon at the second timepoint.

	WT **Mean ± SEM**	***Ccr6*-/-** **Mean ± SEM**	**Winnie x *Ccr6*-/-** **Mean ± SEM**	**Winnie** **Mean ± SEM**
16-22 weeks	0.006 ± 0.0003	0.012 ± 0.0003	0.014 ± 0.0003	0.015 ± 0.0003

A significant difference in the CCL20 percentage expression in the colon existed between WT and Winnie (****p <0.0001) and Winnie x *Ccr6*-/- and Winnie (*p < 0.05) at the second timepoint [Table 33, Figure 24 (a) A-D, b(i)].

3.5.2 Phosphorylated Phosphoinositide 3-kinase (PI3K^{P}) expression pattern in the colon.

Table 34. PI3K^{P} percentage expression in the colon at the second timepoint.

	WT **Mean ± SEM**	***Ccr6*-/-** **Mean ± SEM**	**Winnie x *Ccr6*-/-** **Mean ± SEM**	**Winnie** **Mean ± SEM**
16-22 weeks	0.05 ± 0.001	0.011 ± 0.001	0.014 ± 0.0003	0.03 ± 0.001

A significant difference in the PI3K^{P} percentage expression in the colon existed between WT and Winnie (****p <0.0001) and Winnie x *Ccr6*-/- and Winnie (****p < 0.0001) at the second timepoint [Table 34, Figure 24 (a) E-H, b(ii)].

3.5.3 Phosphorylated Akt (Akt^P) expression pattern in the colon.

Table 35. AKT^P percentage expression in the colon.

	WT **Mean ± SEM**	***Ccr6-/-*** **Mean ± SEM**	**Winnie x *Ccr6-/-*** **Mean ± SEM**	**Winnie** **Mean ± SEM**
16-22 weeks	0.007 ± 0.0003	0.009 ± 0.001	0.02 ± 0.001	0.015 ± 0.0003

A significant difference in the AKT^P percentage expression in the colon existed between WT and Winnie (****p <0.0001) and Winnie x *Ccr6-/-* and Winnie (****p < 0.0001) at the second timepoint [Table 35, Figure 24(a) I-L b(iii)].

(a)

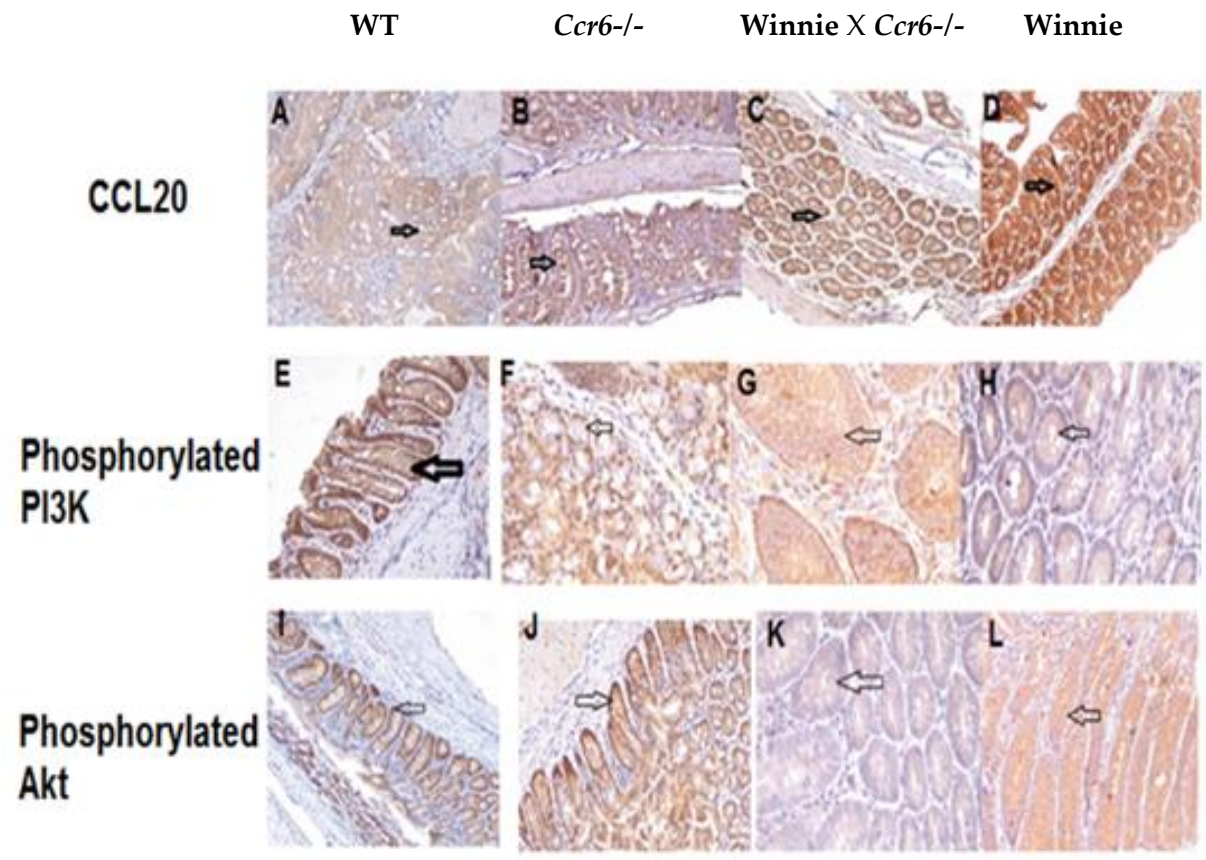

b) (i)

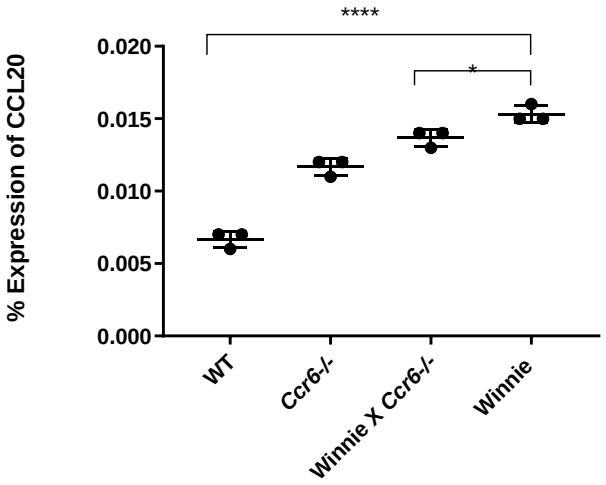
****
*
0.020
0.015
0.010
0.005
0.000
% Expression of CCL20
WT
Ccr6-/-
Winnie X Ccr6-/-
Winnie

(b)(ii)

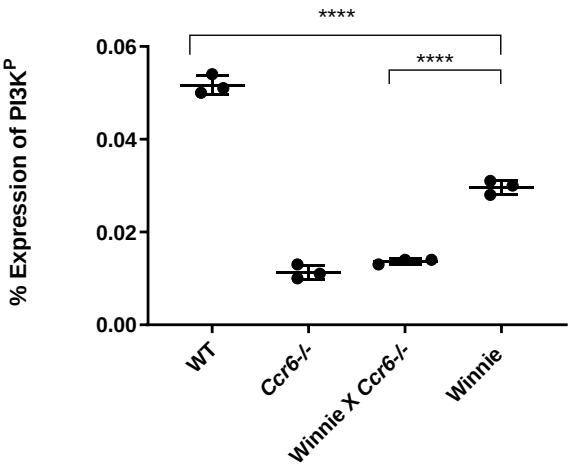
****
****
0.06
0.04
0.02
0.00
% Expression of PI3K P
WT
Ccr6-/-
Winnie X Ccr6-/-
Winnie

(b)(iii)

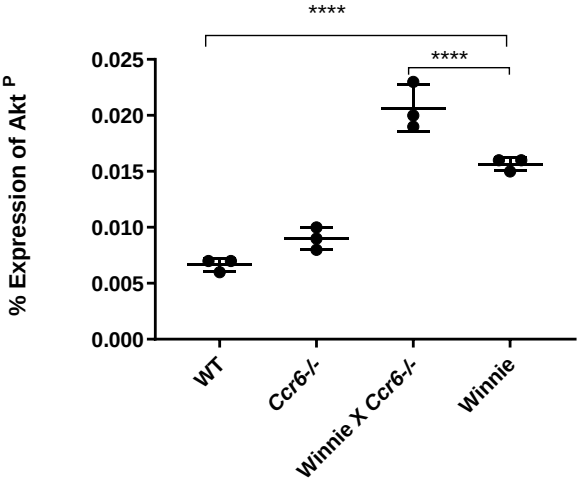
****
****
0.025
0.020
0.015
0.010
0.005
0.000
% Expression of Akt P
WT
Ccr6-/-
Winnie X Ccr6-/-
Winnie

Figure 24. Comparison of the CCL20 [Table 33, (a)(A-D), (b)(i)], phosphorylated PI3K [Table 34, (a) (E-H), (b)(ii)] and phosphorylated Akt [Table 35, (a) (I-L), (b)(iii)] mean percentage expression pattern in the colon in the four genotypes at 16-22 weeks. Arrow indicates brown colour which determines the presence of DAB chromogen bound to anti-CCL20 -anti-mouse primary antibody, anti-$PI3K^{P}$ - anti-mouse primary antibody, anti-Akt^{P} - anti-mouse primary antibody respectively, magnified at x200. The mean percentage (%) expression of (b)(i) CCl20, (b)(ii) $PI3K^{P}$ and (b)(iii) Akt^{P} quantified by Fiji image J software. Percentage expression of intensity was calculated by the formula; optical density (OD) = log (maximum intensity/mean intensity), where max intensity = 255 for 8-bit images using Fiji Image J Version 1.64 software for windows 7 (Scijava Software Inc, USA). Data expressed as mean $\pm$ SEM by one-way analysis of variance (ANOVA) and Tukey's multiple comparison test, n=3 independent experiments in duplicate. (* $p< 0.05$, ** $p<0.01$, *** $p<0.001$, **** $p< 0.0001$).

3.6 *Ccr6*-deficiency suppress the TH1 and TH17 lymphocyte immune responses during colitis and upregulates IL-10.

Table 36. The cytokine expression evaluated by RT-PCR, divided into respective immune responses of the T helper lymphocyte populations.

TH1	**TH2**	**TH17**	**Treg**
IFN-γ	IL-4	IL-17A	IL-10
TNF-α	IL-6	IL-23R	
IL-18	IL-13		

3.6.1 TH1 cytokine mRNA expression in the colon.

Table 37. Mean fold change expression of mRNA in IFN-γ normalized to WT.

	WT **Mean ± SEM**	***Ccr6*-/-** **Mean ± SEM**	**Winnie x *Ccr6*-/-** **Mean ± SEM**	**Winnie** **Mean ± SEM**
8 weeks	1.0 ± 0	0.7 ± 0.3	0.9 ± 0.7	10.0 ± 0.2
16-22 weeks	1.0 ± 0	2.0 ± 0.1	3.0 ± 0.2	3.0 ± 0.2

A significant difference in the mean fold change expression of mRNA in IFN-γ existed between Winnie x *Ccr6*-/- and Winnie (****p <0.0001) at the first timepoint and between the WT and Winnie (****p <0.0001) at both timepoints [Table 37, Figure 25 (A)].

Table 38. Fold change expression of mRNA in TNF-α normalized to WT.

	WT **Mean ± SEM**	***Ccr6*-/-** **Mean ± SEM**	**Winnie x *Ccr6*-/-** **Mean ± SEM**	**Winnie** **Mean ± SEM**
8 weeks	1.0 ± 0	0.94 ± 0.04	2.6 ± 0.1	10 ± 0.2
16-22 weeks	1.0 + 0	1.0 ± 0.2	3.3 ± 0.1	4.7 ± 0.3

A significant difference in the mean fold change expression of mRNA in TNF-α existed between Winnie x *Ccr6*-/- and Winnie (****p <0.0001) at the first timepoint and between the WT and Winnie (****p <0.0001) at both timepoints [Table 38, Figure 25 (A)].

Table 39. Fold change expression of mRNA in IL-18 normalized to WT.

	WT **Mean ± SEM**	***Ccr6*-/-** **Mean ± SEM**	**Winnie x *Ccr6*-/-** **Mean ± SEM**	**Winnie** **Mean ± SEM**
8 weeks	1.0 ± 0	1.0 ± 0.02	5.0 ± 0.2	39.17 ± 1.0
16-22 weeks	1.0 + 0	12.0 ± 0.2	5.0 ± 0.23	12.3 ± 0.4

A significant difference in the mean fold change expression of mRNA in IL-18 existed between Winnie x *Ccr6-/-* and Winnie (****p <0.0001), WT and Winnie (**** p< 0.0001) at both timepoints and between *Ccr6-/-* and both Winnie x *Ccr6-/-* and Winnie (****p <0.0001) at the first timepoint [Table 39, Figure 25 (A)]

3.6.2 TH2 cytokine mRNA expression in the colon.

Table 40. Fold change expression of mRNA in IL-4 normalized to WT.

	WT **Mean ± SEM**	***Ccr6-/-*** **Mean ± SEM**	**Winnie x *Ccr6-/-*** **Mean ± SEM**	**Winnie** **Mean ± SEM**
8 weeks	1.0 ± 0	0.3 ± 0.1	1.15 ± 0.2	35.0 + 0.4
16-22 weeks	1.0 + 0	0.5 ± 0.1	5.6 ± 0.4	8.0 ± 0.2

A significant difference in the mean fold change expression of mRNA in IL-4 existed between the WT and Winnie (****p <0.0001), WT and Winnie x *Ccr6-/-* (****p <0.0001) and between Winnie x *Ccr6-/-* and Winnie (****p <0.0001) at both timepoints [Table 40, Figure 25 (B)].

Table 41. Fold change expression of mRNA in IL-6 normalized to WT.

	WT **Mean ± SEM**	***Ccr6-/-*** **Mean ± SEM**	**Winnie x *Ccr6-/-*** **Mean ± SEM**	**Winnie** **Mean ± SEM**
8 weeks	1.0 ± 0	0.4 ± 0.02	3.0 ± 0.12	9.0 ± 0.2
16-22 weeks	1.0 + 0	1.12 ± 0.14	1.2 ± 0.24	3.0 ± 0.2

A significant difference in the mean fold change expression of mRNA in IL-6 existed between the WT and Winnie (****p <0.0001) at both timepoints and Winnie x *Ccr6-/-*

and between Winnie x *Ccr6-/-* and Winnie (****p <0.0001) at the second timepoint [Table 41, Figure 25 (B)].

Table 42. Fold change expression of mRNA in IL-13 normalized to WT.

	WT **Mean ± SEM**	***Ccr6-/-*** **Mean ± SEM**	**Winnie x *Ccr6-/-*** **Mean ± SEM**	**Winnie** **Mean ± SEM**
8 weeks	1.0 ± 0	0.4 ± 0.1	2.0 ± 0.23	22.0 ± 0.44
16-22 weeks	1.0 + 0	1.1 + 0.14	4.0 ± 0.3	5.0 ± 0.2

A significant difference in the mean fold change expression of mRNA in IL-13 existed between Winnie x *Ccr6-/-* and Winnie (****p <0.0001) at the first timepoint and between the WT and Winnie (****p <0.0001) at both timepoints [Table 42, Figure 25 (B)].

3.6.3 TH17 cytokine mRNA expression in the colon.

Table 43. Fold change expression of mRNA in IL-17A normalized to WT.

	WT **Mean ± SEM**	***Ccr6-/-*** **Mean ± SEM**	**Winnie x *Ccr6-/-*** **Mean ± SEM**	**Winnie** **Mean ± SEM**
8 weeks	1.0 ± 0	1.13 ± 0.14	2.5 ± 0.3	35.0 ± 0.5
16-22 weeks	1.0 + 0	0.93 ± 0.04	0.63 ± 0.1	1.2 ± 0.12

A significant difference in the mean fold change expression of mRNA in IL-17A existed between the WT and Winnie x *Ccr6-/-* (****p <0.0001) and Winnie x *Ccr6-/-* and Winnie (****p <0.0001) at the second timepoint [Table 43, Figure 25 (C)].

Table 44. Fold change expression of mRNA in IL-23R normalized to WT.

	WT **Mean ± SEM**	***Ccr6*-/-** **Mean ± SEM**	**Winnie x *Ccr6*-/-** **Mean ± SEM**	**Winnie** **Mean ± SEM**
8 weeks	1.0 ± 0	0.3 ± 0.01	1.0 ± 0.5	62.0 ± 0.3
16-22 weeks	1.0 + 0	0.3 ± 0.01	2.0 ± 0.03	2.0 ± 0.13

A significant difference in the mean fold change expression of mRNA in IL-23R existed between the WT and Winnie x *Ccr6*-/- (****p <0.0001) and Winnie x *Ccr6*-/- and Winnie (****p <0.0001) at the second timepoint [Table 44, Figure 25 (C)].

3.6.4 Anti-inflammatory (Treg) cytokine mRNA expression in the colon.

Table 45. Fold change expression of mRNA in IL-10 normalized to WT.

	WT **Mean ± SEM**	***Ccr6*-/-** **Mean ± SEM**	**Winnie x *Ccr6*-/-** **Mean ± SEM**	**Winnie** **Mean ± SEM**
8 weeks	1.0 ± 0	2.0 ± 0.1	1.0 ± 0.2	70.0 ± 1.5
16-22 weeks	1.0 + 0	2.6 ± 0.1	4.3 ± 0.2	4.2 ± 0.12

A significant difference in the mean fold change expression of mRNA in IL-10 existed between the WT and Winnie x *Ccr6*-/- (****p <0.0001) and Winnie x *Ccr6*-/- and Winnie (****p <0.0001) at the second timepoint [Table 45, Figure 25 (D)].

(A) **TH1 Immune Response**

IFN-γ (8 Weeks)

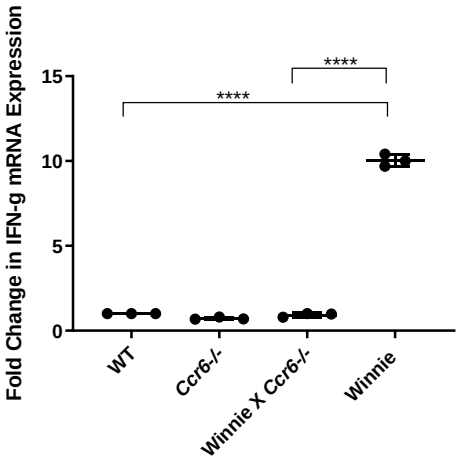

IFN-γ (16-22 weeks)

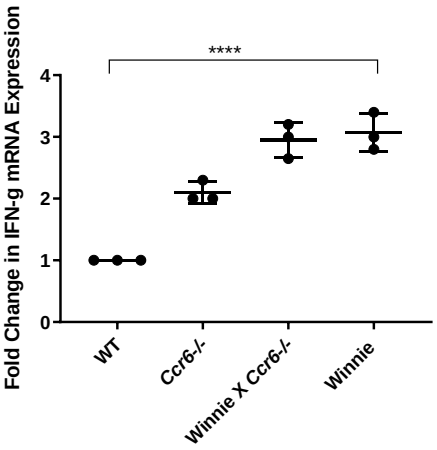

TNF- α (8 Weeks)

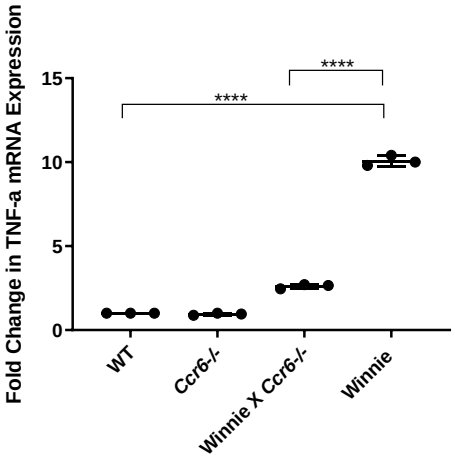

TNF-α (16-22 weeks)

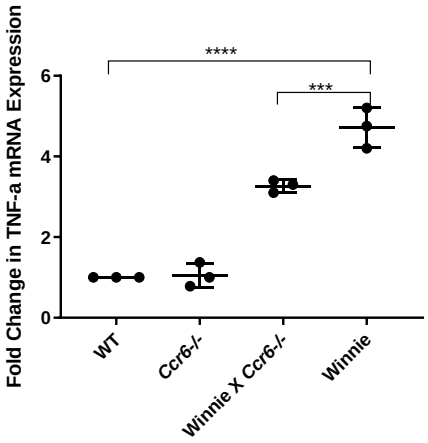

IL-18 (8 Weeks)

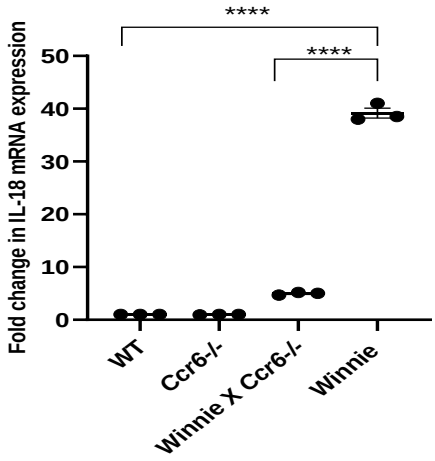

IL-18 (16-22 weeks)

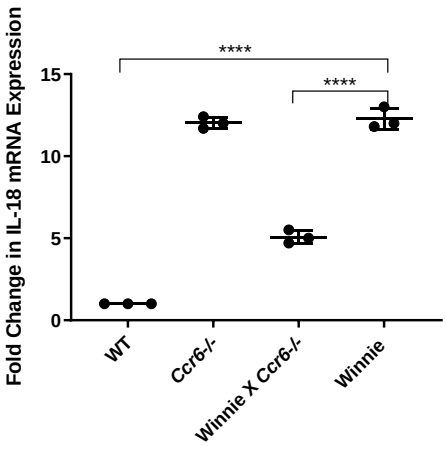

(B) **TH2 Immune Response**

IL-4 (8 Weeks)

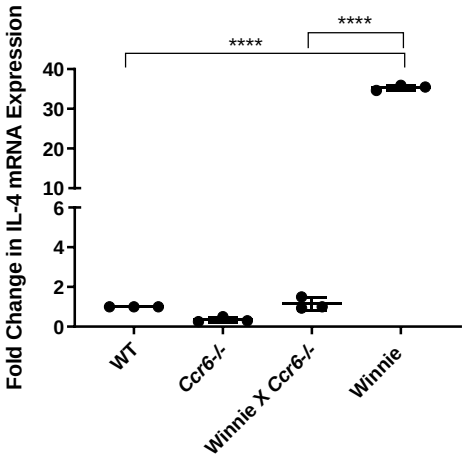

IL-4 (16-22 weeks)

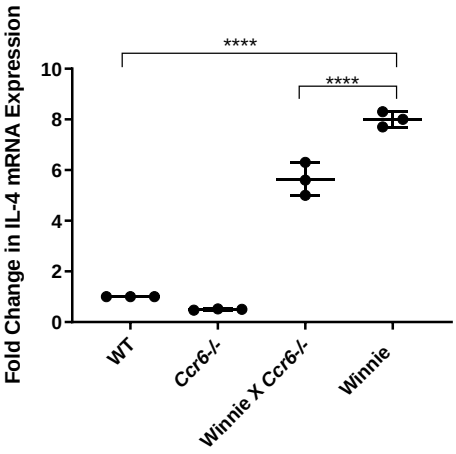

IL-6 (8 Weeks)

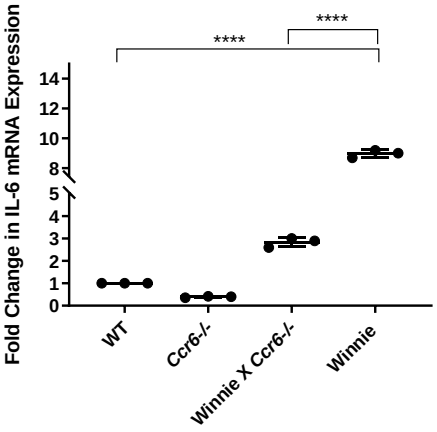

IL-6 (16-22 weeks)

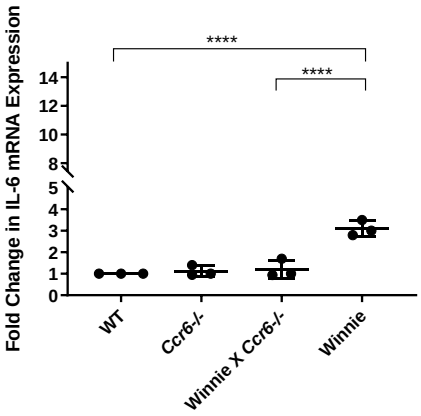

IL-13 (8 Weeks)

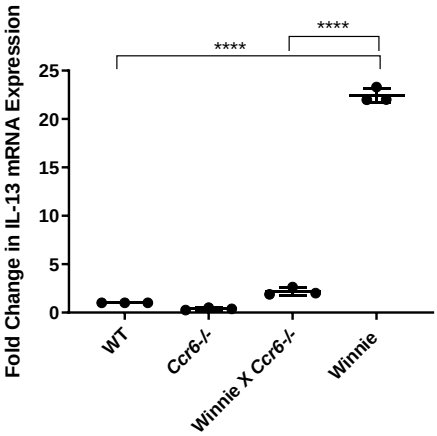

IL-13 (16-22 weeks)

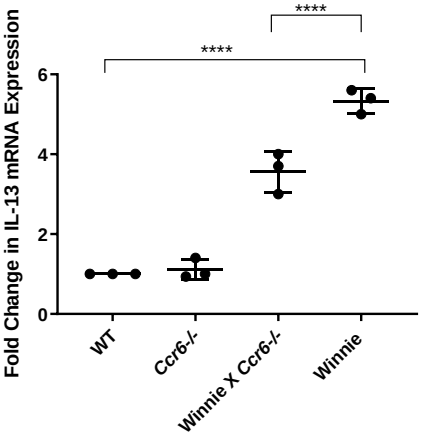

(C) **TH17 Immune Response**

IL-17A (8 Weeks)

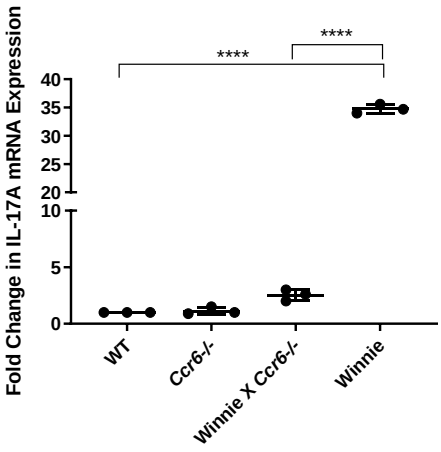

IL-17A (16-22 Weeks)

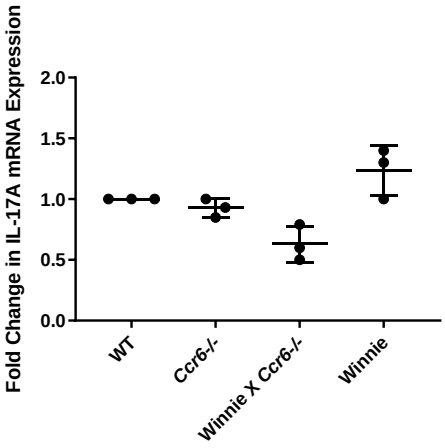

IL-23R (8 Weeks)

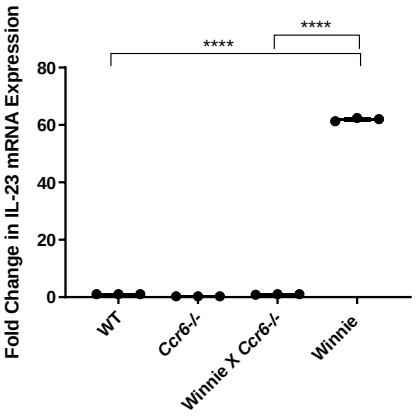

IL-23R (16-22 Weeks)

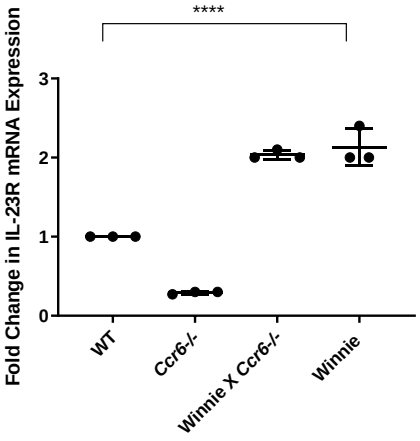

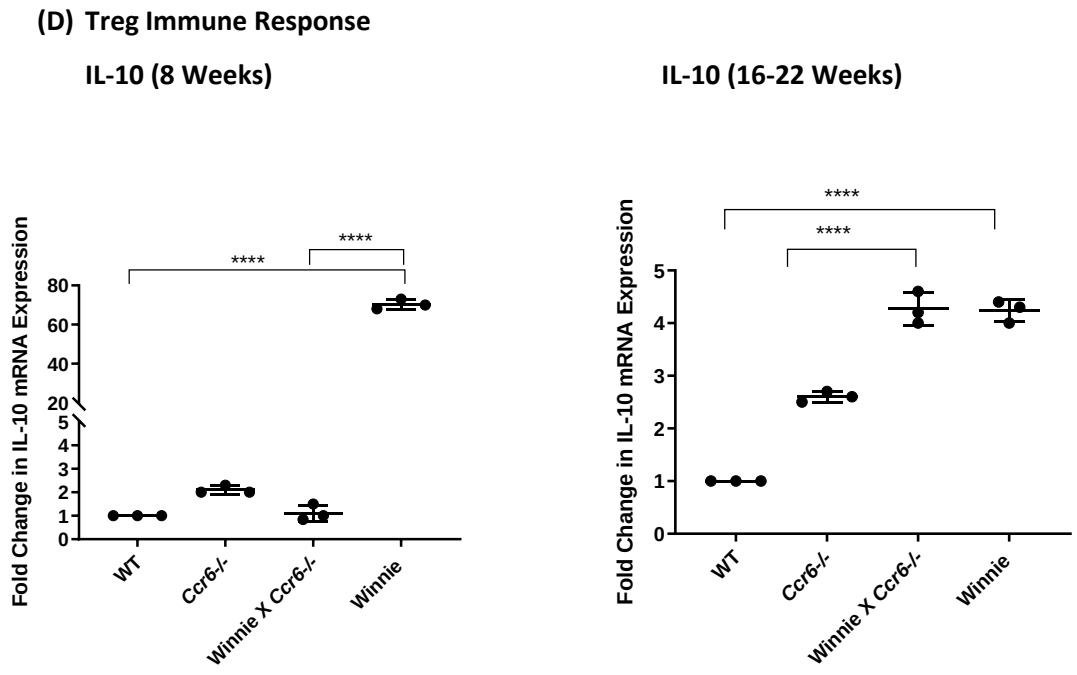

Figure 25. Fold change in mRNA expression of (A) IFN-g, TNF-α, IL-18, (B) IL-4, IL-6, IL-13, (C) IL-17A, IL-23R, (D) IL-10 at 8 weeks and 16-22 weeks. Cycle of threshold (CT) values were normalised to *Gapdh* and CT calculated using the method of $2^{-\Delta CT}$. Data expressed as mean $\pm$ SEM by one-way analysis of variance (ANOVA) and Tukey's multiple comparison test, n=3 independent experiments in duplicate. (**p<0.01, *** p<0.001, ****p<0.0001).

4.0 Discussion

The purpose of this investigation was threefold: (i) to identify the phenotype of Winnie x *Ccr6*-/-, a novel colitis mouse model, and to evaluate the immunological impact of *Ccr6* gene deficiency, (ii) in multi-organ pathophysiology and (iii) it's role in molecular signalling, during the manifestation of spontaneous chronic colitis. The results of this study have demonstrated that CCR6 plays a pathogenic role during the development of chronic colitis. As a direct result of *Ccr6*-deficiency during the continuance of colitis in Winnie, the following salient features were observed: (i) distinct reduction of inflammation in the colon, spleen and liver; (ii) absence of renal

pathology; (iii) suppressed TH1, TH17 immune responses with upregulated TH2 and Treg immune responses in the colon; (iv) restrained production and egression of lymphocytes from the spleen; (v) high lymphocyte proliferation within the mesenteric lymph nodes; and (vi) increased production of CCL20 and phosphorylated Akt (Akt^P) with decreased production of phosphorylated PI3K ($PI3K^P$) in the colon.

Both human and mice systems have provided evidence for the inflammatory role played by the CCR6-CCL20 axis in the progression and pathogenicity of several autoimmune disorders, as well as IBD (42). Winnie x *Ccr6*-/- was derived from crossing littermates of Winnie mice (Figure 5), which were a male with m/m, *Ccr6*-/- and a female with m/m, *Ccr6*-/- which produced a double homozygous knockout (m/m and *Ccr6*-/-) and all the mice groups investigated in this study were of C57BL/6J mouse (strain) background. The experimental model thus produced a similar but relatively less severe intestinal inflammation that mimics human colitis (119).

The Winnie mouse model, as a tool which resembles chronic colitis has multiple advantages in comparison to other contrived colitis models which include: (i) chemically induced models such as DSS and TNBS - induced colitis (which has no need to use toxic chemicals) (120), (121), (ii) adoptive T cell transfer induced colitis (induced in an artificial immune deficient system and lacks adaptive immunity) (108) and (iii) genetically engineered models of colitis (which show complete deficiency of immune functions) (122). This is because, in Winnie x *Ccr6*-/-, (i) the disease manifests as spontaneous colitis (123), (110); (ii) it mimics human UC (124); (iii) it doesn't cause severe tissue damage (110); and (iv) it maintains an intact, normal immune system in comparison to T cell transfer models (110). Additionally, inflammation in Winnie naturally occurred at 6 weeks (124) and was found to progress with age by the present study.

A gain in the colon weight is considered as a sign of increasing inflammation (Table 14, Figure 7), however, it may have been due to either natural growth (as there was a difference of about 12 weeks between the first and second timepoints and the BMI was

not calculated), increased fat metabolism and/or concurrent inflammation. However, *Ccr6* - deficiency appears to reduce fat metabolism as CCR6-expressing adipocytes are implicated in obesity (42). Although all the mice involved in this study were fed with the same diet, autoclaved water and were raised in a temperature and humidity controlled aseptic environment, they displayed varying growth rates and susceptibility to inflammation, which indicated differences in the gut microbiome, physiology and the genetic makeup.

The body weight (Table 16, Figure 9) progressively decreased in Winnie owing to the developing inflammation because colitis takes full effect as early as 8 weeks of age. Winnie x *Ccr6*-/- did not lose weight to the same extent as Winnie and indicated subdued inflammation and suppression of weight - losing physiological mechanisms that were responsible for Winnie's remarkable weight loss. In the experimental model, both the weight gain mechanisms and features of inflammation in the colon tissue such as, fluid retention, oedema, reddening, vasculature and tissue injury, were all moderate and reduced, than those of Winnie (Table 20, Figures 11, 13) (123).

The physiological mechanisms which increased fat metabolism and inflammation because of ER or oxidative stress (due to misfolded protein response) may become the reasons for the significant weight increase in the colon and the loss of body weight observed in Winnie, acting alongside impaired innate and adaptive immunity (125). All the mice in this study were fed with a normal chow diet which contained less than 10% of saturated fat, since prolonged high fat diets (HFD) had induced low-grade chronic intestinal inflammation in mice. Diets high in saturated fat are a known risk factor in the development of human IBD (125).

The gross colon morphology (Table 18, Figure 11), the moderate DAI (Table 19, Figure 12), and the auxiliary inflammation that was visible in Winnie x *Ccr6*-/-, are further validated by its colon histology scores [Table 20, Figure 13 (b)] and the immunological (cytokine) profile (Figure 36) which may have arisen from the loss of CCR6 – driven immune mechanisms in the *Ccr6*-deficient mice that were tested. All the pre-clinical

parameters described above lead to the conclusion that *Ccr6* deficiency renders Winnie with reduced colitis.

Our data is in complete agreement with the results obtained by several research groups that had utilised the *Ccr6*- deficient mouse systems. For example, *Ccr6*-deficient mice induced by DSS had displayed reduced susceptibility to the disease (40) while TNBS - induced colitis was attenuated by blocking the release of CCL20 (126). The adoptive transfer of $CCR6^{+}$ CD4 T cells into recipient recombination activation gene 2 (Rag2-/-) mice also caused aggravated disease (127).

The CCR6-CCL20 axis plays a pivotal role in maintaining immune homeostasis in the gut (39). It produces immune tolerance against the plethora of infectious luminal microbes which penetrate the gut mucosa and simultaneously step up immunity against many other disease-causing secondary contributing factors. When the purported immune tolerance breaks down, the phenomenal TH17 *Vs* Treg imbalance paradigm comes into play either by increased multiplication of pro-inflammatory immune cells such as $CCR6^{+}$TH17 and $CCR6^{+}$TH1, or by immune mechanisms that suppress the production of $FOXP3^{+}$ -induced $CCR6^{+}$Treg cells (127). These mechanisms are empowered by CCR6 which mainly functions in the roles of directing T lymphocyte development and differentiation, and immune cell chemotaxis which stimulate a cascade of accessory molecules and cytokines in the colon.

The attenuation of inflammation was corroborated by the colonic histomorphology [with increased goblet cell numbers (Figure 14] which stimulated an increased production of mucus) seen in the study model in comparison to Winnie [which has deficient mucus generation (Figure 14 (b)]. Features of acute disease histology were less prominent in Winnie x *Ccr6* -/- with all the general criteria used in the assessment being markedly reduced, showing a milder inflammatory status which correlated well with the pre-clinical parameters.

In addition to having pathology within the gastrointestinal tract, IBD patients also exhibit secondary organ pathologies termed as extraintestinal manifestations (128). The spleen, liver and kidneys which are immune-related organs of secondary lymphoid origin were examined as the systemic diseases - hepatitis and glomerular nephritis stem within these organs, where CCR6 played a pivotal role in initiating inflammation (65), (129), (130), (131). There was a significant difference in the histopathology scores and the recurring spread of inflammation in colon tissue between Winnie x *Ccr6*-/- and Winnie and the same trend was continued in spleen (Table 22, Figure 16) and liver (Table 24, Figure 18) histopathological scores at the second time point (at 16-22 weeks of age) of this study.

It is evident that inflammation in the colon also renders them with splenomegaly although the available literature on spleen weight is inconclusive because colitis had mostly induced hypo-splenism in colitis patients (132). Spleen size was not related to site or extent of disease, or to recurrence, but a wide variation of spleen size was seen within inflammatory bowel disease which suggests that more sophisticated tests of splenic function might show a closer correlation with disease patterns (133). Splenomegaly had resulted in Winnie mice probably because of inflammation in the colon during the late disease stage as the red pulp mostly contains lymphocytes, macrophages and a higher proportion of red blood cells (133).

The liver weight (Table 23, Figure 17) indicated that inflammation in the gut was slow to spread to the liver *via* the gut-liver axis. Dissemination of inflammatory cells from the gut across the hepatic portal circulation did not appear to spread the inflammation in mice during early disease, as there was no infiltration of immune cells in the portal tracts, which was also confirmed by their liver histomorphology.

A similar trend to the spleen weight variation was observed in the liver weight with a progressive weight increase from the WT to Winnie during the late disease stage. It is well known that hepatobiliary complications are associated with colitis in clinical investigations (134) and similarly, infiltration of inflammatory cells were observed in

the liver histology specimens. The inflammation was more in Winnie compared to Winnie x *Ccr6*-/-, again confirming that *Ccr6*-deficiency could attenuate inflammation in the liver and there is dissemination of immune cells *via* the gut liver axis in Winnie mice during the late disease stage of colitis.

Liver pathology (Table 24, Figure 18) indicated significant lobular inflammation in Winnie with milder inflammation in the *Ccr6*-deficient Winnie (135). There are reports of concomitant hepatobiliary manifestations in IBD patients, the most common complication being primary sclerosing cholangitis (PSC) (136). Consistent with the mild inflammation seen in this study, there were no granulomas, hepatic abscesses, amyloidosis, and gallstones which are traditionally observed in CD or PSC and autoimmune hepatitis which are usually described in UC patients (136). One of the significant observations from this investigation was that *Ccr6*-deficiency serves to reduce the disease severity in the liver and spleen of the colitis-afflicted mice.

The kidney weight (Table 25, Figure 19) showed significant differences which indicated impaired renal growth. However, renal histology scores (Table 26, Figure 20) showed that the kidneys were free of inflammation in all the genotypes that were tested. In Winnie mice, colitis failed to induce any signs of renal infection or inflammation even at the second time point albeit there was evidence of worsened inflammation in *Ccr6*-deficient nephritic mice (65), because, compared to their WT, *Ccr6* -deficiency in those mice had induced reduced infiltration of regulatory T cells (Treg cells) and TH17 cells but not the TH1 type into the kidney tissue (137).

$CCR6^{+}$ TH17 cells possess dual capability; of either transforming into anti-inflammatory, Treg cells or remaining as the pro-inflammatory TH17. This is a critical turning point in IBD immunopathogenesis which is ascribed to an imbalance of the TH17/Treg paradigm associated with disease resolution (138), (89). The quantification of TH17 and Treg cell subsets would have been more informative although it was considered as fitting beyond the scope of this study. The genetic resilience and impaired migratory capacity of immune cells to the kidneys also may have been the

reasons behind Winnie mice not becoming susceptible to renal disease even during the late stages of colitis.

$CD4^+$, $CD8^+$ (T cells) and $CD19^+$ (B cells) are major surface markers of the T and B lymphocyte repertoire in the spleen. A declining trend of $CD4^+$, $CD8^+$ and $CD19^+$ immune cell percentages in the spleen was observed at the second time point in Winnie and Winnie x *Ccr6*-/- with the WT having the highest percentage of the T cells (Table 27-29, Figure 21-22).

Heightened inflammation in Winnie could have caused an imbalance in the immune responses of T and B lymphocytes [probably within the TH1, TH2, TH17, Treg and the regulatory B cells (Breg) subsets] produced in the spleen because they are fewer in number. The impact of *Ccr6*-deficiency on lymphocyte production in the spleen was to suppress the effector cell mobilization and cause dysfunctional lymphocyte egression from the spleen. FTY720, an inhibitor of the sphingosine 1 phosphate receptor (SIP1) agonist, has been shown to restrict CD4 T lymphocyte egression from lymph nodes during the disease course of allergic diarrhoea (139). *Ccr6* - deficiency in Winnie perhaps produced similar SIP1 receptor inhibition reactivity resulting in diminished CD4 lymphocyte egression from the spleen during chronic colitis.

The activated, effector T cells perpetuate inflammation in the gut and hence, cause tissue destruction in the gut-mucosal system (140). $CD4^+$ T cells in the intestines of IBD patients were markedly high possibly owing to enhanced influx and activation with decreased apoptosis (141). Several gut-homing receptors such as CCR9 and $\alpha 4\beta 7$ are selectively induced on T cells during their priming in intestinal inflamed sites (142). A study which had blocked the migration of activated leukocytes into the inflamed tissue by specific antibodies such as vedolizumab had appeared highly effective (140). Nevertheless, T cells remain the key players in IBD. Targeting either T-cell migration or the use of regulatory T cells appear to be the most promising T-cell -activated therapies in colitis (141). Hence *Ccr6*-deficiency which induced negative chemotaxis

of leukocytes may have contributed towards alleviation of inflammation in the colon (140), (143).

Both immunodeficient SCID and Rag1-/- mice showed no disease development when given mature $CD4^+$ CD45RB High T cells. The reason was that the donor cells consisted of regulatory T cells which up-regulated immune tolerance, and were present among the mature effector T cell population, whereas the recipient mice given either partially or naïve T cells developed a wasting disease (144).

The present study has shown that *Ccr6*-deficiency serves to attenuate disease and plays a beneficial role owing to defective chemotaxis of proinflammatory immune cells with subsequent suppression of proinflammatory cytokines in the colon (Table 37-39, Figure 25) (39). However, the role played by CCR6 in an inflammatory setting remains obscure, because there are opposing arguments that CCR6-deficiency aggravates disease in mice having colitis (145). CCR6(+) Treg cells were characterized as antigen-activated and IL-10-producing in the steady-state, and preferentially migrated to the colon during inflammation to attenuate the severity of disease (146).

A remarkable increase in splenic $CD19^+$ (representing B lymphocytes) was observed during early disease in all the genotypes (Table 29, Figure 22). B-cell depletion has so far only been studied in ulcerative colitis where rituximab (anti-CD20) therapy had failed (143). A study involving the distribution of regulatory B cells ($CD5^+$ B cells) in the $CD19^+ CD3^-$ B cell population from blood and intestinal tissue during colitis, had recorded a significant decrease in the CD and UC patients than in the controls (147). Results of our study could be correlated with evidence that the pathogenesis of UC involves exhaustion of the regulatory B cell (Breg) cohort, resulting in a failure to control B cell activity (147). Thus, the results we have obtained suggest that improving regulatory B cell numbers and function may provide a complementary approach for the treatment of therapy-resistant UC (147). A separate study of B and T cell proliferation capacity needs to be carried out to further confirm high antigen sampling, priming of effector cells, immune responsivity and clonal selection in the B

and T cell groups, in the genotypes tested. A marked increase in B lymphocyte percentages in both the spleen and MLN during both early and late timepoints were observed in our study model which may have included the regulatory B cell component within our total B cell cohorts.

Ccr6-deficiency acts to suppress the T and B lymphocyte expression in the MLN during early disease (Table 30-32, Figure 23). It may be that antigen sampling by the dendritic cells and macrophages which leads to the priming of effector lymphocytes is impaired by their inability to chemotactically migrate to the MLN. Notwithstanding the *Ccr6-* gene deficiency, which impaired chemotaxis of migratory immune cells and the T cell development and differentiation, the *Ccr6-/-* and Winnie x *Ccr6-/-* had produced an increase in T and B cell marker percentages between early and late disease stages and appeared to mount a combined, active, cellular and humoral immune response. They also displayed the capacity to respond to infections *via* T and B cell repertoires in the MLN, possibly indicating the ability to promote immune tolerance in a preclinical colitis setting.

There was a significant increase in the TH1 cytokine mRNA expressions in Winnie (Table 37-39, Figure 25) which indicated severe inflammation and attenuation of disease in Winnie x *Ccr6-/-,* during the early timepoint. It is possible that a lowered TH1 immune response occurs owing to *Ccr6-* deficiency in Winnie mice and hence it acts to decrease the pro-inflammatory cytokine release in the colon tissue resulting in diminished inflammation. These differences may have resulted due to differences in pathogenesis, increased immune suppression mechanisms or the microbiota within the genotypes although they were littermates and were fed the same diet, housed in the same environment, but different cages.

Results of our study indicate that *Ccr6*-deficiency does not heavily induce IFN-γ (Table 37) and TNF-α (Table 38) production during early inflammation in colitis, and at the second time point remains below than that of Winnie, is corroborated by published data which had revealed a robust production of IFN-γ in the gut of DSS-

treated WT mice, associated with severe intestinal inflammation (148). Neutralization antibody against IFN-γ had partially but significantly ameliorated disease (149). IFN-γ is also involved in regulating intestinal epithelial cell homeostasis, cell proliferation and apoptosis through converging beta- catenin signalling pathways (150), and activating the major histocompatibility complex class II (MHC II) on antigen-presenting cells and non-immune cells (151).

The beneficial attribute of IFN-γ is that it also bears anti-inflammatory properties that may be supported by the observations made at the latter time point in the present study. It was shown in a mouse model of *Salmonella typhimurium*- induced colitis, that animals lacking IFN-γ, the severity of intestinal inflammation was markedly attenuated (152). Conventionally, IFN-γ is produced during the innate immune response to bacterial infections by natural killer (NK) cells and NKT cells with both $CD4^+$ and $CD8^+$ T cells becoming the sources at later stages that are responsible for eliciting adaptive immune responses (152). Moreover, IFN-γ has been identified as a negative regulator of IL-23 – mediated experimental colitis (153).

High levels of TNF-α in the intestinal mucosa is associated with the development of relapses and sustaining chronic inflammatory activity, which in our study model was conspicuously reduced. Intestinal homing of memory T lymphocytes were shown to augment TNF-α levels in relapsing UC patients along with higher NF-kB nuclear translocation in lamina propria mononuclear cells taken from IBD patients (154). According to Arora and Shen (2014), excessive production of TNF-α occurs from activated macrophages and T lymphocytes leading to further activation of macrophages and T cells as well as recruitment of neutrophils, culminating in a vicious cycle of heightened colonic inflammation (155).

The targeted deletion of Nuclear Factor -kappa B essential modulator (NEMO), also known as IKK-γ mouse model, develops into colitis due to the lack of NF-kB pathway resulting in elevated sensitivity of colonic epithelial cells to TNF-α and apoptosis, causing spontaneous and severe chronic intestinal inflammation. However, these

models lack the ability to represent the true immunogenicity of natural human colitis (156).

A similar pattern was observed in the cytokine mRNA expression in TH2 cytokines (IL-4, IL-6 and IL-13; Table 40 -42) and TH17 cytokines (IL-17A and IL-23R; Table 43-44). However, the anti-inflammatory cytokine, IL-10, mRNA expression (Table 45) was the lowest in Winnie x *Ccr6-/-* and was the highest in Winnie at 8 weeks. Although IL-10 was produced in excess, during early disease, it did not seem to contribute to dampen the inflammation in Winnie. Although Winnie displays a high IL-10 expression, and theoretically, it should promote colonisation of more Treg cells in the colon tissue, there seemed to be a different mechanism that determined the TH17/Treg imbalance in Winnie. The suppressed IL-10 expression in Winnie x *Ccr6-/-* also did not appear to aggravate inflammation in the experimental model, either. It could be explained either by the absence of CCR6+ immune cells such as TH1, TH17 and/or Treg cells owing to defective migratory capacity to the colonic mucosa or there was upregulation of immune tolerance *via* regulatory T and B cells which served to curtail inflammation.

The TH2 cells produce IL-4, IL-10 and IL-13 which are known to inhibit TH1-mediated immune responses (157) those of which were evident in Winnie x *Ccr6-/-*. Published data reveal that the expression of IL-4 mRNA was reduced in IBD patients due to the loss of balance between proinflammatory and anti-inflammatory effects (158). IL-4 is mainly produced by activated lymphocytes and its main function is to inhibit formation of macrophage colonies (158). IL-4 causes a significant reduction in inflammation *via* suppression of vascular endothelial growth factor (VEGF) produced by peripheral blood mononuclear cells in patients having active CD and UC (157).

IL-6 is involved in IBD pathophysiology as a proinflammatory cytokine and (157) and its level in the colon is correlated with disease severity (159). Reportedly IL-6 acts to induce T and B cell differentiation, stimulating the survival and proliferation of intestinal epithelial cells, acute phase proteins in hepatocytes and maturation of

megakaryocytes (159). IL-6 had induced inflammation and epithelial homeostasis in the colon during chronic colitis (160). Increased IL-6 activity leads to upregulating the nuclear translocation of STAT3, which is important for the dichotomous TH17 or Treg imbalance paradigm which occurs in IBD and for maintaining anti-apoptotic activity in the lamina propria of the colon (161).

IL-13 not only contributes to pathology but also mediates TH2-like immune responses (162). IL-13 can directly act on macrophages driving the differentiation towards the M2 phenotype (163). *Ccr6*- deficiency had increased IL-13 towards late disease compared to Winnie and the WT, and the biological effects of IL-13 demonstrate that it elicits a more favourable response in colitis. However, in Winnie, IL-13 immune mechanisms appeared to be upregulated with severity of disease.

In our study, *Ccr6*-deficiency significantly induced a moderately high IL-10 mRNA expression (a 4-fold increase compared to the WT – Table 45, Figure 25) during the late stage of inflammation which had suppressed the inflammation in Winnie x *Ccr6*-/-. IL-10 is an established anti-inflammatory cytokine produced by T cells, B cells and monocytes when stimulated by an antigenic stimulus. IL-10 is known to downregulate MHC II molecules which diminish the antigen presenting capacity of cells thus inhibiting the production of IL-6, interleukin -1 beta (IL-1β) and TNF-α (157).

Similarly, IL-17A mRNA expression (Table 43, Figure 25) and the IL-23R mRNA expression (Table 44, Figure 25) were moderately elevated in Winnie x *Ccr6*-/- at the second time point, indicating the priming of $TH17^+$ immune cells, like that of Winnie. Since IL-23 is a natural stimulator of $IL\text{-}17^+$ cells, *Ccr6*-deficiency in Winnie could be upregulating the TH17 expression from which a certain proportion of TH17 lymphocytes are converted into Treg cells and hence act to reduce the inflammation in the gut, spleen and liver. CCR6 stimulates the phosphorylation of AKT leading to mTOR and STAT3 signalling which culminate in upregulating the IL-17A-driven $CD4^+$ T helper cell differentiation into TH17 and Treg subsets and the simultaneous suppression of the $FOXP3^+$ -triggered Treg activation (127).

Inhibition of IL-17 had exacerbated CD and weakened epithelial barrier integrity, thus exhibiting its potency for activating disease resolution. IL-23 inhibition had attenuated CD as well as promoting the development of the regulatory T cells (164). In another study, antibodies targeting IL-23 had ameliorated colitis (165). Results of our study are consistent with these observations. The protein encoded by the *IL23R* gene is a subunit of the receptor for IL23A/IL23. This protein pairs with the receptor molecule IL12RB1/IL12Rbeta1, and both are required for IL23A signalling and is associated constitutively with Janus kinase 2 (JAK2), and also binds to transcription activator STAT3 in a ligand-dependent manner (166). T cells, which mediate immune responses during disease, are influenced by multiple factors including the cytokine milieu, microbial species, metabolites and signalling molecules which end up determining the outcome of disease (167).

Patients with UC or CD who have persistent chronic inflammation of the colon for more than 8 to 10 years are in a very high risk of developing metastatic colorectal cancer (CRC). Approximately 25 to 30% of patients with a history of pan-colitis for more than 30 years develop colorectal cancer, because of prolonged exposure of the colon to chronic inflammation. The tissue infiltrating pro-inflammatory cells are thought to drive the neoplastic changes in the inflamed colon leading to CRC (168). To understand the signalling pathways that cause inflammation in the colon tissue is critical for effective prevention and therapy of chronic inflammatory diseases. This study has therefore, explored the CCL20, $PI3K^{P}$ and AKT^{P} activity in the colitis mouse models we had used.

CCL20 is a known inflammatory bio marker in colitis (169). The percentage expression of CCL20 in colon tissue (Table 33, Figure 24) was lowest in the WT and highest in Winnie while Winnie x *Ccr6*-/- was intermediate at the second time point. A significant difference in CCL20 expression existed between Winnie x *Ccr6*-/- and Winnie towards late disease.

The PI3K / AKT pathway is active in cells infiltrating inflamed human colon tissue. This pathway sustains the recruitment of inflammatory cells through a positive feedback loop (168). A range of chemo-attractants activate G protein-coupled receptors (GPCRs) such as CCR6, receptor tyrosine kinases (RTKs) and Toll-like / IL-1 receptors (TLR/IL1Rs) and initiate inflammation by activating PI3K (168). Knowledge of the cellular source of PI3K activity in healthy, inflamed tissues is therefore important for understanding how PI3K activity causes colitis and predisposes IBD patients to cancer. This knowledge will lead to understanding the mode of action of PI3K targeting drugs that are currently being tested for prevention and treatment of IBD.

$PI3K^P$ is at the starting point of CCR6 receptor activation pathway (Figure 1) and hence, aids chemotactic navigation of lymphocytes and other CCR6 expressing cell types to the colon, during inflammation. The colonic $PI3K^P$ percentage expression in this study (Table 34, Figure 24) has indicated the suppression of chemotaxis in T and B lymphocytes to the gut and secondary lymphoid organs during colitis which have advantages as well as disadvantages. On one hand it appeared to promote cell mediated immune tolerance leading to tissue restitution and on the other hand it upregulates the release of proinflammatory cytokines, free radicals, nitric oxide (NO), reactive oxygen species (ROS) and metabolites that caused oxidative stress and exacerbated inflammation in the gut (170). However, the lowered expression of $PI3K^P$ in colon tissue in the *Ccr6*-deficient mice could be helping in either early resolution of disease or to keep the inflammation contained.

Ccr6-deficiency in Winnie induced downregulation of $PI3K^P$ expression in the colonic epithelial tissue. The CCR6-activation pathway is also stimulated by $PI3K^P$ which directs actin polymerisation leading to enhanced migratory capacity of CCR6-bearing immune cells. The PI3K/AKT/mTOR/PTEN signalling network plays an important role in metabolism and inflammation under physiological conditions. The effective

targeting of this signalling cascade with pharmacological modulators may also result in successful treatment of patients with inflammation (170).

A study has reported the measuring of DAI and histological scores of mice after treatment with a PI3K inhibitor (Wortmannin), where both mice (with DSS colitis) and UC patients, showed a significant decrease in the DAI and tissue-morphology which suggested that PI3K inhibition contributed towards attenuating colitis (171).

However, this same study had shown a lowering of phosphorylated Akt alongside the declining DAI, although in the present study, *Ccr6*-deficiency had stimulated a significant increase in Akt^{P} (Table 45, Figure 24) compared to the WT and Winnie. This indicates to us that phosphorylated Akt performs multiple roles in activating both beneficial and non-beneficial immune pathways in colitis and needs further investigation.

Akt^{P} is a well- known biomarker in the CCR6-upregulated Akt-mTOR pathway which helps to determine the tilt of TH17/Treg imbalance that produces resolution of colitis (127). Akt, which is also known as Protein kinase B (PKB), is a serine/threonine-specific protein kinase that plays a key role in multiple cellular processes (Figure 26) such as; glucose metabolism, apoptosis, cell proliferation, transcription and cell migration (172). The Akt-stimulated glucose metabolism could aid the tissue repair and restitution in the gut (173). The mild to moderate inflammation seen in Winnie x *Ccr6*-/- could depend upon a different Akt^{P}-driven immune mechanism that is involved in colitis resolution. The Winnie x *Ccr6*-/- produced elevated levels of phosphorylated Akt, which stimulates the Nuclear factor kappa beta (NF-kB) pathway, with a concomitant decrease in TNF-α production in the colon which probably had produced the low level of inflammation (154). Further investigation is needed to establish the contribution made by $PI3K^{P}$ and Akt^{P} during colitis in the four genotypes included in my study.

The limitations of my study include lack of functional studies on the immune cell repertoires and quantification of regulatory T cells and other T lymphocyte cohorts as well as detailed screening of the proteins involved in molecular signalling, which again was considered as beyond the scope of a Masters study.

Recent genome wide association studies (GWAS) illustrated *Ccr6* as a predisposing genetic locus in IBD patients, a mechanism by which CCR6 imparts immunological modulation. This study has highlighted a functional role for CCR6 in the pathogenicity of spontaneous chronic colitis and implies that CCR6 could be utilised as a functional therapeutic target in IBD. The proven functional efficacy of CCR6-inhibition (Table 46, Figure 3) in psoriasis, rheumatoid arthritis (RA), multiple sclerosis (MS), carcinoma and experimental autoimmune encephalitis (EAE), could be replicated in IBD as well (73). Recent research had shown the direct involvement of CCR6 with AKT/mTOR pathway which contributes to the TH17/Treg imbalance (that is considered as the prime immunological factor) and that it influences the resolution of colitis (127). In conclusion, it is proposed to further evaluate the potency of CCR6 -inhibition as an active drug target in the clinical studies of colitis.

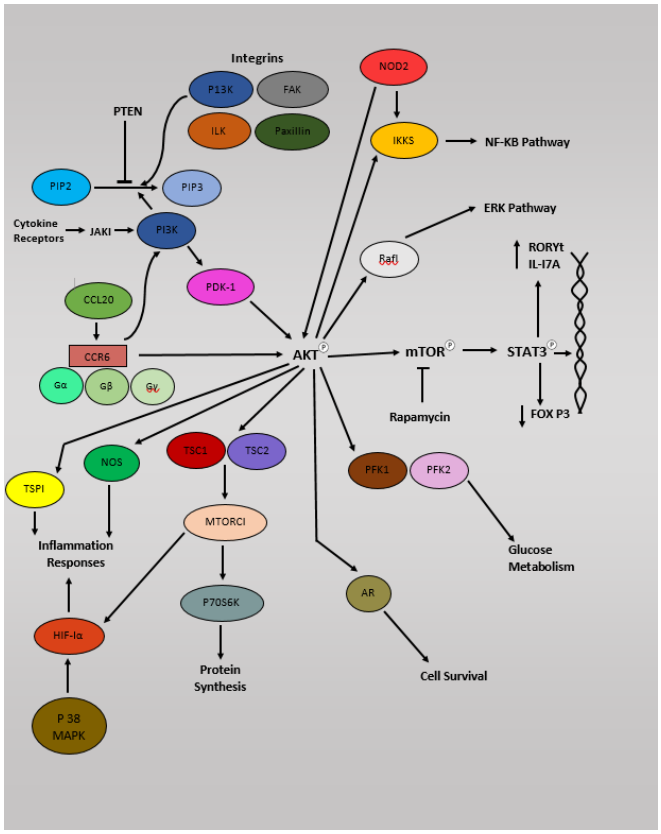

Figure 26. Some possible immune pathways involving PI3K and Akt^{P}.

Legend: Phosphatidylinositol 4,5-bisphosphate (PIP2), Phosphatidylinositol (3,4,5)-trisphosphate (PIP3), Phosphatase and tensin homolog (PTEN), Phosphoinositide 3-kinases (PI3K), 3-Phosphoinositide-dependent protein kinase 1 (PDK1), C-C Chemokine Ligand 20 (CCL20), C-C Chemokine Receptor 6 (CCR6), Guanine nucleotide binding proteins -alpha subunit (Gα), Guanine nucleotide binding protein – beta subunit (Gβ), Guanine nucleotide binding protein -gamma subunit (Gγ), Thrombospondin-1 (TSP1), Nitric oxide synthase (NOS), Hypoxia-inducible factor 1-alpha (HIF-1α), P38 Mitogen Activated Protein Kinases (p38 MAPK), Tuberous Sclerosis 1 (TSC1), Tuberous Sclerosis 2 (TSC2), Mammalian Target of Rapamycin (mTOR), Mammalian Target of Rapamycin Complex 1 (mTOR C1), Ribosomal Protein S6 Kinase beta - 1 (P70S6K), Phosphofructokinase -1 (PFK-1), Phosphofructokinase-2 (PFK-2), Androgen Receptor (AR), Protein Kinase B (Akt), Phosphorylated Signal Transducer of Activation of Transcription 3 (STAT3^{P}), Forkhead Box P3 (FOXP3), RAR-related orphan receptor gamma (t) (RORγt), Interleukin 17 A (IL-17A), Raf-1

Proto-Oncogene, Serine/Threonine Kinase (Raf-1), Inhibitor of Kappa B Kinases (IKKS), Nucleotide-binding oligomerization domain-containing protein 2 (NOD2), Focal Adhesion Kinase in Integrin (FAK), Integrin-Linked Kinase (ILK), Janus kinase 1 (JAK-1).

5.0 Future Directions

Further studies are required to gain deeper knowledge of the exact mechanisms of the CCR6–CCL20 axis. Extensive studies into immune and therapeutic functions of the CCR6–CCL20 axis with the use of novel inhibitors need to gain momentum, as there is a profound gap in immunological research into the treatment options for autoimmune and inflammatory disorders. New interventions with synthetic cellular, molecular, or nanoparticle inhibitors and derivatives of herbal and anti-toxic metabolites could be utilized to mimic or block the numerous biochemical pathways through which the CCR6–CCL20 axis is involved in disease promotion. Given the skewed immune regulation inducted by CCR6 and CCL20 partners in producing an imbalanced TH17 and Treg populations, which tilt immune homeostasis into inflammation, the invention of a vaccine may even become possible to boost T and B memory lymphocyte subsets of choice, coupled with selective inhibition of these two chemokines. Comprehensive randomized, placebo-controlled, clinical trials on the therapeutic use of the CCR6–CCL20 axis could become useful to thoroughly evaluate the benefits and disadvantages of using inhibitors of this axis, in humans.

Most of the studies undertaken have utilized multiple animal models which may not be a true depiction of human colitis. Therefore, pre-clinical studies involving the relevant IBD animal models (spontaneous colitis) or human tissue (organoids and spheroids) would be preferable options. Investigations into novel paradigms such as ILC behaviour, ER stress, gut-specific microbiome, intestinal apoptosis, and metabolomics need to be encouraged with special reference to CCR6 mediation. Goal-oriented, specifically targeted innovative research models are needed to construct the

broader context surrounding the CCR6–CCL20 immune modulation, which will open avenues to test more effective therapeutic interventions to treat IBD in the future.

Preclinical models such as CCR6/CCL20 double knockouts as well as humanized murine clones and randomized clinical trials utilizing antibodies, novel CCR6 inhibitors, and deeper investigation of TH22 cells associated with inflammatory response are suggested as future initiatives which might bring us closer to elucidating the immunogenic contributions of the chemokine receptor 6. Studies utilizing proteomics and metabolomics methodologies, combined with the CCR6 biology, may also be useful in identifying the multiple immune pathways that are dysregulated in IBD. A comparison of immune mechanisms with those delineated so far in other autoimmune disorders may also be useful, given the shared genetic and molecular etiologic factors.

The CCR6/CCL20 axis demonstrates a vital role in determining the disease outcome of inflammatory disorders and cancer metastasis in multiple organ systems in the human body (42). Effective blocking of the CCR6 signal transduction pathway using novel biochemical interventions (Figure 3) might prove to be a useful therapeutic strategy in regulating pro-disease - inducing cell chemotaxis within inflammatory microenvironments. Most of the research has been centred on animal models which do not depict the true clinical picture, and therefore there remains an urgent need for the evaluation of the chemokine receptor 6 and its ligand in expanded *in vivo* and *ex vivo* clinical studies.

6.0 Conclusion

Ccr6-deficiency in the Winnie mouse model indicated that it could potentially promote the immune mechanisms in the colon which augments attenuation of colonic inflammation during spontaneous chronic colitis. *Ccr6*-deficiency plays an important role in the pathogenesis of colon, spleen and liver during colitis by acting to lessen the severity of disease which involved these organs. It is indicated that the immune

activation pathways steered by phosphorylated PI3K and phosphorylated Akt possibly contribute to reduce inflammation in the gut in pre-clinical models.

7.0 References

1. Zhang Y-Z, Li Y-Y. Inflammatory bowel disease: pathogenesis. World journal of gastroenterology: WJG. 2014;20(1):91.

2. Hrabe JE, Byrn JC, Button AM, Zamba GK, Kapadia MR, Mezhir JJ. A matched case-control study of IBD-associated colorectal cancer: IBD portends worse outcome. Journal of surgical oncology. 2014;109(2):117-21.

3. Bernstein CN, Singh S, Graff LA, Walker JR, Miller N, Cheang M. A prospective population-based study of triggers of symptomatic flares in IBD. The American journal of gastroenterology. 2010;105(9):1994.

4. Zimmerman J. Extraintestinal symptoms in irritable bowel syndrome and inflammatory bowel diseases: nature, severity, and relationship to gastrointestinal symptoms. Digestive diseases and sciences. 2003;48(4):743-9.

5. Olaison G, Smedh K, Sjödahl R. Natural course of Crohn's disease after ileocolic resection: endoscopically visualised ileal ulcers preceding symptoms. Gut. 1992;33(3):331-5.

6. Scaldaferri F, Pizzoferrato M, Lopetuso LR, Musca T, Ingravalle F, Sicignano LL, et al. Nutrition and IBD: malnutrition and/or sarcopenia? A practical guide. Gastroenterology research and practice. 2017;2017.

7. Mendoza J, Lana R, Taxonera C, Alba C, Izquierdo S, Diaz-Rubio M. Extraintestinal manifestations in inflammatory bowel disease: differences between Crohn's disease and ulcerative colitis. Medicina clinica. 2005;125(8):297-300.

8. Baumgart DC, Sandborn WJ. Crohn's disease. The Lancet. 2012;380(9853):1590-605.

9. Marks C, Ritchie JK, Lockhart-Mummery H. Anal fistulas in Crohn's disease. British Journal of Surgery. 1981;68(8):525-7.

10. Greenstein AJ, Janowitz HD, Sachar DB. The extra-intestinal complications of Crohn's disease and ulcerative colitis: a study of 700 patients. Medicine. 1976;55(5):401-12.

11. Johnston RD, Logan RF. What is the peak age for onset of IBD? Inflammatory bowel diseases. 2008;14(suppl_2):S4-S5.

12. Plevinsky J, Gumidyala A, Fishman L. Transition experience of young adults with inflammatory bowel diseases (IBD): a mixed methods study. Child: care, health and development. 2015;41(5):755-61.

13. Sewitch MJ, Abrahamowicz M, Bitton A, Daly D, Wild GE, Cohen A, et al. Psychological distress, social support, and disease activity in patients with inflammatory bowel disease. The American journal of gastroenterology. 2001;96(5):1470.

14. Kaplan GG. The global burden of IBD: from 2015 to 2025. Nature reviews Gastroenterology & hepatology. 2015;12(12):720.

15. Dahlhamer JM. Prevalence of inflammatory bowel disease among adults aged≥ 18 years—United States, 2015. MMWR Morbidity and mortality weekly report. 2016;65.

16. Ng SC, Shi HY, Hamidi N, Underwood FE, Tang W, Benchimol EI, et al. Worldwide incidence and prevalence of inflammatory bowel disease in the 21st century: a systematic review of population-based studies. The Lancet. 2017;390(10114):2769-78.

17. Wilson J, Hair C, Knight R, Catto-Smith A, Bell S, Kamm M, et al. High incidence of inflammatory bowel disease in Australia: A prospective population-based Australian incidence study. Inflammatory bowel diseases. 2010;16(9):1550-6.

18. Massuger W, Moore GT, Andrews JM, Kilkenny MF, Reyneke M, Knowles S, et al. Crohn's & Colitis Australia inflammatory bowel disease audit: measuring the quality of care in Australia. Internal medicine journal. 2019;49(7):859-66.

19. Niewiadomski O, Studd C, Wilson J, Williams J, Hair C, Knight R, et al. Influence of food and lifestyle on the risk of developing inflammatory bowel disease. Internal medicine journal. 2016;46(6):669-76.

20. Niewiadomski O, Studd C, Hair C, Wilson J, McNeill J, Knight R, et al. Health care cost analysis in a population-based inception cohort of inflammatory bowel disease patients in the first year of diagnosis. Journal of Crohn's and Colitis. 2015;9(11):988-96.

21. Strober W, Fuss I, Mannon P. The fundamental basis of inflammatory bowel disease. The Journal of clinical investigation. 2007;117(3):514-21.

22. Arpaia N, Rudensky AY. Microbial metabolites control gut inflammatory responses. Proceedings of the National Academy of Sciences. 2014;111(6):2058-9.

23. Siegmund B, Zeitz M. Innate and adaptive immunity in inflammatory bowel disease. World journal of gastroenterology: WJG. 2011;17(27):3178.

24. Rajan T. Inflammatory bowel disease: maladaptation of the vigilant genotype in a hyper-clean world? Perspectives in biology and medicine. 2006;49(2):171-7.

25. Logan I, Bowlus CL. The geoepidemiology of autoimmune intestinal diseases. Autoimmunity reviews. 2010;9(5):A372-A8.

26. Ye BD, McGovern DP. Genetic variation in IBD: progress, clues to pathogenesis and possible clinical utility. Expert review of clinical immunology. 2016;12(10):1091-107.

27. Gordon H, Trier Moller F, Andersen V, Harbord M. Heritability in inflammatory bowel disease: from the first twin study to genome-wide association studies. Inflammatory bowel diseases. 2015;21(6):1428-34.

28. Rogler G, Vavricka S. Exposome in IBD: recent insights in environmental factors that influence the onset and course of IBD. Inflammatory bowel diseases. 2014;21(2):400-8.

29. Shouval DS, Rufo PA. The role of environmental factors in the pathogenesis of inflammatory bowel diseases: a review. JAMA pediatrics. 2017;171(10):999-1005.

30. Crespo I, San-Miguel B, Prause C, Marroni N, Cuevas MJ, González-Gallego J, et al. Glutamine treatment attenuates endoplasmic reticulum stress and apoptosis in TNBS-induced colitis. PloS one. 2012;7(11):e50407.

31. Kaser A, Zeissig S, Blumberg RS. Genes and environment: how will our concepts on the pathophysiology of IBD develop in the future? Digestive diseases. 2010;28(3):395-405.

32. Mokrowiecka A, Gasiorowska A, Malecka-Panas E. pANCA and ASCA in the diagnosis of different subtypes of inflammatory bowel disease. Hepato-gastroenterology. 2007;54(77):1443-8.

33. Sutherland AD, Gearry RB, Frizelle FA. Review of fecal biomarkers in inflammatory bowel disease. Diseases of the colon & rectum. 2008;51(8):1283-91.

34. Larson DW, Pemberton JH. Current concepts and controversies in surgery for IBD. Gastroenterology. 2004;126(6):1611-9.

35. Wheat CL, Ko CW, Clark-Snustad K, Grembowski D, Thornton TA, Devine B. Inflammatory Bowel Disease (IBD) pharmacotherapy and the risk of serious infection: a systematic review and network meta-analysis. BMC gastroenterology. 2017;17(1):52.

36. Rawla P, Sunkara T, Raj JP. Role of biologics and biosimilars in inflammatory bowel disease: current trends and future perspectives. Journal of inflammation research. 2018;11:215.

37. Manuc T-EM, Manuc MM, Diculescu MM. Recent insights into the molecular pathogenesis of Crohn's disease: a review of emerging therapeutic targets. Clinical and experimental gastroenterology. 2016;9:59.

38. Love BL. Management of patients with inflammatory bowel disease: current and future treatments. Acute pain. 2019;10:00.

39. Ito T, Carson IV WF, Cavassani KA, Connett JM, Kunkel SL. CCR6 as a mediator of immunity in the lung and gut. Experimental cell research. 2011;317(5):613-9.

40. Lee A, Eri R, Lyons AB, Grimm M, Korner H. CC chemokine ligand 20 and its cognate receptor CCR6 in mucosal T cell immunology and inflammatory bowel disease: odd couple or axis of evil? Frontiers in immunology. 2013;4:194.

41. Murdoch C, Finn A. Chemokine receptors and their role in inflammation and infectious diseases. Blood, The Journal of the American Society of Hematology. 2000;95(10):3032-43.

42. Ranasinghe R, Eri R. Pleiotropic immune functions of chemokine receptor 6 in health and disease. Medicines. 2018;5(3):69.

43. Zlotnik A, Morales J, Hedrick JA. Recent advances in chemokines and chemokine receptors. Critical reviews in immunology. 1999;19(1):1-47.

44. Lee AY, Phan TK, Hulett MD, Körner H. The relationship between CCR6 and its binding partners: Does the CCR6–CCL20 axis have to be extended? Cytokine. 2015;72(1):97-101.

45. Grainger DJ, Reckless J. Broad-spectrum chemokine inhibitors (BSCIs) and their anti-inflammatory effects in vivo. Biochemical pharmacology. 2003;65(7):1027-34.

46. Rot A, Von Andrian UH. Chemokines in innate and adaptive host defense: basic chemokinese grammar for immune cells. Annu Rev Immunol. 2004;22:891-928.

47. Williams IR. CCR6 and CCL20: partners in intestinal immunity and lymphorganogenesis. Annals of the New York Academy of Sciences. 2006;1072(1):52-61.

48. Klein M, Brouwer MC, Angele B, Geldhoff M, Marquez G, Varona R, et al. Leukocyte attraction by CCL20 and its receptor CCR6 in humans and mice with pneumococcal meningitis. PloS one. 2014;9(4).

49. Cook DN, Prosser DM, Forster R, Zhang J, Kuklin NA, Abbondanzo SJ, et al. CCR6 mediates dendritic cell localization, lymphocyte homeostasis, and immune responses in mucosal tissue. Immunity. 2000;12(5):495-503.

50. Luster AD. The role of chemokines in linking innate and adaptive immunity. Current opinion in immunology. 2002;14(1):129-35.

51. Baba M, Imai T, Nishimura M, Kakizaki M, Takagi S, Hieshima K, et al. Identification of CCR6, the specific receptor for a novel lymphocyte-directed CC chemokine LARC. Journal of Biological Chemistry. 1997;272(23):14893-8.

52. Yamazaki T, Yang XO, Chung Y, Fukunaga A, Nurieva R, Pappu B, et al. CCR6 regulates the migration of inflammatory and regulatory T cells. The Journal of Immunology. 2008;181(12):8391-401.

53. Ranasinghe R, Eri R. CCR6–CCL20-Mediated Immunologic Pathways in Inflammatory Bowel Disease. Gastrointestinal Disorders. 2019;1(1):15-29.

54. Doucet M, Jayaraman S, Swenson E, Tusing B, Weber KL, Kominsky SL. CCL20/CCR6 signaling regulates bone mass accrual in mice. Journal of Bone and Mineral Research. 2016;31(7):1381-90.

55. Krzysiek R, Lefevre EA, Bernard Jrm, Foussat A, Galanaud P, Louache F, et al. Regulation of CCR6 chemokine receptor expression and responsiveness to macrophage inflammatory protein-3α/CCL20 in human B cells. Blood, The Journal of the American Society of Hematology. 2000;96(7):2338-45.

56. Yang D, Chertov O, Bykovskaia S, Chen Q, Buffo M, Shogan J, et al. β-defensins: linking innate and adaptive immunity through dendritic and T cell CCR6. Science. 1999;286(5439):525-8.

57. Vongsa RA, Zimmerman NP, Dwinell MB. CCR6 regulation of the actin cytoskeleton orchestrates human beta defensin-2-and CCL20-mediated restitution of colonic epithelial cells. Journal of Biological Chemistry. 2009;284(15):10034-45.

58. Hughes CE, Nibbs RJ. A guide to chemokines and their receptors. The FEBS journal. 2018;285(16):2944-71.

59. Mackay CR. Chemokine receptors and T cell chemotaxis. Journal of Experimental Medicine. 1996;184(3):799-802.

60. Weiss ER, Kelleher DJ, Woon C-W, Soparkar S, Osawa S, Heasley L, et al. Receptor activation of G proteins. The FASEB journal. 1988;2(13):2841-8.

61. Wong MM, Fish EN, editors. Chemokines: attractive mediators of the immune response. Seminars in immunology; 2003: Elsevier.

62. Zissel G, Höhne K, Kilic A, Maier C, Ploenes T, Prasse A, et al. CCR6 is a receptor for CCL18 expressed on human lung fibroblasts from IPF lungs. Eur Respiratory Soc; 2011.

63. Facco M, Baesso I, Miorin M, Bortoli M, Cabrelle A, Boscaro E, et al. Expression and role of CCR6/CCL20 chemokine axis in pulmonary sarcoidosis. Journal of leukocyte biology. 2007;82(4):946-55.

64. Hammerich L, Bangen JM, Govaere O, Zimmermann HW, Gassler N, Huss S, et al. Chemokine receptor CCR6-dependent accumulation of γδ T cells in injured liver restricts hepatic inflammation and fibrosis. Hepatology. 2014;59(2):630-42.

65. Turner J-E, Paust H-J, Steinmetz OM, Peters A, Riedel J-H, Erhardt A, et al. CCR6 recruits regulatory T cells and Th17 cells to the kidney in glomerulonephritis. Journal of the American Society of Nephrology. 2010;21(6):974-85.

66. Alikhan MA, Huynh M, Kitching AR, Ooi JD. Regulatory T cells in renal disease. Clinical & translational immunology. 2018;7(1):e1004.

67. Ransohoff RM, Trettel F. Editorial Research Topic “Chemokines and chemokine receptors in brain homeostasis”. Frontiers in Cellular Neuroscience. 2015;9:132.

68. Arunachalam P, Ludewig P, Melich P, Arumugam TV, Gerloff C, Prinz I, et al. CCR6 (CC Chemokine Receptor 6) is essential for the migration of detrimental natural interleukin-17–producing γδ T cells in stroke. Stroke. 2017;48(7):1957-65.

69. Hedrick MN, Lonsdorf AS, Hwang ST, Farber JM. CCR6 as a possible therapeutic target in psoriasis. Expert opinion on therapeutic targets. 2010;14(9):911-22.

70. Bonelli M, Puchner A, Goeschl L, Hayer S, Niederreiter B, Smolen JS, et al. 02.06 Ccr6 modulates severity of arthritis in T cell dependent manner. BMJ Publishing Group Ltd; 2017.

71. Fakhoury M, Negrulj R, Mooranian A, Al-Salami H. Inflammatory bowel disease: clinical aspects and treatments. Journal of inflammation research. 2014;7:113.

72. Pedros C, Duguet F, Saoudi A, Chabod M. Disrupted regulatory T cell homeostasis in inflammatory bowel diseases. World journal of gastroenterology. 2016;22(3):974.

73. Ranasinghe R, Eri R. Modulation of the CCR6-CCL20 Axis: A Potential Therapeutic Target in Inflammation and Cancer. Medicina. 2018;54(5):88.

74. Ranasinghe R, Eri R. CCR6–CCL20 Axis in IBD: What Have We Learnt in the Last 20 Years? Gastrointestinal Disorders. 2019;1(1):57-74.

75. Yang F, Wang D, Li Y, Sang L, Zhu J, Wang J, et al. Th1/Th2 balance and Th17/Treg-mediated immunity in relation to murine resistance to dextran sulfate-induced colitis. Journal of immunology research. 2017;2017.

76. Zenewicz LA, Antov A, Flavell RA. CD4 T-cell differentiation and inflammatory bowel disease. Trends in molecular medicine. 2009;15(5):199-207.

77. Gálvez J. Role of Th17 cells in the pathogenesis of human IBD. ISRN inflammation. 2014;2014.

78. Comerford I, Bunting M, Fenix K, Haylock-Jacobs S, Litchfield W, Harata-Lee Y, et al. An immune paradox: how can the same chemokine axis regulate both immune tolerance and activation? CCR6/CCL20: a chemokine axis balancing immunological tolerance and inflammation in autoimmune disease. Bioessays. 2010;32(12):1067-76.

79. El-behi M, Rostami A, Ciric B. Current views on the roles of Th1 and Th17 cells in experimental autoimmune encephalomyelitis. Journal of Neuroimmune Pharmacology. 2010;5(2):189-97.

80. Costantino CM, Baecher-Allan CM, Hafler DA. Human regulatory T cells and autoimmunity. European journal of immunology. 2008;38(4):921-4.

81. Zhang W, Nie L, Wang Y, Wang X-p, Zhao H, Dongol S, et al. CCL20 secretion from the nucleus pulposus improves the recruitment of CCR6-expressing Th17 cells to degenerated IVD tissues. PloS one. 2013;8(6):e66286.

82. Geremia A, Biancheri P, Allan P, Corazza GR, Di Sabatino A. Innate and adaptive immunity in inflammatory bowel disease. Autoimmunity reviews. 2014;13(1):3-10.

83. Skovdahl HK, van Beelen Granlund A, Østvik AE, Bruland T, Bakke I, Torp SH, et al. Expression of CCL20 and its corresponding receptor CCR6 is enhanced in active inflammatory bowel disease, and TLR3 mediates CCL20 expression in colonic epithelial cells. PloS one. 2015;10(11).

84. Skovdahl HK, Damås JK, Granlund AvB, Østvik AE, Doseth B, Bruland T, et al. CC Motif Ligand 20 (CCL20) and CC Motif Chemokine Receptor 6 (CCR6) in Human Peripheral Blood Mononuclear Cells: Dysregulated in Ulcerative Colitis and a Potential Role for CCL20 in IL-1β Release. International journal of molecular sciences. 2018;19(10):3257.

85. Steinbach EC, Gipson GR, Sheikh SZ. Induction of Murine Intestinal Inflammation by Adoptive Transfer of Effector CD4+ CD45RBhigh T Cells into Immunodeficient Mice. JoVE (Journal of Visualized Experiments). 2015(98):e52533.

86. Guan Q. A Comprehensive Review and Update on the Pathogenesis of Inflammatory Bowel Disease. Journal of Immunology Research. 2019;2019.

87. Brand S. Crohn's disease: Th1, Th17 or both? The change of a paradigm: new immunological and genetic insights implicate Th17 cells in the pathogenesis of Crohn's disease. Gut. 2009;58(8):1152-67.

88. Parkes M, Cortes A, Van Heel DA, Brown MA. Genetic insights into common pathways and complex relationships among immune-mediated diseases. Nature Reviews Genetics. 2013;14(9):661.

89. Ueno A, Ghosh A, Hung D, Li J, Jijon H. Th17 plasticity and its changes associated with inflammatory bowel disease. World journal of gastroenterology. 2015;21(43):12283.

90. Griffin MD, Ritter T, Mahon BP. Immunological aspects of allogeneic mesenchymal stem cell therapies. Human gene therapy. 2010;21(12):1641-55.

91. Boden EK, Snapper SB. Regulatory T cells in inflammatory bowel disease. Current opinion in gastroenterology. 2008;24(6):733-41.

92. Öhman L, Åström RG, Hultgren Hörnquist E. Impaired B cell responses to orally administered antigens in lamina propria but not Peyer's patches of Gαi2-deficient mice prior to colitis. Immunology. 2005;115(2):271-8.

93. Mebratu Y, Tesfaigzi Y. How ERK1/2 activation controls cell proliferation and cell death: Is subcellular localization the answer? Cell cycle. 2009;8(8):1168-75.

94. Geremia A, Arancibia-Cárcamo CV. Innate lymphoid cells in intestinal inflammation. Frontiers in immunology. 2017;8:1296.

95. Geremia A, Arancibia-Cárcamo CV, Fleming MP, Rust N, Singh B, Mortensen NJ, et al. IL-23–responsive innate lymphoid cells are increased in inflammatory bowel disease. Journal of Experimental Medicine. 2011;208(6):1127-33.

96. Kara EE, Comerford I, Bastow CR, Fenix KA, Litchfield W, Handel TM, et al. Distinct chemokine receptor axes regulate Th9 cell trafficking to allergic and autoimmune inflammatory sites. The Journal of Immunology. 2013;191(3):1110-7.

97. Lu Y, Hong S, Li H, Park J, Hong B, Wang L, et al. Th9 cells promote antitumor immune responses in vivo. The Journal of clinical investigation. 2012;122(11):4160-71.

98. Goto Y, Kiyono H. Epithelial barrier: an interface for the cross-communication between gut flora and immune system. Immunological reviews. 2012;245(1):147-63.

99. Kucharzik T, Maaser C, Lügering A, Kagnoff M, Mayer L, Targan S, et al. Recent understanding of IBD pathogenesis: implications for future therapies. Inflammatory bowel diseases. 2006;12(11):1068-83.

100. Tsuji NM, Kosaka A. Oral tolerance: intestinal homeostasis and antigen-specific regulatory T cells. Trends in immunology. 2008;29(11):532-40.

101. Siddiqui K, Powrie F. CD103+ GALT DCs promote Foxp3+ regulatory T cells. Mucosal immunology. 2008;1(1s):S34.

102. Habtezion A, Nguyen LP, Hadeiba H, Butcher EC. Leukocyte trafficking to the small intestine and colon. Gastroenterology. 2016;150(2):340-54.

103. Cerutti A. The regulation of IgA class switching. Nature reviews immunology. 2008;8(6):421.

104. Basheer W, Kunde D, Eri R. Role of Chemokine Ligand CCL20 and its Receptor CCR6 in Intestinal Inflammation. Immunology and Infectious diseases. 2013;1(2):30-7.

105. Wang C, Kang SG, Lee J, Sun Z, Kim CH. The roles of CCR6 in migration of Th17 cells and regulation of effector T-cell balance in the gut. Mucosal immunology. 2009;2(2):173.

106. Varona R, Cadenas V, Flores J, Martínez-A C, Márquez G. CCR6 has a non-redundant role in the development of inflammatory bowel disease. European journal of immunology. 2003;33(10):2937-46.

107. Mizoguchi A. Animal models of inflammatory bowel disease. Progress in molecular biology and translational science. 105: Elsevier; 2012. p. 263-320.

108. Eri R, McGuckin MA, Wadley R. T cell transfer model of colitis: a great tool to assess the contribution of T cells in chronic intestinal inflammation. Leucocytes: Springer; 2012. p. 261-75.

109. Rahman AA, Robinson AM, Jovanovska V, Eri R, Nurgali K. Alterations in the distal colon innervation in Winnie mouse model of spontaneous chronic colitis. Cell and tissue research. 2015;362(3):497-512.

110. Robinson AM, Rahman AA, Carbone SE, Randall-Demllo S, Filippone R, Bornstein JC, et al. Alterations of colonic function in the Winnie mouse model of spontaneous chronic colitis. American Journal of Physiology-Gastrointestinal and Liver Physiology. 2016;312(1):G85-G102.

111. Eri R, Adams R, Tran T, Tong H, Das I, Roche D, et al. An intestinal epithelial defect conferring ER stress results in inflammation involving both innate and adaptive immunity. Mucosal immunology. 2011;4(3):354.

112. McGuckin MA, Eri RD, Das I, Lourie R, Florin TH. Intestinal secretory cell ER stress and inflammation. Portland Press Ltd.; 2011.

113. Robinson AM, Gondalia SV, Karpe AV, Eri R, Beale DJ, Morrison PD, et al. Fecal microbiota and metabolome in a mouse model of spontaneous chronic colitis: Relevance to human inflammatory bowel disease. Inflammatory bowel diseases. 2016;22(12):2767-87.

114. van Vlerken-Ysla LE, Rios-Doria J, Moynihan J, Shan L, Hollingsworth RE, Herbst R, et al. Targeting the CCL20-CCR6 axis as a novel opportunity to stimulataneously modulate cancer stem cells and the tumor-immune infiltrate by a dual anti-cancer mechanism. AACR; 2017.

115. Meyer L, Simian D, Lubascher J, Acuna R, Figueroa C, Silva G, et al. Adverse events associated with the treatment of inflammatory bowel disease. Revista Médica de Chile. 2015;143(1):7-13.

116. Kim JS, Sklarz T, Banks LB, Gohil M, Waickman AT, Skuli N, et al. Natural and inducible T H 17 cells are regulated differently by Akt and mTOR pathways. Nature immunology. 2013;14(6):611.

117. Basheer W. Genetic ablation of CCR6 confers differential exacerbation in a spontaneous colitis model: University of Tasmania; 2018.

118. Ibrahim KE, Al-Mutary MG, Bakhiet AO, Khan HA. Histopathology of the liver, kidney, and spleen of mice exposed to gold nanoparticles. Molecules. 2018;23(8):1848.

119. Heazlewood CK, Cook MC, Eri R, Price GR, Tauro SB, Taupin D, et al. Aberrant mucin assembly in mice causes endoplasmic reticulum stress and spontaneous inflammation resembling ulcerative colitis. PLoS medicine. 2008;5(3):e54.

120. Chassaing B, Aitken JD, Malleshappa M, Vijay-Kumar M. Dextran sulfate sodium (DSS)-induced colitis in mice. Current protocols in immunology. 2014;104(1):15.25. 1-15.25. 14.

121. Antoniou E, Margonis GA, Angelou A, Pikouli A, Argiri P, Karavokyros I, et al. The TNBS-induced colitis animal model: An overview. Annals of medicine and surgery. 2016;11:9-15.

122. Mizoguchi A, Takeuchi T, Himuro H, Okada T, Mizoguchi E. Genetically engineered mouse models for studying inflammatory bowel disease. The Journal of pathology. 2016;238(2):205-19.

123. Rahman AA, Robinson AM, Brookes SJ, Eri R, Nurgali K. Rectal prolapse in Winnie mice with spontaneous chronic colitis: changes in intrinsic and extrinsic innervation of the rectum. Cell and tissue research. 2016;366(2):285-99.

124. Perera AP, Fernando R, Shinde T, Gundamaraju R, Southam B, Sohal SS, et al. MCC950, a specific small molecule inhibitor of NLRP3 inflammasome attenuates colonic inflammation in spontaneous colitis mice. Scientific reports. 2018;8(1):8618.

125. Gulhane M, Murray L, Lourie R, Tong H, Sheng YH, Wang R, et al. High fat diets induce colonic epithelial cell stress and inflammation that is reversed by IL-22. Scientific reports. 2016;6(1):1-17.

126. Katchar K, Kelly CP, Keates S, O'Brien MJ, Keates AC. MIP-3α neutralizing monoclonal antibody protects against TNBS-induced colonic injury and inflammation in mice. American journal of physiology-gastrointestinal and liver physiology. 2007;292(5):G1263-G71.

127. Kulkarni N, Meitei HT, Sonar SA, Sharma PK, Mujeeb VR, Srivastava S, et al. CCR6 signaling inhibits suppressor function of induced-Treg during gut inflammation. Journal of autoimmunity. 2018;88:121-30.

128. Mateer SW, Cardona J, Marks E, Goggin BJ, Hua S, Keely S. Ex vivo intestinal sacs to assess mucosal permeability in models of gastrointestinal disease. JoVE (Journal of Visualized Experiments). 2016(108):e53250.

129. Welsh-Bacic D, Lindenmeyer M, Cohen CD, Draganovici D, Mandelbaum J, Edenhofer I, et al. Expression of the chemokine receptor CCR6 in human renal inflammation. Nephrology dialysis transplantation. 2010;26(4):1211-20.

130. Oo YH, Banz V, Kavanagh D, Liaskou E, Withers DR, Humphreys E, et al. CXCR3-dependent recruitment and CCR6-mediated positioning of Th-17 cells in the inflamed liver. Journal of hepatology. 2012;57(5):1044-51.

131. Arsent'eva N, Semenov A, Lyubimova N, Ostankov YV, Elezo D, Kudryavtsev I, et al. Chemokine receptors CXCR3 and CCR6 and their ligands in the liver and blood of patients with chronic hepatitis C. Bulletin of experimental biology and medicine. 2015;160(2):252-5.

132. Ryan F, Smart R, Holdsworth C, Preston F. Hyposplenism in inflammatory bowel disease. Gut. 1978;19(1):50-5.

133. Pereira J, Hughes L, Young H. Spleen size in patients with inflammatory bowel disease. Diseases of the colon & rectum. 1987;30(6):403-9.

134. Fousekis FS, Theopistos VI, Katsanos KH, Tsianos EV, Christodoulou DK. Hepatobiliary manifestations and complications in inflammatory bowel disease: A review. Gastroenterology research. 2018;11(2):83.

135. Egresi A, Kovács Á, Szilvás Á, Blázovics A. Gut-liver axis in inflammatory bowel disease. A retrospective study. Orvosi hetilap. 2017;158(26):1014-21.

136. Silva J, Brito BS, Silva INdN, Nóbrega VG, da Silva MCS, Gomes HDdN, et al. Frequency of Hepatobiliary Manifestations and Concomitant Liver Disease in Inflammatory Bowel Disease Patients. BioMed research international. 2019;2019.

137. Paust H-J, Turner J-E, Riedel J-H, Disteldorf E, Peters A, Schmidt T, et al. Chemokines play a critical role in the cross-regulation of Th1 and Th17 immune responses in murine crescentic glomerulonephritis. Kidney international. 2012;82(1):72-83.

138. Raza A, Yousaf W, Giannella R, Shata MT, Kaser, Tsironi, et al. Th17 cells: interactions with predisposing factors in the immunopathogenesis of inflammatory bowel disease. Expert review of clinical immunology. 2012;8(2):161-8.

139. Cyster JG, Schwab SR. Sphingosine-1-phosphate and lymphocyte egress from lymphoid organs. Annual review of immunology. 2012;30:69-94.

140. Arseneau K, Cominelli F. Targeting leukocyte trafficking for the treatment of inflammatory bowel disease. Clinical Pharmacology & Therapeutics. 2015;97(1):22-8.

141. Imam T, Park S, Kaplan MH, Olson MR. Effector T helper cell subsets in inflammatory bowel diseases. Frontiers in immunology. 2018;9:1212.

142. Bamias G, J Clark D, Rivera-Nieves J. Leukocyte traffic blockade as a therapeutic strategy in inflammatory bowel disease. Current drug targets. 2013;14(12):1490-500.

143. Gerner R, Moschen A, Tilg H. Targeting T and B lymphocytes in inflammatory bowel diseases: lessons from clinical trials. Digestive Diseases. 2013;31(3-4):328-35.

144. Kanai T, Kawamura T, Dohi T, Makita S, Nemoto Y, Totsuka T, et al. TH1/TH2-mediated colitis induced by adoptive transfer of CD4+ CD45RBhigh T lymphocytes into nude mice. Inflammatory bowel diseases. 2006;12(2):89-99.

145. Wunderlich CM, Ackermann PJ, Ostermann AL, Adams-Quack P, Vogt MC, Tran M-L, et al. Obesity exacerbates colitis-associated cancer via IL-6-regulated macrophage polarisation and CCL-20/CCR-6-mediated lymphocyte recruitment. Nature communications. 2018;9(1):1646.

146. Kitamura K, Farber JM, Kelsall BL. CCR6 marks regulatory T cells as a colon-tropic, IL-10–producing phenotype. The Journal of Immunology. 2010;185(6):3295-304.

147. Wang X, Zhu Y, Zhang M, Wang H, Jiang Y, Gao P. Ulcerative colitis is characterized by a decrease in regulatory B cells. Journal of Crohn's and Colitis. 2016;10(10):1212-23.

148. Ito R, Shin-Ya M, Kishida T, Urano A, Takada R, Sakagami J, et al. Interferon-gamma is causatively involved in experimental inflammatory bowel disease in mice. Clinical & Experimental Immunology. 2006;146(2):330-8.

149. Obermeier F, Kojouharoff G, Hans W, Schölmerich J, Gross V, Falk W. Interferon-gamma (IFN-γ)-and tumour necrosis factor (TNF)-induced nitric oxide as toxic effector molecule in chronic dextran sulphate sodium (DSS)-induced colitis in mice. Clinical and experimental immunology. 1999;116(2):238.

150. Nava P, Koch S, Laukoetter MG, Lee WY, Kolegraff K, Capaldo CT, et al. Interferon-γ regulates intestinal epithelial homeostasis through converging β-catenin signaling pathways. Immunity. 2010;32(3):392-402.

151. Thelemann C, Eren RO, Coutaz M, Brasseit J, Bouzourene H, Rosa M, et al. Interferon-γ induces expression of MHC class II on intestinal epithelial cells and protects mice from colitis. PloS one. 2014;9(1):e86844.

152. Spees AM, Kingsbury DD, Wangdi T, Xavier MN, Tsolis RM, Bäumler AJ. Neutrophils are a source of gamma interferon during acute Salmonella enterica serovar Typhimurium colitis. Infection and immunity. 2014;82(4):1692-7.

153. Sheikh SZ, Matsuoka K, Kobayashi T, Li F, Rubinas T, Plevy SE. Cutting edge: IFN-γ is a negative regulator of IL-23 in murine macrophages and experimental colitis. The Journal of Immunology. 2010;184(8):4069-73.

154. Sands BE, Kaplan GG. The role of TNFα in ulcerative colitis. The Journal of Clinical Pharmacology. 2007;47(8):930-41.

155. Arora Z, Shen B. Biological therapy for ulcerative colitis. Gastroenterology report. 2014;3(2):103-9.

156. Shibata W, Maeda S, Hikiba Y, Yanai A, Ohmae T, Sakamoto K, et al. Cutting edge: the IκB kinase (IKK) inhibitor, NEMO-binding domain peptide, blocks inflammatory injury in murine colitis. The Journal of Immunology. 2007;179(5):2681-5.

157. Roda G, Marocchi M, Sartini A, Roda E. Cytokine networks in ulcerative colitis. Ulcers. 2011;2011.

158. Xiong J, Lin Y-H, Bi L-H, Wang J-D, Bai Y, Liu S-D. Effects of interleukin-4 or interleukin-10 gene therapy on trinitrobenzenesulfonic acid-induced murine colitis. BMC gastroenterology. 2013;13(1):165.

159. Mitsuyama K, MATSUMOTO S, Masuda J, Yamasaki H, Kuwaki K, Takedatsu H, et al. Therapeutic strategies for targeting the IL-6/STAT3 cytokine signaling pathway in inflammatory bowel disease. Anticancer Research. 2007;27(6A):3749-56.

160. Takač B, Mihaljević S, Štefanić M, Glavaš-Obrovac L, Kibel A, Samardžija M. Importance of interleukin 6 in pathogenesis of inflammatory bowel disease. Collegium antropologicum. 2014;38(2):659-64.

161. Atreya R, Neurath MF. Involvement of IL-6 in the pathogenesis of inflammatory bowel disease and colon cancer. Clinical reviews in allergy & immunology. 2005;28(3):187-95.

162. Giuffrida P, Caprioli F, Facciotti F, Di Sabatino A. The role of interleukin-13 in chronic inflammatory intestinal disorders. Autoimmunity reviews. 2019.

163. Xu Y-W, Xing R-X, Zhang W-H, Li L, Wu Y, Hu J, et al. Toxoplasma ROP16I/III ameliorated inflammatory bowel diseases via inducing M2 phenotype of macrophages. World Journal of Gastroenterology. 2019;25(45):6634.

164. Maxwell JR, Zhang Y, Brown WA, Smith CL, Byrne FR, Fiorino M, et al. Differential roles for interleukin-23 and interleukin-17 in intestinal immunoregulation. Immunity. 2015;43(4):739-50.

165. Whibley N, Gaffen SL. Gut-busters: IL-17 ain't afraid of no IL-23. Immunity. 2015;43(4):620-2.

166. Sun R, Hedl M, Abraham C. IL23 group> IL23R recycling and amplifies innate receptor-induced signalling and cytokines in human macrophages, and the IBD-protective IL23R R381Q variant modulates these outcomes. Gut. 2020;69(2):264-73.

167. Ueno A, Jeffery L, Kobayashi T, Hibi T, Ghosh S, Jijon H. Th17 plasticity and its relevance to inflammatory bowel disease. Journal of autoimmunity. 2018;87:38-49.

168. Khan MW, Keshavarzian A, Gounaris E, Melson JE, Cheon EC, Blatner NR, et al. PI3K/AKT signaling is essential for communication between tissue-infiltrating mast cells, macrophages, and epithelial cells in colitis-induced cancer. Clinical Cancer Research. 2013;19(9):2342-54.

169. Lee H-J, Choi S-C, Lee M-H, Oh H-M, Choi E-Y, Choi E-J, et al. Increased expression of MIP-3α/CCL20 in peripheral blood mononuclear cells from patients with ulcerative colitis and its down-regulation by sulfasalazine and glucocorticoid treatment. Inflammatory bowel diseases. 2005;11(12):1070-9.

170. Tokuhira N, Kitagishi Y, Suzuki M, Minami A, Nakanishi A, Ono Y, et al. PI3K/AKT/PTEN pathway as a target for Crohn's disease therapy. International journal of molecular medicine. 2015;35(1):10-6.

171. Huang XL, Xu J, Zhang XH, Qiu BY, Peng L, Zhang M, et al. PI3K/Akt signaling pathway is involved in the pathogenesis of ulcerative colitis. Inflammation research. 2011;60(8):727-34.

172. Yap TA, Garrett MD, Walton MI, Raynaud F, de Bono JS, Workman P. Targeting the PI3K–AKT–mTOR pathway: progress, pitfalls, and promises. Current opinion in pharmacology. 2008;8(4):393-412.

173. Whiteman EL, Cho H, Birnbaum MJ. Role of Akt/protein kinase B in metabolism. Trends in Endocrinology & Metabolism. 2002;13(10):444-51.

174. Robert R, Juglair L, Lim EX, Ang C, Wang CJ, Ebert G, et al. A fully humanized IgG-like bispecific antibody for effective dual targeting of CXCR3 and CCR6. PloS one. 2017;12(9):e0184278.

175. Jaen J, Dairaghi D, Leleti M, Powers J, Wang Y, Zhang P, et al. FRI0002 Inhibition of chemokine receptors ccr1 and ccr6 as promising therapies for rheumatoid arthritis. Annals of the Rheumatic Diseases. 2013;72(Suppl 3):A369-A.

176. Bouma G, Zamuner S, Hicks K, Want A, Oliveira J, Choudhury A, et al. CCL20 neutralization by a monoclonal antibody in healthy subjects selectively inhibits recruitment of CCR6+ cells in an experimental suction blister. British Journal of Clinical Pharmacology. 2017;83(9):1976-90.

177. Getschman A, Imai Y, Larsen O, Peterson F, Wu X, Rosenkilde M, et al. Protein engineering of the chemokine CCL20 prevents psoriasiform dermatitis in an IL-23–dependent murine model. Proceedings of the National Academy of Sciences. 2017;114(47):12460-5.

178. Lee AY, Körner H. CCR6 and CCL20: emerging players in the pathogenesis of rheumatoid arthritis. Immunology and cell biology. 2014;92(4):354-8.

179. Hirata T, Osuga Y, Takamura M, Kodama A, Hirota Y, Koga K, et al. Recruitment of CCR6-expressing Th17 cells by CCL 20 secreted from IL-1β-, TNF-α-, and IL-17A-stimulated endometriotic stromal cells. Endocrinology. 2010;151(11):5468-76.

180. Eskandarpour M, Alexander R, Adamson P, Calder VL. Pharmacological inhibition of bromodomain proteins suppresses retinal inflammatory disease and downregulates retinal Th17 cells. The Journal of Immunology. 2017;198(3):1093-103.

181. Dairaghi D, Zhang P, Leleti M, Berahovich R, Ebsworth K, Ertl L, et al. Inhibition Of Chemokine Receptors CCR1 and CCR6 As Promising Therapies For Autoimmune Diseases Such As Rheumatoid Arthritis and Psoriasis.: 1792. Arthritis & Rheumatism. 2013;65.

182. Klamar CR. Development of a robust and improved system for studying interactions between CCL20 and CCR6 using both recombinant and chemically synthesized rhesus macaque chemokines: University of Pittsburgh; 2010.

183. Blázquez AB, Knight AK, Getachew H, Bromberg JS, Lira SA, Mayer L, et al. A functional role for CCR6 on proallergic T cells in the gastrointestinal tract. Gastroenterology. 2010;138(1):275-84. e4.

184. Ito M, Teshima K, Ikeda S, Kitadate A, Watanabe A, Nara M, et al. MicroRNA-150 inhibits tumor invasion and metastasis by targeting the chemokine receptor CCR6, in advanced cutaneous T-cell lymphoma. Blood. 2014;123(10):1499-511.

185. Lee S-M, Yang H, Tartar D, Gao B, Luo X, Ye S, et al. Prevention and treatment of diabetes with resveratrol in a non-obese mouse model of type 1 diabetes. Diabetologia. 2011;54(5):1136-46.

8.0 Appendix

8.1 Types of inhibitors used against the CCR6–CCL20 axis.

Table 46. Types of inhibitors used against the CCR6–CCL20 axis, their common names, the immune cells involved, experimental outcomes, and diseases involved.

Type of Inhibitor	Name of Inhibitor	Nature of Inhibitor	Immune Cells / Cytokines Involved	Experimental Outcome	Name of Disease/ Model	Ref
Anti-hCCR6 mAbs		CCR6 Inhibitor	T_H17, B cells	Reduced inflammatory cell infiltration	Experimental Autoimmune Encephalitis (EAE)	(174)
Anti-CCR6 Abs	CO339589	CCR6 inhibitor	NK cells PBMC	Reduced disease	RA, psoriasis, MS	(175)
Anti CCL20 Abs	WO2017011559A1	CCL20 inhibitor	T_H17, T_{reg}	Inhibits CSC activity, tumorigenesis	Carcinoma	(114)

	GSK3050002	CCL20 inhibitor	T_H17	Reduced cell chemotaxis	Suction blister in skin	(176)
		CCL20 inhibitor	γδ T cells	Reduced immune cell infiltration to skin	Imiquimod (IMQ) induced psoriasiform dermatitis	(177)
Anti-TNF-α Abs	Infliximab Tocilizumab	Indirect CCL20 inhibitor	Synoviocytes	Inhibits TNF-α induced CCL20 upregulation	RA	(178)
Inhibitors of p38, 42, 44	MAPK Inhibitors	Indirect CCL20 inhibitor	T_H17	Reduced pro-inflammatory cytokines, suppressed CCL20	Ovarian endometritis	(179)
Partial Agonists	AOP-RANTES	Partial CCR6 inhibitor	T_H17	Reduced inflammato	Psoriasiform dermatitis	(177)

				ry cell chemotaxis		
Bispecific Abs	Humanised IgG-like BsAb	CCR6 and CXCR3 inhibitors	T_H17	Blocks cell chemotaxis	Murine model	(174)
BET Proteins		Gene regulator	T_H17, T_{reg}	Reduced inflammation	Posterior uveitis	(180)
Small Molecule Inhibitors	CCX9664	CCR6 inhibitor	T_H17	Reduced disease	Rheumatoid arthritiis (RA)	(181)
Botanical Inhibitors	EGCG, Gallotannin	CCL20 inhibitor	T_H17	Inhibited cell chemotaxis	Rhesus Macaque model	(182)
Sphingosine 1 PO4 R agonist	FTY720		$CD4^+$T Cells	Inhibited egress of lymphocytes from LNs	Allergic diarrhea	(183)
microRNA	MiR-150	CCR6 inhibitor	CTCL cells	Reduced metastasis	Cutaneous T cell	(184)

					lymphoma (CTCL)	
Polyphenol compound	Resveratrol	Sirtuin-1 activator	T_H17, macrophages	Reduced disease, inflammatory cytokines	Type-1 diabetes, RA, lupus, EAE	(185)
CCR6R Peptide Mimetics	ECL-2	CCL20 inhibitor	$CCR6^+$ cells	Reduced cell chemotaxis	Rhesus Macaque model	(182)

Legend: MAPK—mitogen activated protein kinase, p—protein, CCL20—CC chemokine ligand 20, mAbs—monoclonal antibodies, BsAb—bispecific antibodies CCR6—CC chemokine receptor 6, hCCR6—humanised CCR6, Abs—antibodies, IL—interleukin, TNF-α—tumor necrosis factor-alpha, BET—bromodomain extraterminal proteins, PO_4—phosphate, R—receptor, RNA—ribonucleic acid, AOP-RANTES—amino oxy pentane regulated on activation, normal T cell expressed and secreted. NK—natural killer, PBMC—peripheral blood mononuclear cells, IMQ—Imiquimod, T_H17—T helper subset 17, T_{reg}—regulatory T reg cell, $\gamma\delta$ T cell—gamma delta T cell, EGCG—Epigallocatechin gallate, Ref—references to inhibitors, MS—multiple sclerosis, RA—rheumatoid arthritis.

8.2 Ethics Approval Permit

Animal Ethics Committee

ETHICS APPROVAL PERMIT

Office of Research Services
Phone : 03 62266236
Fax: 03 62267148
animal.ethics@utas.edu.au

To: Associate Professor Raj Eri

From: Mel Perry

Date: 05 September 2018

Project: A0017451 - Immune Profiling in a CCR6 Deficient Model of Spontaneous Inflammatory Bowel Disease

Approved on: 05 September 2018

Approval expires: 04 September 2021

1st Annual Report due: 05 September 2019

Please read this permit carefully as **approval may be withdrawn** for non-compliance with the conditions stated below.

The Animal Ethics Committee has approved the above project and a copy of the initial application document is attached. The approval is subject to the review and AEC approval of an annual report which is due before the approval anniversary**. Please note the due date in your diary.**

As the Responsible Investigator, you MUST ensure that:

1. All aspects of the work conform to the requirements of the current edition of the *Australian code of practice for the care and use of animals for scientific purposes* 8th edition 2013
2. The project is conducted in accordance with the provisions of the Tasmanian Veterinary Surgeons Act 1987 and Veterinary Surgeons Regulations 2012. If the project involves a veterinary service or other animal service, it is **your responsibility** to contact the University Veterinarian to discuss the legal requirements of competency assessment.
3. It is the responsibility of institutions and researchers to be aware of and conduct research in accordance with both general and specific legal requirements, wherever relevant

4. The University Veterinarian and the Animal Ethics Committee are promptly notified of any unexpected event which was not considered in the initial application and impacts on the welfare of any animal directly or indirectly involved in the project.
5. You contact the University Veterinarian to advise when and where your experiments will be conducted. Sufficient notice needs to be given so that an inspection can be easily arranged.
6. In the event of any unexpected death, you contact the University Veterinarian to perform an autopsy.
7. A full record is maintained of all animals used in this project. If at any stage you anticipate the need to use additional animals this must be communicated to the committee before use. Using additional animals without AEC approval is a breach of your ethics permit.
8. That all investigators complete the MyLo Animal Ethics Online Training module every three years.

The project is approved for a maximum of 3 years. If the project is to continue past the expiry date, a new initial application will need to be submitted.

If the investigation necessitates a Parks & Wildlife permit or other permits, you are required to send copies to animal.ethics@utas.edu.au before commencing work.

Executive Officer
Animal Ethics Committee

University of Tasmania

Animal Ethics Committee

Ethics Number: A0017451
Project Name:
Immune Profiling in a CCR6 Deficient Model of Spontaneous Inflammatory Bowel Disease
Chief Investigator: Associate Professor Raj Eri
School: Health Sciences
Person responsible for day-to-day care:
Ethics start date: 05 September 2018
Ethics approved to: 04 September 2021
Emergency Contact: